

Exponentially accurate open quantum simulation via randomized dissipation with minimal ancilla

Jumpei Kato,^{1,2,3,*} Kaito Wada,^{3,†} Kosuke Ito,^{2,4} and Naoki Yamamoto^{2,5}

¹*Mitsubishi UFJ Financial Group, Inc. and MUFG Bank, Ltd., 4-10-2 Nakano, Nakano-ku, Tokyo 164-0001, Japan*

²*Quantum Computing Center, Keio University, Hiyoshi 3-14-1, Kohoku, Yokohama 223-8522, Japan*

³*Graduate School of Science and Technology, Keio University, 3-14-1 Hiyoshi, Kohoku, Yokohama 223-8522, Japan*

⁴*Advanced Material Engineering Division, Toyota Motor Corporation, 1200 Mishuku, Susono, Shizuoka 410-1193, Japan*

⁵*Department of Applied Physics and Physico-Informatics, Keio University, Hiyoshi 3-14-1, Kohoku, Yokohama 223-8522, Japan*

Simulating open quantum systems is an essential technique for understanding complex physical phenomena and advancing quantum technologies. Some quantum algorithms for simulating Lindblad dynamics achieve logarithmically short circuit depth in terms of accuracy ε by coherently encoding all possible jump processes with a large ancilla consumption. Minimizing the space complexity while achieving such a logarithmic depth remains an important challenge. In this work, we present a quantum algorithm for simulating general Lindblad dynamics with multiple jump operators aimed at an observable estimation, that achieves both a logarithmically short circuit depth and a minimum ancilla size. Toward simulating an exponentially accurate Taylor expansion of the Lindblad propagator to ensure the circuit depth of $\mathcal{O}(\log(1/\varepsilon))$, we develop a novel random circuit compilation method that leverages dissipative processes with only a single jump operator; importantly, the proposed method requires the minimal-size, $4 + \lceil \log M \rceil$, ancilla qubits where each single jump operator has at most M Pauli strings. This work represents a significant step towards making open quantum system simulations more feasible on early fault-tolerant quantum computing devices.

Introduction.— Analysis and simulation of open quantum systems [1–4] are indispensable for understanding complex quantum phenomena found in e.g., many-body quantum systems. It can also be used for synthesizing quantum systems having useful functionalities in the framework of reservoir engineering [5, 6], and moreover for devising noise mitigation techniques in quantum computation [7]. Such studies are usually based on the Lindblad equation or Gorini–Kossakowski–Sudarshan–Lindblad equation [8, 9]:

$$\frac{d\rho}{dt} = \mathcal{L}(\rho) := -i[H, \rho] + \sum_{k=1}^K \left(L_k \rho L_k^\dagger - \frac{1}{2} \{ L_k^\dagger L_k, \rho \} \right), \quad (1)$$

where H and $\{L_k\}_{k=1}^K$ are the Hamiltonian and jump operators of a target system, respectively.

Quantum computation offers a promising approach for simulating the dynamics of quantum systems [10]. There are several efficient approaches to simulate the Lindblad equation via unitary dynamics of quantum computation, based on Trotter-type decomposition [11–17], vectorized Lindblad equation [18–20], and sample-based simulation [21, 22]. In particular, the previous works for open quantum systems [23–25] achieve a logarithmically short circuit depth with respect to accuracy, likewise the case of closed systems via the state-of-the-art

methods for Hamiltonian simulation (HS) [26–28]. However, they need to simultaneously encode *all* possible jump processes in a quantum circuit, via linear combination of unitaries (LCU) method followed by oblivious amplitude amplification (OAA), leading to a large consumption of ancilla qubits and complicated controlled operations. Very recently, Ref. [29] introduces a HS-based method achieving Q -th order approximation without OAA, while it still requires large amount of ancilla qubits in addition to a highly accurate simulation of a dilated Hamiltonian comprised of an exponentially large number of terms $\mathcal{O}(K^Q)$.

On the other hand, recently, the importance of reducing ancilla qubits has been demonstrated in various quantum algorithms [30–35], especially in the early stage of fault-tolerant quantum computers, where only a limited amount of quantum resources is available. However, for open quantum system simulations, only limited attention has been paid to improving space complexity while guaranteeing high accuracy. This is possibly because it is challenging to achieve both the reduction of ancilla qubits boosting the simulation accuracy for non-unitary dynamics with advanced coherent techniques. Note that we may use near-term quantum algorithms [36–38] that work with fewer ancilla qubits, but they require many samples for accurate simulation. Therefore, significant progress in reducing space overhead, together with high accuracy and constant sampling overhead, has yet to be achieved.

Summary of the result.— In this work, we present a quantum algorithm for estimating the expectation value

* jumpei.kato@keio.jp

† wkai1013keio840@keio.jp; J.K. and K.W. contributed equally to this work.

Algorithm	Circuit depth	Additional qubits
Channel LCU [23]	$\mathcal{O}(\tau \text{polylog}(\tau/\varepsilon))$	$\mathcal{O}(\log(1/\varepsilon) \log(MK/\varepsilon))$
Higher order HS (Qth order) [29]	$\mathcal{O}(\tau (\tau/\varepsilon)^{\frac{1}{Q}})$	$\Omega(Q \log(MK))$
Vectorization [19]	$\mathcal{O}(\tau^2/\varepsilon)$	$n + 1$
Our work	$\mathcal{O}(\tau^2 \log(\tau/\varepsilon))$	$4 + \lceil \log_2 M \rceil$

TABLE I. Circuit depth and additional qubits for n -qubit Lindblad simulation algorithms. K is the number of jump operators, each of which consists of M Pauli strings, and $Q > 0$ is an integer. For simplicity, we omit the dependence of depth on parameters except for rescaled time $\tau = t \|\mathcal{L}\|_{\text{pauli}}$ and accuracy ε . Remarkably, the gate complexity in our method does not depend on either K or the number m of Pauli strings in the system Hamiltonian, whereas other methods may rely on one or both. The last two algorithms are applicable only for the expectation value estimation.

$\text{Tr}[O\rho(t)]$ of a given observable O with respect to $\rho(t)$ evolved by Eq. (1), rather than the tracking of full state $\rho(t)$ focused in the previous works. Given a Hamiltonian H and jump operators $\{L_k\}_{k=1}^K$ specified by n -qubit Pauli strings $\{P_{kj}\}$ as

$$H = \sum_{j=1}^m \alpha_{0j} P_{0j}, \quad L_k = \sum_{j=1}^M \alpha_{kj} P_{kj}, \quad (2)$$

for $\alpha_{0j} \in \mathbb{R}, \alpha_{kj} \in \mathbb{C}$, our algorithm requires $\mathcal{O}(\|O\|^2/\varepsilon^2)$ samples from quantum circuits with the logarithmic depth $\mathcal{O}(t^2 \log(t/\varepsilon))$ for a given estimation error ε . Notably, while the scaling of depth is yet worse in t than Ref. [23, 29] shown in Table I, the number of additional ancilla qubits is only $4 + \lceil \log_2 M \rceil$ for the number of Pauli strings M of each single jump operator in Eq. (2). Our ancilla count depends solely on M , whereas other proposals have the dependence of M, K, ε , or n . In particular, the independence from K offers a significant advantage for open systems with large K , e.g., in the presence of collective decay, K scales exponentially regarding system qubits n [39].

Our algorithm works as follows. The quantum circuits are composed of r randomly chosen sequential blocks, shown in Fig. 1. In each block, we simulate Hamiltonian dynamics or dissipative process, which is further stochastically decomposed into minimal units, i.e., a single Pauli rotation and a single jump process. As a result, the total gate complexity does not depend on either the number m of Pauli strings in Hamiltonian H or the number K of jump operators L_k . A similar feature on m can be found in random compilers such as qDRIFT [31, 40]. The very recent randomization approaches for Lindblad simulation [39, 41] have similar features while they do not establish the logarithmic depth.

To realize each dissipative process with a single jump on a quantum circuit, we develop an improved version of the method via LCU combined with OAA invented by Ref. [23]. This requires minimal-size ancilla qubits for a

general single jump process, given by at most $3 + \lceil \log_2 M \rceil$ qubits. Although the previous method introduces approximation errors, our improved version allows for the exact simulation of jump processes thanks to an error recovery operation. Finally, by averaging the (weighted) measurement outputs from these randomized circuits, we can estimate the expectation value with a constant sampling overhead (more precisely, its value can be close to 1).

Our idea is founded on decomposing the dynamical map $e^{t\mathcal{L}}$ via the transfer matrix representation of superoperators (i.e., a linear map on the space of linear operators) [42, 43]. Although the transfer matrix formalism usually introduces an extended ancilla system with the same dimension as the target system [18, 19], we establish an effective simulation formalism for superoperators using quantum circuits without doubling the target system size. This formalism allows us to effectively simulate an exponentially accurate Taylor expansion of the transfer matrix of $e^{t\mathcal{L}}$ on the circuits. Below we describe key features of our algorithm, which is summarized in Theorem 1.

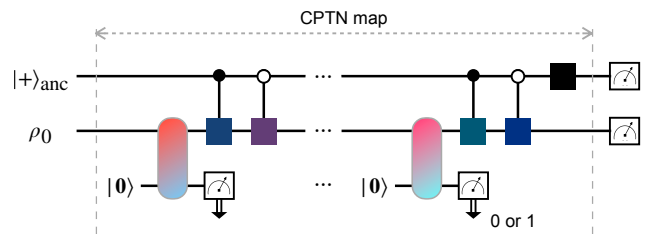


FIG. 1. Quantum circuit of sampled $\widetilde{\mathcal{W}}_v$ for simulating the decomposition of $e^{t\mathcal{L}}$ in Theorem 1. The colored blocks denote unitary gates, which can be constructed from the input model. The mid-circuit measurement and qubit reset allow us to effectively simulate the CPTN maps \mathcal{W}_v by the quantum circuits. The quantum register $|0\rangle$ contains at most $3 + \lceil \log_2 M \rceil$ qubits.

Decomposition of $e^{t\mathcal{L}}$.— We first provide a theorem giving an exact decomposition of the dynamical map $e^{t\mathcal{L}}$ in the form of a linear combination of generalized Hadamard-test circuits $\{\widetilde{\mathcal{W}}_v\}$; each circuit is illustrated in Fig. 1. In the theorem, the upper bound of the total coefficients, Eq. (4), is essential to realize an efficient random compilation.

Theorem 1. *Let \mathcal{L} be an n -qubit Lindblad superoperator with a Hamiltonian H and jump operators $\{L_k\}_{k=1}^K$ that are specified by Eq. (2), and let $\|\mathcal{L}\|_{\text{pauli}} := 2(\alpha_0 + \sum_{k=1}^K \alpha_k^2)$ for $\alpha_k := \sum_j |\alpha_{kj}|$. Then, for any $t > 0$ and any positive integer $r \geq t \|\mathcal{L}\|_{\text{pauli}}$, there exists a linear decomposition*

$$e^{t\mathcal{L}}(\bullet) = \sum_{v \in \mathcal{S}} c_v \text{Tr}_{\text{anc}}[(X_{\text{anc}} \otimes \mathbf{1}) \widetilde{\mathcal{W}}_v(|+\rangle \langle +|_{\text{anc}} \otimes \bullet)] \quad (3)$$

for some indices set S , real values $c_v > 0$, and $(n+1)$ -qubit completely positive trace non-increasing (CPTN) maps $\{\widetilde{\mathcal{W}}_v\}$, such that

$$\sum_{v \in S} c_v \leq e^{2\|\mathcal{L}\|_{\text{Pauli}}^2 t^2 / r}. \quad (4)$$

Furthermore, for any v , the $(n+1)$ -qubit CPTN map $\widetilde{\mathcal{W}}_v$ can be effectively simulated by a quantum circuit on the $n+1$ qubits system and additional $3 + \lceil \log_2 M \rceil$ qubits ancilla system with mid-circuit measurement and qubit reset.

The constructive proof of Theorem 1 is provided in Appendix B1. In the following, we show a sketch of the proof that is built on the framework of the *transfer matrix* of superoperators [42, 43], which greatly simplifies involved calculations for the higher powers of superoperators. We follow the convention that treats any n -qubit operator A as a column-stacking 4^n -dimensional vector $|A\rangle$. Under this notation, a general superoperator \mathcal{E} can be written as a $4^n \times 4^n$ matrix $S(\mathcal{E})$, which is often called the transfer matrix of \mathcal{E} . For instance, for a superoperator $A \bullet B^\dagger$, we have $S(A \bullet B^\dagger) = \overline{B} \otimes A$, where \overline{B} denotes the entrywise complex conjugation of B . Also, we often use the fact that $S(\Phi' \circ \Phi) = S(\Phi')S(\Phi)$ for any superoperators Φ and Φ' . In this framework, the Lindblad equation Eq. (1) can be written as

$$\frac{d}{dt} |\rho\rangle\rangle = G |\rho\rangle\rangle, \quad (5)$$

where $G = S(\mathcal{L})$ is the transfer matrix of \mathcal{L}

$$G = -i\mathbf{1} \otimes H + iH^\dagger \otimes \mathbf{1} + \sum_{k=1}^K \left(\overline{L}_k \otimes L_k - \frac{1}{2} \mathbf{1} \otimes L_k^\dagger L_k - \frac{1}{2} L_k^\dagger \overline{L}_k \otimes \mathbf{1} \right). \quad (6)$$

Also, the transfer matrix of $e^{t\mathcal{L}}$ is given by e^{tG} .

Sketch of the proof. We aim to have the decomposition of Eq. (3) through that of e^{tG} on the extended space. As the first step, we decompose e^{tG} as a linear combination of (the transfer matrix of) superoperators \mathcal{W}_v that can be written as a product of the following two-type superoperators: (A) CPTN maps and (B) convex combinations of asymmetric forms $U \bullet V^\dagger$ with (possibly distinct) unitaries U and V . Then, we translate the composite map \mathcal{W}_v into the form $\text{Tr}_{\text{anc}}[\dots]$ of Eq. (3). For simplicity, we refer to a type-(B) superoperator composed of asymmetric forms $e^{i\theta} P \bullet Q^\dagger$ for some $\theta \in \mathbb{R}$ and $P, Q \in \{I, X, Y, Z\}^{\otimes n}$ as an *asymmetric Pauli mixture*.

Let us consider the Taylor expansion of $e^{(t/r)G}$:

$$e^{(t/r)G} = \sum_l \frac{(t/r)^{2l}}{(2l)!} G^{2l} G', \quad (7)$$

where $G' := \mathbf{1} \otimes \mathbf{1} + tG/r(2l+1)$. From the assumption of the access model (2), we can represent $G/\|\mathcal{L}\|_{\text{Pauli}}$ as an asymmetric Pauli mixture. Then, defining $\alpha := 2\alpha_0 + \sum_k \alpha_k^2$ and $\tau_l := \alpha t/r(2l+1)$ for simplicity, we expand G' into the sum of the following terms for $k = 1, 2, \dots, K$:

$$\frac{\alpha_k^2}{\alpha} \left\{ S(\mathcal{B}_{kl}) - \frac{\tau_l^2}{4} \frac{L_k^\dagger \overline{L}_k}{\alpha_k^2} \otimes \frac{L_k^\dagger L_k}{\alpha_k^2} \right\}, \quad (8)$$

$$\frac{\alpha_0}{\alpha} \left(2 \cdot \mathbf{1} \otimes \mathbf{1} + \mathbf{1} \otimes \frac{-i\tau_l H}{\alpha_0} + \frac{i\tau_l H^\dagger}{\alpha_0} \otimes \mathbf{1} \right), \quad (9)$$

where \mathcal{B}_{kl} is the CP map of the simplest dissipative operator defined as

$$\mathcal{B}_{kl}(\bullet) = \sqrt{\tau_l} \frac{L_k}{\alpha_k} \bullet \left(\sqrt{\tau_l} \frac{L_k}{\alpha_k} \right)^\dagger + \left(\mathbf{1} - \frac{\tau_l}{2} \frac{L_k^\dagger L_k}{\alpha_k^2} \right) \bullet \left(\mathbf{1} - \frac{\tau_l}{2} \frac{L_k^\dagger L_k}{\alpha_k^2} \right)^\dagger. \quad (10)$$

To derive the equality Eq. (3) satisfying Eq. (4), it is crucial to find an *exact* linear decomposition of G' with type-(A, B) superoperators such that the norm of coefficients scales as $1 + \mathcal{O}((t/r)^2)$ [44].

To exactly simulate the CP map \mathcal{B}_{kl} , we cannot use the standard method for quantum channel implementation [23] that relies on the LCU for channels followed by OAA. This is because the method provides an (explicit) quantum circuit to effectively simulate a CPTN map $\mathcal{B}_{kl}^{(\text{approx})}$ that only approximates the target CP map when it lacks trace-preserving property; see Appendix B2. To overcome this difficulty, we develop a new technique for the exact simulation of *general* CP maps. This technique allows us to simulate \mathcal{B}_{kl} with the help of random sampling of *correction* superoperator \mathcal{R}_{kl} . That is, we construct a superoperator \mathcal{R}_{kl} to recover the approximation error such that

$$\mathcal{B}_{kl} = \mathcal{B}_{kl}^{(\text{approx})} + \mathcal{R}_{kl} \quad (11)$$

holds; importantly, while \mathcal{R}_{kl} is generally not a CP map, it can be written as an asymmetric Pauli mixture up to a normalization factor of the order $\mathcal{O}(\tau_l^2)$. As a result, we have a linear decomposition of Eq. (8) with a small sum of coefficients $\alpha_k^2/\alpha + \mathcal{O}(\tau_l^2)$, using an exactly simulatable type-(A) superoperator $\mathcal{B}_{kl}^{(\text{approx})}$ and an asymmetric Pauli mixture.

As for the decomposition of Eq. (9), we can apply the decomposition method for Hamiltonian simulation in

Ref. [31], which provides

$$\begin{aligned} & \mathbf{1} \otimes \mathbf{1} + \mathbf{1} \otimes \frac{-i\tau_l H}{\alpha_0} \\ &= \sqrt{1 + \tau_l^2} \sum_{j=1}^m \frac{|\alpha_{0j}|}{\alpha_0} \cdot \mathbf{1} \otimes e^{-i\theta_l \text{sgn}(\alpha_{0j}) P_{0j}}, \end{aligned} \quad (12)$$

where $\theta_l := \arccos(\{1 + \tau_l^2\}^{-1/2})$. By applying the similar decomposition for the term of $i\tau_l H^T/\alpha_0$, Eq. (9) with the normalization factor $2\alpha_0\sqrt{1 + \tau_l^2}/\alpha$ can be written as a type-(B) superoperator with asymmetric forms of $\mathbf{1} \otimes U$ or $\bar{V} \otimes \mathbf{1}$ with some Pauli rotation gates U and V .

Therefore, combining the above results together with Eq. (7), we arrive at a linear decomposition of $e^{(t/r)G}$ with composite maps of type-(A, B) superoperators. This immediately leads to a linear decomposition of e^{tG} as $e^{tG} = \sum_v c_v S(\mathcal{W}_v)$ for some indices v , $c_v \geq 0$, and composite maps \mathcal{W}_v . Since the norm of coefficients in the decomposition scales as $1 + \mathcal{O}((t/r)^2)$, the upper bound of the sum of coefficients is obtained as

$$\sum_{v \in S} c_v = \left(\sum_{l=0}^{\infty} \frac{(\tau/r)^{2l}}{(2l)!} (1 + \mathcal{O}(\tau_l^2)) \right)^r \leq e^{2r^2/r}, \quad (13)$$

where $\tau = t\|\mathcal{L}\|_{\text{pauli}}$. Thus, we have Eq. (4); the detailed derivation is provided in Appendix B 1.

In the final step toward obtaining Eq. (3), we introduce the following translation rule from \mathcal{W}_v to the CPTN map $\widetilde{\mathcal{W}}_v$ on the $n + 1$ qubits:

$$\widetilde{\mathcal{W}}_v : \begin{pmatrix} A_{00} & A_{01} \\ A_{10} & A_{11} \end{pmatrix} \mapsto \begin{pmatrix} * & \mathcal{W}_v(A_{01}) \\ \mathcal{J} \circ \mathcal{W}_v \circ \mathcal{J}(A_{10}) & * \end{pmatrix}, \quad (14)$$

where $A_{ij} := \langle i|_{\text{anc}} A |j\rangle_{\text{anc}}$ and \mathcal{J} is an anti-linear map that $\mathcal{J} : A \mapsto A^\dagger$. We can obtain such $\widetilde{\mathcal{W}}_v$ from \mathcal{W}_v by the following simple replacement; for type-(A), the CPTN map $\Phi(\bullet)$ is replaced with $\mathcal{I}_{\text{anc}} \otimes \Phi$, and for type-(B), $\sum_i p_i U_i \bullet V_i^\dagger$ is replaced with the mixed unitary channel $\sum_i p_i \mathcal{U}_i$ defined as

$$\mathcal{U}_i = |0\rangle\langle 0|_{\text{anc}} \otimes U_i + |1\rangle\langle 1|_{\text{anc}} \otimes V_i. \quad (15)$$

The details for the translation rule are provided in Appendix B 3. Therefore, making the measurement of X_{anc} , we obtain Eq. (3) thanks to $e^{t\mathcal{L}} = \mathcal{J} \circ e^{t\mathcal{L}} \circ \mathcal{J}$ from the Hermitian-preserving property of $e^{t\mathcal{L}}$.

To simulate the $(n + 1)$ -qubit CPTN map $\widetilde{\mathcal{W}}_v$, we need to introduce additional $3 + \lceil \log_2 M \rceil$ qubits. This additional qubits are required for quantum circuits, obtained from the standard method [23], to effectively simulate the CPTN maps $\mathcal{B}_{kl}^{(\text{approx})}$. They are measured by the computational basis in the middle of the entire circuit and

then reset for the next $\mathcal{B}_{kl}^{(\text{approx})}$. Performing a classical post-processing on the final outputs in order to drop an unnecessary part of the CPTP process by unitary circuit, we can effectively realize CPTN maps using the circuits illustrated in Fig. 1. \square

Theorem 1 clarifies the complexity to simulate a target open system is well reflected by that of $\widetilde{\mathcal{W}}_v$, which can be indeed effectively simulated on a device. Actually, the additional space overhead and the total gate complexity for each circuit for $\widetilde{\mathcal{W}}_v$ does not depend on either the number m of Pauli strings in a Hamiltonian H or the number K of jump operators, while the collection of $\widetilde{\mathcal{W}}_v$ recovers the full dynamics $e^{t\mathcal{L}}$.

Moreover, toward developing a practically effective algorithm for estimating the expectation value $\text{Tr}[O\rho(t)]$, let us discuss the maximal circuit depth for $\widetilde{\mathcal{W}}_v$. The decomposition (3) is attributed to the Taylor series expansion Eq. (7); the CPTN map $\widetilde{\mathcal{W}}_v$ contains $2l$ sequential applications of the mixed unitary channel, which may result in a large depth circuit without any truncation. However, the Taylor expansion is exponentially accurate with respect to the truncation order Q , meaning that we only need circuits with $l \leq Q = \mathcal{O}(\log(r/\Delta))$ to achieve accuracy Δ/r for each segment. Therefore, we have a finite subset S_Δ of S satisfying the following properties: (i) Eq. (3) holds up to error Δ , and (ii) the circuit depth for $\widetilde{\mathcal{W}}_v$ is $\mathcal{O}(rQ) = \mathcal{O}(r \log(r/\Delta))$ for all $v \in S_\Delta$. In addition, we can efficiently sample the explicit circuit for $\widetilde{\mathcal{W}}_v$ according to the distribution proportional to c_v for $v \in S_\Delta$; see Algorithm 1 in Appendix C. With these preliminaries, we now describe our main algorithm in what follows.

Main algorithm.— Our quantum algorithm for estimating $\text{Tr}[O\rho(t)]$ works as follows. First, we randomly generate a quantum circuit from the set $\{\widetilde{\mathcal{W}}_v\}$ according to the probability distribution $\{c_v/C\}$, where

$$C := \sum_{v \in S_\Delta} c_v \leq \sum_{v \in S} c_v \leq e^{2\|\mathcal{L}\|_{\text{pauli}}^2 t^2/r}. \quad (16)$$

The sampled circuit contains (possibly multi-round) mid-circuit measurement with binary outcome(s) $b \in \{0, 1\}$ and qubit reset for realizing the CPTN property of $\widetilde{\mathcal{W}}_v$. Then, running the quantum circuit with the initial state $|+\rangle\langle +|_{\text{anc}} \otimes \rho_0$ followed by the measurement for observable $X_{\text{anc}} \otimes O$ at the end of the circuit, we record measurement results (b_X, b_O) and a collection of mid-circuit measurement outcomes $\mathbf{b} = (b_1, b_2, \dots)$ ($b_i \in \{0, 1\}$). By repeating the above procedure N times independently, we calculate the average of the obtained results as

$$\varphi_N = \frac{C}{N} \sum_{i=1}^N b_X^{(i)} b_O^{(i)} \delta_{\mathbf{b}^{(i)}, \mathbf{0}} \quad (17)$$

where i denotes the trial index; this quantity serves as an estimator for $\text{Tr}[O\rho(t)]$. Note that the CPTN map

is effectively realized by dropping an unnecessary part of the CPTP process by the quantum circuit, through the classical post-processing of $\delta_{\mathbf{b}^{(i)}, \mathbf{0}}$; see the end of the sketch of proof for Theorem 1.

Using the construction of φ_N , we prove the existence of a quantum algorithm to achieve our goal in the following theorem.

Theorem 2. *For any Hamiltonian H and jump operators $\{L_k\}_{k=1}^K$ specified by Eq. (2), there exists a quantum algorithm that estimates the expectation value of an observable O for the n -qubit Lindblad dynamics Eq. (1) with the use of additional $4 + \lceil \log_2 M \rceil$ ancilla qubits, where M is the number of Pauli strings contained in a single jump operator L_k . For given additive error ε , δ , and simulation time t , this algorithm outputs an ε -close estimate for the expectation value with at least $1 - \delta$ probability, using $\mathcal{O}(\|O\|^2 \log(1/\delta)/\varepsilon^2)$ samples from the set of quantum circuits the maximal depth of which is*

$$\mathcal{O}\left(\|\mathcal{L}\|_{\text{pauli}}^2 t^2 \frac{\log(\|O\| \|\mathcal{L}\|_{\text{pauli}} t / \varepsilon)}{\log \log(\|O\| \|\mathcal{L}\|_{\text{pauli}} t / \varepsilon)}\right). \quad (18)$$

The sketch of the proof is as follows; see the full proof in Appendix C. The estimator φ_N for the true expectation value has a bias of magnitude at most $\Delta\|O\|$, where $\|O\|$ denotes the operator norm of O . Thus, taking $\Delta = \mathcal{O}(\|O\|/\varepsilon)$, we conclude that $N = \mathcal{O}(C^2\|O\|^2 \log(1/\delta)/\varepsilon^2)$ samples are sufficient to assure that φ_N has an additive error ε with a high probability due to the Hoeffding's inequality. Here, the factor C represents the sampling overhead in the proposed algorithm, because our problem can be solved by $\mathcal{O}(\|O\|^2 \log(1/\delta)/\varepsilon^2)$ calls of some quantum algorithm that directly prepares $\rho(t)$ (when we use no amplitude estimation). The sampling overhead C , which is upper bounded as Eq. (16), is controllable in our method by adjusting the circuit depth or equivalently the time slicing r . In particular, we can make $C = \mathcal{O}(1)$ by taking $r = \mathcal{O}(\|\mathcal{L}\|_{\text{pauli}}^2 t^2)$. Therefore, this choice of r combined with Theorem 1 (more precisely, the truncated version of the decomposition) completes the proof of Theorem 2.

Numerical simulation.— Here, we provide a numerical validation for the proposed algorithm. The tested instance is a two-level system with decay rate γ , described by the following Hamiltonian and jump operator:

$$H = -\frac{\delta}{2}Z - \frac{\Omega}{2}X, \quad L = \sqrt{\gamma} \frac{X - iY}{2}. \quad (19)$$

Figure 2 shows the results of estimating the excited state population, meaning that $O = |0\rangle\langle 0|$. The calculated values are in good agreement with the exact solution, which successfully captures the characteristic dynamics. Detailed description of the simulation setup and supplementary results are provided in Appendix D.

Conclusion.— We presented a quantum algorithm for estimating the physical properties of the general Lindblad dynamics, which has an exponentially short circuit

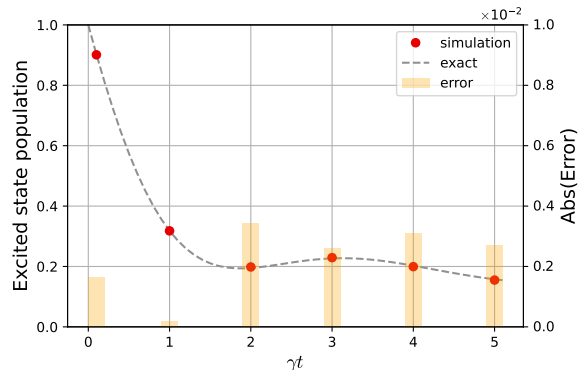


FIG. 2. Excited state population of the two level atom with parameters $\delta = \Omega = \gamma = 1$. The initial state $|0\rangle\langle 0|$ is evolved until time $t = 5$. The *exact* solution is obtained by QuTiP, and the *simulation* shows the mean value of Eq. (17) obtained from 2×10^4 samples. The *error* indicates the absolute error between *exact* and *simulation* for the single experiment on the right axis.

depth $\mathcal{O}(\log(1/\varepsilon))$ to achieve an accuracy ε and a nearly constant ancilla qubits $4 + \lceil \log_2(M) \rceil$. Thanks to the low computational resource, this algorithm has a potential to reveal undiscovered physical phenomena that must require high precision estimation. We also would like to emphasize the importance of newly developed techniques for superoperator simulation, such as the translation method of transfer matrices and the exact CP map simulation via OAA together with the recovery operation. Actually, they are widely applicable techniques for many problems beyond open system simulations.

We leave some questions open for future investigation. A particularly interesting question is on the relationship between our algorithm and the formulation via stochastic Schrödinger equation (SSE) [45], a widely applicable stochastic simulation method for open quantum systems. In fact, our algorithm also uses stochastic applications of unitary or jump operations to simulate the Lindblad master equation. However, our dissipative process is not physical unlike the case of SSE, because it is described as the composition of the minimal dissipation \mathcal{B}_{kl} and (possibly non-physical) superoperators $U \bullet V^\dagger$. Exploring the connection to SSE could offer some physical interpretation of our algorithm and thereby enable improvement of it in both implementability and computational complexity perspectives.

ACKNOWLEDGMENTS

K.W. was supported by JSPS KAKENHI Grant Number JP24KJ1963. J.K. acknowledges support by SIP Grant Number JPJ012367. This work was supported by MEXT Quantum Leap Flagship Program Grants No.

-
- [1] H.-P. Breuer and F. Petruccione, *The theory of open quantum systems* (Oxford University Press, 2007).
- [2] H. M. Wiseman and G. J. Milburn, *Quantum Measurement and Control* (Cambridge University Press, 2009).
- [3] A. J. Daley, Quantum trajectories and open many-body quantum systems, *Adv. Phys.* **63**, 77 (2014).
- [4] U. Weiss, *Quantum dissipative systems* (WORLD SCIENTIFIC, 2012).
- [5] J. Poyatos, J. I. Cirac, and P. Zoller, Quantum reservoir engineering with laser cooled trapped ions, *Physical review letters* **77**, 4728 (1996).
- [6] S. Haroche and J.-M. Raimond, *Exploring the quantum: Atoms, cavities, and photons*, Oxford Graduate Texts (Oxford University Press, 2006).
- [7] E. Van Den Berg, Z. K. Mineev, A. Kandala, and K. Temme, Probabilistic error cancellation with sparse Pauli-Lindblad models on noisy quantum processors, *Nature physics* **19**, 1116 (2023).
- [8] G. Lindblad, On the generators of quantum dynamical semigroups, *Communications in mathematical physics* **48**, 119 (1976).
- [9] V. Gorini, A. Kossakowski, and E. C. G. Sudarshan, Completely positive dynamical semigroups of N-level systems, *Journal of Mathematical Physics* **17**, 821 (1976).
- [10] S. Lloyd, Universal quantum simulators, *Science* **273**, 1073 (1996).
- [11] M. Kliesch, T. Barthel, C. Gogolin, M. Kastoryano, and J. Eisert, Dissipative quantum Church-Turing theorem, *Phys. Rev. Lett.* **107**, 120501 (2011).
- [12] T. Barthel and M. Kliesch, Quasilocality and efficient simulation of Markovian quantum dynamics, *Phys. Rev. Lett.* **108**, 230504 (2012).
- [13] A. M. Childs and T. Li, Efficient simulation of sparse Markovian quantum dynamics, *Quantum Information & Computation* **17**, 901 (2017).
- [14] J. Han, W. Cai, L. Hu, X. Mu, Y. Ma, Y. Xu, W. Wang, H. Wang, Y. P. Song, C.-L. Zou, and L. Sun, Experimental simulation of open quantum system dynamics via Trotterization, *Phys. Rev. Lett.* **127**, 020504 (2021).
- [15] D. Bacon, A. M. Childs, I. L. Chuang, J. Kempe, D. W. Leung, and X. Zhou, Universal simulation of Markovian quantum dynamics, *Phys. Rev. A* **64**, 062302 (2001).
- [16] R. Sweke, I. Sinayskiy, D. Bernard, and F. Petruccione, Universal simulation of Markovian open quantum systems, *Phys. Rev. A* **91**, 062308 (2015).
- [17] M. Jo and M. Kim, Simulating open quantum many-body systems using optimised circuits in digital quantum simulation, arXiv preprint arXiv:2203.14295 <https://doi.org/10.48550/arXiv.2203.14295> (2022).
- [18] A. W. Schlimgen, K. Head-Marsden, L. M. Sager, P. Narang, and D. A. Mazziotti, Quantum simulation of the Lindblad equation using a unitary decomposition of operators, *Phys. Rev. Res.* **4**, 023216 (2022).
- [19] H. Kamakari, S.-N. Sun, M. Motta, and A. J. Minnich, Digital quantum simulation of open quantum systems using quantum imaginary-time evolution, *PRX quantum* **3** (2022).
- [20] T. M. Watad and N. H. Lindner, Variational quantum algorithms for simulation of Lindblad dynamics, *Quantum Sci. Technol.* **9**, 025015 (2024).
- [21] D. Patel and M. M. Wilde, Wave matrix Lindbladization I: Quantum programs for simulating Markovian dynamics, *Open Syst. Inf. Dyn.* **30** (2023).
- [22] D. Patel and M. M. Wilde, Wave matrix Lindbladization II: General Lindbladians, linear combinations, and polynomials, *Open Syst. Inf. Dyn.* **30** (2023).
- [23] R. Cleve and C. Wang, Efficient quantum algorithms for simulating Lindblad evolution (Schloss Dagstuhl - Leibniz-Zentrum für Informatik, 2016).
- [24] X. Li and C. Wang, Simulating Markovian open quantum systems using higher-order series expansion (Schloss Dagstuhl - Leibniz-Zentrum für Informatik, 2023).
- [25] C.-F. Chen, M. J. Kastoryano, F. G. Brandão, and A. Gilyén, Quantum thermal state preparation, arXiv preprint arXiv:2303.18224 <https://doi.org/10.48550/arXiv.2303.18224> (2023).
- [26] D. W. Berry, A. M. Childs, R. Cleve, R. Kothari, and R. D. Somma, Simulating Hamiltonian dynamics with a truncated Taylor series, *Phys. Rev. Lett.* **114**, 090502 (2015).
- [27] G. H. Low and I. L. Chuang, Optimal Hamiltonian simulation by quantum signal processing, *Physical review letters* **118**, 010501 (2017).
- [28] G. H. Low and I. L. Chuang, Hamiltonian Simulation by Qubitization, *Quantum* **3**, 163 (2019).
- [29] Z. Ding, X. Li, and L. Lin, Simulating open quantum systems using Hamiltonian simulations, *PRX quantum* **5** (2024).
- [30] L. Lin and Y. Tong, Heisenberg-limited ground-state energy estimation for early fault-tolerant quantum computers, *PRX Quantum* **3**, 010318 (2022).
- [31] K. Wan, M. Berta, and E. T. Campbell, Randomized quantum algorithm for statistical phase estimation, *Phys. Rev. Lett.* **129**, 030503 (2022).
- [32] D. An, J.-P. Liu, and L. Lin, Linear combination of Hamiltonian simulation for nonunitary dynamics with optimal state preparation cost, *Phys. Rev. Lett.* **131**, 150603 (2023).

- [33] K. Wada, K. Fukuchi, and N. Yamamoto, Quantum-enhanced mean value estimation via adaptive measurement, *Quantum* **8**, 1463 (2024).
- [34] S. Wang, S. McArdle, and M. Berta, Qubit-efficient randomized quantum algorithms for linear algebra, *PRX quantum* **5** (2024).
- [35] A. Katabarwa, K. Gratsea, A. Caesura, and P. D. Johnson, Early fault-tolerant quantum computing, *PRX quantum* **5** (2024).
- [36] S. Endo, J. Sun, Y. Li, S. C. Benjamin, and X. Yuan, Variational quantum simulation of general processes, *Phys. Rev. Lett.* **125**, 010501 (2020).
- [37] T. Haug and K. Bharti, Generalized quantum assisted simulator, *Quantum Science and Technology* **7**, 045019 (2022).
- [38] Z. Liu, L.-M. Duan, and D.-L. Deng, Solving quantum master equations with deep quantum neural networks, *Phys. Rev. Res.* **4** (2022).
- [39] S. Peng, X. Sun, Q. Zhao, and H. Zhou, Quantum-trajectory-inspired Lindbladian simulation, arXiv preprint arXiv:2408.10505 <https://doi.org/10.48550/arXiv.2408.10505> (2024).
- [40] E. Campbell, Random compiler for fast Hamiltonian simulation, *Phys. Rev. Lett.* **123**, 070503 (2019).
- [41] H. Chen, B. Li, J. Lu, and L. Ying, A randomized method for simulating Lindblad equations and thermal state preparation, arXiv preprint arXiv:2407.06594 <https://doi.org/10.48550/arXiv.2407.06594> (2024).
- [42] C. J. Wood, J. D. Biamonte, and D. G. Cory, Tensor networks and graphical calculus for open quantum systems, arXiv preprint arXiv:1111.6950 <https://doi.org/10.48550/arXiv.1111.6950> (2011).
- [43] E. Nielsen, J. K. Gamble, K. Rudinger, T. Scholten, K. Young, and R. Blume-Kohout, Gate Set Tomography, *Quantum* **5**, 557 (2021).
- [44] Although we can naively decompose G' as an asymmetric Pauli mixture up to the normalization factor $1 + \mathcal{O}(t/r)$, this normalization factor is too large to achieve Eq. (4). $1 + \mathcal{O}(t/r)$ scaling naively provides an upper bound $e^{\|\mathcal{L}\|_{\text{pauli}} t/r}$.
- [45] C. Gardiner and P. Zoller, *Quantum noise: a handbook of Markovian and non-Markovian quantum stochastic methods with applications to quantum optics* (Springer Science & Business Media, 2004).
- [46] B. Baumgartner, An inequality for the trace of matrix products, using absolute values, arXiv preprint arXiv:1106.6189 <https://doi.org/10.48550/arXiv.1106.6189> (2011).
- [47] J. Watrous, Notes on super-operator norms induced by Schatten norms, *Quantum Info. Comput.* **5**, 58–68 (2005).
- [48] A. M. Childs and N. Wiebe, Hamiltonian simulation using linear combinations of unitary operations, arXiv preprint arXiv:1202.5822 <https://doi.org/10.26421/QIC12.11-12> (2012).
- [49] D. W. Berry, A. M. Childs, and R. Kothari, Hamiltonian simulation with nearly optimal dependence on all parameters, in *2015 IEEE 56th annual symposium on foundations of computer science* (IEEE, 2015) pp. 792–809.
- [50] D. W. Berry, A. M. Childs, R. Cleve, R. Kothari, and R. D. Somma, Exponential improvement in precision for simulating sparse Hamiltonians, in *Proceedings of the 46th Annual ACM SIGACT Symposium on Theory of Computing* (2014) pp. 283–292.
- [51] A. Gilyén, Y. Su, G. H. Low, and N. Wiebe, Quantum singular value transformation and beyond: exponential improvements for quantum matrix arithmetics, in *Proceedings of the 51st Annual ACM SIGACT Symposium on Theory of Computing* (2019) pp. 193–204.
- [52] S. Chakraborty, Implementing any linear combination of unitaries on intermediate-term quantum computers, *Quantum* **8**, 1496 (2024).
- [53] N. Suri, J. Barreto, S. Hadfield, N. Wiebe, F. Wudarski, and J. Marshall, Two-unitary decomposition algorithm and open quantum system simulation, *Quantum* **7**, 1002 (2023).
- [54] A. W. Schlimgen, K. Head-Marsden, L. M. Sager, P. Narang, and D. A. Mazziotti, Quantum simulation of the Lindblad equation using a unitary decomposition of operators, *Phys. Rev. Res.* **4**, 023216 (2022).
- [55] J. R. Johansson, P. D. Nation, and F. Nori, QuTiP: An open-source python framework for the dynamics of open quantum systems, *Comput. Phys. Commun.* **183**, 1760 (2012).
- [56] J. R. Johansson, P. D. Nation, and F. Nori, QuTiP 2: A python framework for the dynamics of open quantum systems, *Comput. Phys. Commun.* **184**, 1234 (2013).

Appendix A: Preliminary

1. Notation, norm, and vectorization

Let us consider a finite-dimensional Hilbert space H . We write $\mathsf{L}(\mathsf{H})$ as the set of all linear operators on H , which is also a finite-dimensional Hilbert space with the Hilbert-Schmidt inner product, i.e., $\langle A, B \rangle := \text{Tr}[A^\dagger B]$ for $A, B \in \mathsf{L}(\mathsf{H})$. The Schatten p -norm of an operator $A \in \mathsf{L}(\mathsf{H})$ is defined as

$$\|A\|_p := (\text{Tr} [|A|^p])^{1/p}, \quad |A| := \sqrt{A^\dagger A}, \quad p \in [1, \infty]. \quad (\text{A.1})$$

When $p = \infty$, this norm corresponds to the operator norm of A , denoted by $\|A\|$. In particular, for two operators $A, B \in \mathsf{L}(\mathsf{H})$ and parameters $p, q \in [1, \infty]$ such that $1/p + 1/q = 1$, the Hölder's inequality holds:

$$\|AB\|_1 \leq \|A\|_p \|B\|_q. \quad (\text{A.2})$$

Under the same assumption, the following matrix Hölder's inequality also holds [46]:

$$|\text{Tr} [A^\dagger B]| \leq \|A\|_p \|B\|_q. \quad (\text{A.3})$$

For a given superoperator \mathcal{L} , which is a linear map acting on the space of operators $\mathsf{L}(\mathsf{H})$, we define the induced $1 \rightarrow 1$ norm [47] as

$$\|\mathcal{L}\|_{1 \rightarrow 1} := \sup_{A \in \mathsf{L}(\mathsf{H}), A \neq 0} \frac{\|\mathcal{L}(A)\|_1}{\|A\|_1}. \quad (\text{A.4})$$

It is clear from the definition that $\|\mathcal{L}' \circ \mathcal{L}\|_{1 \rightarrow 1} \leq \|\mathcal{L}'\|_{1 \rightarrow 1} \|\mathcal{L}\|_{1 \rightarrow 1}$ holds for any superoperators \mathcal{L} and \mathcal{L}' . Especially, the $1 \rightarrow 1$ norm of completely positive and trace-preserving (CPTP) maps satisfies the following property.

Lemma 1. *For any CPTP map Φ , $\|\Phi\|_{1 \rightarrow 1} = 1$ holds.*

Proof. As shown in [47], for any CPTP map Φ , the supremum in $\|\Phi\|_{1 \rightarrow 1}$ can be restricted to self-adjoint operators as

$$\|\Phi\|_{1 \rightarrow 1} = \sup_{A \in \mathsf{L}(\mathsf{H}), A=A^\dagger, \|A\|_1=1} \|\Phi(A)\|_1. \quad (\text{A.5})$$

Observing that a self-adjoint A with $\|A\|_1 = 1$ has the spectral decomposition $A = \sum_i \lambda_i |v_i\rangle\langle v_i|$ with $\sum_i |\lambda_i| = 1$, we obtain

$$\|\Phi(A)\|_1 \leq \sum_i |\lambda_i| \|\Phi(|v_i\rangle\langle v_i|)\|_1 \leq \max_i \|\Phi(|v_i\rangle\langle v_i|)\|_1 = \max_i \text{Tr}[\Phi(|v_i\rangle\langle v_i|)] = \max_i \text{Tr} |v_i\rangle\langle v_i| = 1, \quad (\text{A.6})$$

where the first equality follows from the fact that $\Phi(|v_i\rangle\langle v_i|) \geq 0$ due to the positivity of Φ , and the second equality follows from the trace-preserving property of Φ . Especially, $A = |v\rangle\langle v|$ with a unit vector $|v\rangle$ attains $\|\Phi(|v\rangle\langle v|)\|_1 = \text{Tr} |v\rangle\langle v| = 1$ in the same way. Therefore, the proof is completed. \square

To distinguish operators and superoperators, we use the italic font and calligraphic font to denote them, respectively, e.g., A is an operator and \mathcal{L} is a superoperator. When it is clear from the context, we omit the subscript $1 \rightarrow 1$ of the norm $\|\bullet\|_{1 \rightarrow 1}$ for superoperators.

Throughout this work, we use *vectorization* to represent operators in $\mathsf{L}(\mathsf{H})$ as vectors [42]. Specifically, taking an orthonormal basis $\{\sigma_\alpha\}_\alpha$ in the Hilbert space $\mathsf{L}(\mathsf{H})$, the vectorization (with respect to the base $\{\sigma_\alpha\}$) maps any operator $A \in \mathsf{L}(\mathsf{H})$ to a vector $|A\rangle\rangle_\sigma$ as

$$A \mapsto |A\rangle\rangle_\sigma := \sum_\alpha \text{Tr}[\sigma_\alpha^\dagger A] |\alpha\rangle, \quad (\text{A.7})$$

where $|\alpha\rangle$ is an orthonormal basis in a $(\dim \mathsf{H})^2$ dimensional Hilbert space. The inner product of vectorized operators $|A\rangle\rangle_\sigma$ and $|B\rangle\rangle_\sigma$ matches the Hilbert-Schmidt inner product as

$$\langle\langle B | A \rangle\rangle_\sigma = \text{Tr}[B^\dagger A] = \langle B, A \rangle. \quad (\text{A.8})$$

In this formalism, a superoperator \mathcal{E} can be written as a matrix $S(\mathcal{E})$ defined as

$$S(\mathcal{E}) := \sum_{\alpha, \beta} \text{Tr}[\sigma_\alpha^\dagger \mathcal{E}(\sigma_\beta)] |\alpha\rangle \langle \beta|. \quad (\text{A.9})$$

This matrix representation is often called the *transfer matrix* of \mathcal{E} [43]. For instance, the expectation value of an observable O with respect to a quantum state ρ evolved by a superoperator \mathcal{E} can be written as

$$\text{Tr}[O\mathcal{E}(\rho)] = \langle\langle O | S(\mathcal{E}) | \rho \rangle\rangle = \langle\langle O | \mathcal{E}(\rho) \rangle\rangle. \quad (\text{A.10})$$

We often use the fact that for any superoperators Φ and Φ' acting on $L(\mathbb{H})$, $S(\Phi \circ \Phi') = S(\Phi)S(\Phi')$ holds. In particular, we use the map from the orthonormal basis $|i\rangle \langle j|$ in $L(\mathbb{H})$ to $|j\rangle |i\rangle \equiv |j\rangle \otimes |i\rangle$ via vectorization, where $|i\rangle$ is the computational basis of \mathbb{H} . That is, we use the column-stacking convention for vectorization. Then, we can write (omitting the subscript of vectorization)

$$|A\rangle\rangle = \sum_{i,j} \langle i | A | j \rangle |j\rangle |i\rangle = \mathbf{1} \otimes A |\mathbf{1}\rangle\rangle, \quad (\text{A.11})$$

where the vectorization $|\mathbf{1}\rangle\rangle$ of the identity operator $\mathbf{1}$ corresponds to the unnormalized maximally entangled state:

$$|\mathbf{1}\rangle\rangle = \sum_i |i\rangle |i\rangle. \quad (\text{A.12})$$

For a superoperator \mathcal{E} , its transfer matrix $S(\mathcal{E})$ via the column-stacking vectorization is given by

$$S(\mathcal{E}) = \sum_{i,j,k,l} \langle k | \mathcal{E}(|i\rangle \langle j|) |l\rangle |l\rangle \langle j| \otimes |k\rangle \langle i|. \quad (\text{A.13})$$

2. Lindblad equation

In this work, we aim to estimate the physical properties of (finite-dimensional) density matrices $\rho(t)$ whose dynamics is governed by the Lindblad equation or Gorini–Kossakowski–Sudarshan–Lindblad equation [8, 9]:

$$\frac{d}{dt}\rho = \mathcal{L}(\rho) := -i[H, \rho] + \sum_{k=1}^K \left(L_k \rho L_k^\dagger - \frac{1}{2} \{L_k^\dagger L_k, \rho\} \right), \quad (\text{A.14})$$

where H denotes the Hamiltonian of a target system, and $\{L_k\}_{k=1}^K$ are linear operators on the target system. The operators $\{L_k\}$ are called jump operators. The superoperator \mathcal{L} acts on the space of linear operators. In addition, the operation in the last term is an anti-commutator i.e., $\{A, B\} := AB + BA$ for operators A and B . The resulting superoperator $e^{t\mathcal{L}}$ generated by \mathcal{L} is a quantum channel (i.e., CPTP map) for any $t \geq 0$, where

$$e^{t\mathcal{L}} := \sum_{q=0}^{\infty} \frac{t^q \mathcal{L}^q}{q!}. \quad (\text{A.15})$$

The superoperator $\mathcal{L}^q := \mathcal{L} \circ \dots \circ \mathcal{L}$ is defined as q sequential applications of \mathcal{L} . We note that $e^{t\mathcal{L}}$ satisfies the semigroup property: for any $t_1, t_2 \geq 0$,

$$e^{t_2\mathcal{L}} \circ e^{t_1\mathcal{L}} = e^{(t_2+t_1)\mathcal{L}}. \quad (\text{A.16})$$

Using the vectorization Eqs. (A.11) and (A.13), the Lindblad equation can be written as

$$\frac{d}{dt} |\rho\rangle\rangle = G |\rho\rangle\rangle, \quad (\text{A.17})$$

where G is the transfer matrix of the superoperator \mathcal{L} :

$$G := S(\mathcal{L}) = -i\mathbf{1} \otimes H + iH^T \otimes \mathbf{1} + \sum_{k=1}^K \left(\overline{L}_k \otimes L_k - \frac{1}{2}\mathbf{1} \otimes L_k^\dagger L_k - \frac{1}{2}L_k^T \overline{L}_k \otimes \mathbf{1} \right). \quad (\text{A.18})$$

The matrix \overline{L}_k denotes the entrywise complex conjugation of L_k . Note that the solution of Eq. (A.17) for an initial state $|\rho(0)\rangle\rangle$ can be formally written as

$$|\rho(t)\rangle\rangle = e^{tG} |\rho(0)\rangle\rangle, \quad \text{where } e^{tG} = \sum_{q=0}^{\infty} \frac{t^q G^q}{q!} = S(e^{t\mathcal{L}}). \quad (\text{A.19})$$

3. Linear combination of unitaries (LCU) and oblivious amplitude amplification (OAA)

Here we introduce two quantum algorithms: linear combination of unitaries (LCU) [48, 49] and oblivious amplitude amplification (OAA) [50], which take crucial roles in our method.

Let $A := \sum_{i=1}^m c_i U_i$ be a linear combination of unitary operators $\{U_i\}_{i=1}^m$ with complex coefficients $c_i \in \mathbb{C}$. Without loss of generality, we assume $c_i > 0$ because the complex phase can be absorbed into U_i . In order to implement A , we use the following two unitary operations. The first one, called PREPARE, encodes the positive coefficients $\{c_i\}_{i=1}^m$ as

$$\text{PRE} : |\mathbf{0}\rangle \mapsto \sum_{i=1}^m \sqrt{\frac{c_i}{\|c\|_1}} |i\rangle,$$

where $\|c\|_1$ denotes the L^1 -norm of the vector $c = (c_1, \dots, c_m)$, and $|\mathbf{0}\rangle$ and $|i\rangle$ denote an initial state and the computational basis in a $\lceil \log_2 m \rceil$ -qubit ancilla system, respectively. The second one, called SELECT, encodes the unitary operators U_i conditioned by the $\lceil \log_2 m \rceil$ -qubit ancilla system:

$$\text{SEL} = \sum_{i=1}^m |i\rangle\langle i| \otimes U_i.$$

Using the two operations PRE and SEL, we can show that the unitary operator

$$W_A := (\text{PRE}^\dagger \otimes \mathbf{1}) \cdot \text{SEL} \cdot (\text{PRE} \otimes \mathbf{1}) \quad (\text{A.20})$$

implements the target operator $A = \sum_{i=1}^m c_i U_i$ as

$$W_A |\mathbf{0}\rangle |\psi\rangle = \frac{1}{\|c\|_1} |\mathbf{0}\rangle A |\psi\rangle + |\tilde{\perp}_\psi\rangle, \quad (\text{A.21})$$

where $|\psi\rangle$ is an arbitrary system state. $|\tilde{\perp}_\psi\rangle$ denotes an unnormalized state that depends on $|\psi\rangle$ and satisfies $\langle \mathbf{0} | \otimes \mathbf{1} \cdot |\tilde{\perp}_\psi\rangle = 0$.

According to Ref. [23], the above LCU method can be further extended to the implementation of a quantum channel $\mathcal{A}(\bullet) = \sum_k A_k \bullet A_k^\dagger$, where each operator A_k ($k = 0, \dots, K-1$) is given by a linear combination of unitary operators as

$$A_k := \sum_{i=1}^m c_{ki} U_{ki}, \quad c_{ki} > 0. \quad (\text{A.22})$$

Using the LCU method, we can construct a unitary operator $W_k := W_{A_k}$ satisfying Eq. (A.21) for the operator A_k , where the normalization factor $\|c\|_1$ is replaced by $\sum_i c_{ki}$. Now, we introduce an additional ancilla system P, and define the following unitary operator

$$\sum_k |k\rangle \langle k|_{\text{P}} \otimes W_k, \quad (\text{A.23})$$

where $\{|k\rangle_{\text{P}}\}$ denotes the computational basis set on P. Also, we define the unitary operator $U_{\text{R,P}}$ preparing a quantum state $|R\rangle$ on the ancilla system P as

$$U_{\text{R,P}} |0\rangle_{\text{P}} = |R\rangle_{\text{P}} := \frac{1}{\sqrt{\sum_k (\sum_i c_{ki})^2}} \sum_k (\sum_i c_{ki}) |k\rangle_{\text{P}}. \quad (\text{A.24})$$

Using the two operations Eq. (A.23) and $U_{\text{R,P}}$, we can directly confirm that for any input state $|\psi\rangle$,

$$\mathbf{1}_{\text{P}} \otimes \langle \mathbf{0} | \otimes \mathbf{1} \cdot \left(\sum_k |k\rangle \langle k|_{\text{P}} \otimes W_k \right) U_{\text{R,P}} \cdot |0\rangle_{\text{P}} |\mathbf{0}\rangle |\psi\rangle = \frac{1}{\sqrt{\sum_k (\sum_i c_{ki})^2}} \sum_k |k\rangle_{\text{P}} \otimes A_k |\psi\rangle. \quad (\text{A.25})$$

In particular, when $\{A_k\}$ are Kraus operators (i.e., $\sum_k A_k^\dagger A_k = \mathbf{1}$), we can implement the quantum channel $\mathcal{A}(|\psi\rangle \langle \psi|) = \sum_k A_k |\psi\rangle \langle \psi| A_k^\dagger$ by measuring $|\mathbf{0}\rangle$ on the quantum state $|0\rangle_{\text{P}} |\mathbf{0}\rangle |\psi\rangle$ evolved by $U_{\text{R,P}}$ and Eq. (A.23). Note that we can also take the input state as an arbitrary density matrix. The success probability for this implementation of a quantum channel is given by $1/\sum_k (\sum_i c_{ki})^2$.

To amplify the above success probability of the LCU method for a quantum channel, we can use the quantum algorithm called the oblivious amplitude amplification (OAA) for isometries [23, 51], as follows. Let U be a unitary operator, and let $\tilde{\Pi}$ and Π be orthogonal projectors. In addition, we assume that $\tilde{\Pi}U\Pi$ takes the following form:

$$\tilde{\Pi}U\Pi = \sqrt{p}W \quad (\text{A.26})$$

with some $p \in (0, 1)$ and a partial isometry W (meaning that $W^\dagger W$ is a projection). Note that $WW^\dagger W = W$ holds in this case. We focus on the case of $p = 1/4$, which is required in our method as explained later. In this special case, the procedure of OAA is much simpler than the general case as follows. Using two unitary operations $2\Pi - \mathbf{1}$ and $2\tilde{\Pi} - \mathbf{1}$, we have

$$\tilde{\Pi}U(2\Pi - \mathbf{1})U^\dagger(2\tilde{\Pi} - \mathbf{1})U\Pi = 4\sqrt{p}^3 WW^\dagger W - 3\sqrt{p}W = (4\sqrt{p}^3 - 3\sqrt{p})W = -W, \quad (\text{A.27})$$

where we used the property of partial isometry $WW^\dagger W = W$ in the second equality.

To clarify the effect of this amplification, we here give an example. Assuming

$$\frac{1}{\sqrt{\sum_k (\sum_i c_{ki})^2}} \geq \frac{1}{2}, \quad (\text{A.28})$$

we add a single-qubit register to the state on the left side of Eq. (A.25) as

$$R_y |0\rangle \otimes \left(\sum_k |k\rangle \langle k|_{\text{P}} \otimes W_k \right) U_{\text{R,P}} \cdot |0\rangle_{\text{P}} |\psi\rangle = \frac{1}{2} |0\rangle \otimes \left(\sum_k |k\rangle_{\text{P}} \otimes |\mathbf{0}\rangle \otimes A_k |\psi\rangle \right) + |\tilde{\perp}'\rangle \quad (\text{A.29})$$

where R_y is a single-qubit rotation such that $R_y : |0\rangle \mapsto (\sqrt{\sum_k (\sum_i c_{ki})^2/2}) |0\rangle + \sqrt{1 - \sum_k (\sum_i c_{ki})^2/4} |1\rangle$, and $|\tilde{\perp}'\rangle$ is an unnormalized quantum state satisfying $\langle 0| \otimes \langle \mathbf{0}| \cdot |\tilde{\perp}'\rangle = 0$. If we take the following U as the unitary operator in Eq. (A.26):

$$U = R_y \otimes \left(\sum_{k=0}^{K-1} |k\rangle \langle k|_{\text{P}} \otimes W_k \right) U_{\text{R,P}} \quad (\text{A.30})$$

and set (assuming the Kraus operators $\{A_k\}_{k=0}^{K-1}$ in $\{W_k\}$ act on the n -qubit system)

$$\begin{aligned} \tilde{\Pi} &= |0\rangle \langle 0| \otimes \mathbf{1}_{\text{P}} \otimes |\mathbf{0}\rangle \langle \mathbf{0}| \otimes \mathbf{1} = \sum_{k=0}^{K-1} \sum_{\mu=1}^{2^n} |0\rangle \langle 0| \otimes |k\rangle \langle k| \otimes |\mathbf{0}\rangle \langle \mathbf{0}| \otimes |\mu\rangle \langle \mu|, \\ \Pi &= |0\rangle \langle 0| \otimes |0\rangle \langle 0|_{\text{P}} \otimes |\mathbf{0}\rangle \langle \mathbf{0}| \otimes \mathbf{1} = \sum_{\mu=1}^{2^n} |0\rangle \langle 0| \otimes |0\rangle \langle 0|_{\text{P}} \otimes |\mathbf{0}\rangle \langle \mathbf{0}| \otimes |\mu\rangle \langle \mu|, \end{aligned}$$

then $\tilde{\Pi}U\Pi$ takes the form of Eq. (A.26) with $p = 1/4$ and the isometry W defined as

$$W = \sum_{\mu,\nu=1}^{2^n} \sum_{k=0}^{K-1} \langle \mu| A_k |\nu\rangle |0\rangle |k\rangle_{\text{P}} |\mathbf{0}\rangle |\mu\rangle \langle 0| \langle 0|_{\text{P}} \langle \mathbf{0}| \langle \nu|. \quad (\text{A.31})$$

Here, we can directly check that W in Eq. (A.31) satisfies $W^\dagger W = \Pi$ if $\{A_k\}$ are Kraus operators of a quantum channel. Therefore, applying the following unitary sequence involving the unitary operator U in Eq. (A.30)

$$U(2\Pi - \mathbf{1})U^\dagger(2\tilde{\Pi} - \mathbf{1})U, \quad (\text{A.32})$$

to the input state $|0\rangle |0\rangle_{\text{P}} |\mathbf{0}\rangle |\psi\rangle$ for any n -qubit state $|\psi\rangle$, we can *deterministically* obtain the target quantum state

$$\sum_k |k\rangle_{\text{P}} \otimes A_k |\psi\rangle \quad (\text{A.33})$$

by measuring the other qubits in the computational basis. This is because the probability of obtaining the measurement result for $|0\rangle \otimes |\mathbf{0}\rangle$, or equivalently the probability of projection onto $\tilde{\Pi}$, is just 1:

$$\left\| \tilde{\Pi}U(2\Pi - \mathbf{1})U^\dagger(2\tilde{\Pi} - \mathbf{1})U |0\rangle |0\rangle_{\text{P}} |\mathbf{0}\rangle |\psi\rangle \right\|^2 = \|-W |0\rangle |0\rangle_{\text{P}} |\mathbf{0}\rangle |\psi\rangle\|^2 = 1. \quad (\text{A.34})$$

4. Review of randomized LCU for Hamiltonian simulation

In this section, we review a random-sampling implementation of a LCU decomposition for the time propagator e^{-iHt} [31, 52]. First, we provide the decomposition for e^{-iHt} derived in [31], which is one of the key components of the proof of our main theorem. Let $H = \sum_i \alpha_i P_i$ with Pauli strings P_i and real coefficients α_i , and let $\alpha = \sum_i |\alpha_i|$. Splitting the total evolution time t into r segments, we expand each segment $e^{-iHt/r}$ via the Taylor expansion as

$$\begin{aligned} e^{-iHt/r} &= \sum_{n=0}^{\infty} \frac{(-iHt/r)^n}{n!} = \sum_{k=0}^{\infty} \frac{(-iHt/r)^{2k}}{(2k)!} \left(I + \frac{-iHt/r}{2k+1} \right) \\ &= \sum_{k=0}^{\infty} \frac{(-iHt/r)^{2k}}{(2k)!} \sum_i \frac{|\alpha_i|}{\alpha} \left(I - i \frac{\alpha t/r}{2k+1} \text{sgn}(\alpha_i) P_i \right) \\ &= \sum_{k=0}^{\infty} \frac{(-iHt/r)^{2k}}{(2k)!} \sum_i \frac{|\alpha_i|}{\alpha} \sqrt{1 + \left(\frac{\alpha t/r}{2k+1} \right)^2} \exp[-i\theta_k \text{sgn}(\alpha_i) P_i], \end{aligned} \quad (\text{A.35})$$

where $\theta_k = \arccos\left(\left\{1 + \left(\frac{\alpha t/r}{2k+1}\right)^2\right\}^{-1/2}\right)$. At the last equality, we have combined the two Pauli gates I and P_i into a single non-Clifford gate. Note that the controlled version of $e^{-i\theta P}$ for any Pauli string P can be implemented with a single-qubit controlled rotation and multiple Clifford gates (CNOT gates). Furthermore, defining the probability distribution $p_i := |\alpha_i|/\alpha$, we have

$$\begin{aligned} e^{-iHt/r} &= \sum_{k=0}^{\infty} \frac{(-i\alpha t/r)^{2k}}{(2k)!} \sum_i \frac{|\alpha_i|}{\alpha} \sqrt{1 + \left(\frac{\alpha t/r}{2k+1} \right)^2} \left(\frac{H}{\alpha} \right)^{2k} \exp[-i\theta_k \text{sgn}(\alpha_i) P_i] \\ &= \sum_{k=0}^{\infty} \frac{(-i\alpha t/r)^{2k}}{(2k)!} \sqrt{1 + \left(\frac{\alpha t/r}{2k+1} \right)^2} \sum_i p_i \left(\sum_j p_j \text{sgn}(\alpha_j) P_j \right)^{2k} \exp[-i\theta_k \text{sgn}(\alpha_i) P_i]. \end{aligned} \quad (\text{A.36})$$

Thus, we obtain a LCU decomposition of the form $e^{-iHt/r} = \sum_m c_m W_m$, where $c_m > 0$ and W_m are implicitly defined through Eq. (A.36). Moreover, it has been shown that the L^1 -norm of the LCU coefficient $\{c_m\}$ is upper bounded by $e^{(\alpha t/r)^2}$ [31]. This scaling is attributed to the grouping of a linear combination of two Paulis into a single unitary in the final line of Eq. (A.35), which improves the corresponding L^1 norm from $1 + \mathcal{O}(t/r)$ to $\sqrt{1 + \mathcal{O}((t/r)^2)} = 1 + \mathcal{O}((t/r)^2)$. This improvement critically reduces the total L^1 -norm. Therefore, we obtain the LCU decomposition of $e^{-iHt} = (e^{-iHt/r})^r$ that has the total L^1 -norm at most $e^{(\alpha t)^2/r}$, which can be summarized as follows.

Lemma 2 (A slightly modified version of Lemma 2 in Ref. [31]). *Let $H = \sum_j \alpha_j P_j$ be a Hermitian operator that is specified as a linear combination of Pauli operators with $\alpha_j \in \mathbb{R}$. For any $t \in \mathbb{R}$ and $r \in \mathbb{N}$, there exists a linear decomposition*

$$e^{-iHt} = \sum_{k \in \mathcal{S}} b_k U_k$$

for some index set \mathcal{S} , $b_k > 0$, and unitaries U_k , such that

$$\sum_{k \in \mathcal{S}} b_k \leq \exp \left[\left(\sum_i |\alpha_i| \right)^2 \frac{t^2}{r} \right].$$

For all $k \in \mathcal{S}$, the non-Clifford cost of controlled- U_k is that of r controlled single-qubit Pauli rotations.

Now, we briefly summarize key ideas of the randomization for efficient simulation of the LCU decomposition of e^{-iHt} . Let U_i and U_j be independent random unitaries following the distribution $\{p_i = b_i/b\}$ with $b := \sum_{k \in \mathcal{S}} b_k$. Then, the expectation value of an observable O can be estimated with the expectation of the random unitaries with the multiplier b^2 :

$$\text{Tr} \left[O \left(\sum_i b_i U_i \right) \rho \left(\sum_j b_j^\dagger U_j^\dagger \right) \right] = b^2 \sum_{i,j} p_i p_j \text{Tr}(O U_i \rho U_j^\dagger) = b^2 \mathbb{E}_{i,j} \left[\text{Tr}(O U_i \rho U_j^\dagger) \right]$$

Observing the right hand side of the equation, we randomly and independently sample U_i and U_j according to the distribution $\{p_i\}$ and run the generalized Hadamard test circuit (Fig. 3). Then, the sampling mean of the measurement outcomes multiplied by b^2 serves as an estimator of the expectation value of the observable.

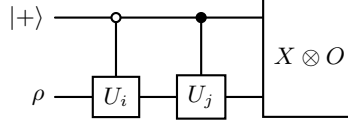


FIG. 3. The circuit for the generalized Hadamard test. U_i and U_j are the unitary operators randomly sampled.

As shown in the previous work [52], by appropriately truncating the Taylor series, this estimation scheme requires $\mathcal{O}(\|O\|^2 b^4 \log(1/\delta)/\varepsilon^2)$ samples of the quantum circuits with the depth at most $\mathcal{O}(\alpha^2 t^2 \log(\alpha t \|O\|/\varepsilon))$, in order to achieve an additive error ε of the final estimation with at least $1 - \delta$ probability, where $\alpha := \sum_i |\alpha_i|$. Remarkably, the circuit depth achieves the logarithmic dependence of ε . The Hamiltonian simulation based on the Taylor series, proposed by [26], also achieves the logarithmic dependence of ε together with a linear dependence on t . However, this algorithm employs LCU and OAA techniques with many additional ancilla qubits and complicated multi-controlled operations. In contrast, the randomized approach uses only one ancilla qubit because it simulates the LCU with the help of random sampling of multiple quantum circuits.

The randomized approach involves a trade-off between the circuit depth and the number of samples. The factor b^2 in the estimator increases the sampling cost because the number of samples scales as $\mathcal{O}(\|O\|^2 b^4 \log(1/\delta)/\varepsilon^2)$. In the Hamiltonian simulation with the truncated Taylor series proposed in Ref. [26], the corresponding L^1 norm of coefficients scales as $e^{\alpha t}$, leading to an exponential increase in the sampling cost when the randomized approach is employed. However, according to Lemma 2, if r is chosen as $r = \mathcal{O}(\alpha^2 t^2)$, the sampling overhead b^2 can be suppressed to $\mathcal{O}(1)$ with respect to α and t .

Appendix B: Decomposition of $e^{t\mathcal{L}}$

In this section, we prove Theorem 1 to derive the decomposition of $e^{t\mathcal{L}}$. Subsection B 1 presents a comprehensive proof, while the essential technical components are described in the subsequent subsections.

- Subsection B 1 provides the proof of Theorem 1. In the proof, we utilize Lemma 5, 8, 10 and the framework described by Proposition 1, 2.
- Subsection B 2 introduces a method to simulate general CP maps. The method allows the exact and efficient simulation for the dissipation. Lemma 3, 4 are the statements for general CP maps, and Lemma 5, 8 are for the special case of our interest.
- Subsection B 3 introduces a general simulation framework for a linear combination of n -qubit superoperators with a form of $\sum c_i U_i \bullet V_i^\dagger$ using $(n+1)$ -qubit quantum circuits. This framework is well summarized in Proposition 1, 2.
- Subsection B 4 shows technical lemmas. In particular, Lemma 10 gives the upper bound of the norm of the decomposition that we derive in Subsection B 1.

1. Proof of Theorem 1

Theorem 1. *Let \mathcal{L} be an n -qubit Lindblad superoperator with a Hamiltonian H and jump operators $\{L_k\}_{k=1}^K$ that are specified by a linear combination of Pauli strings as*

$$H = \sum_{j=1}^m \alpha_{0j} P_{0j}, \quad L_k = \sum_{j=1}^M \alpha_{kj} P_{kj}, \quad (\text{B.1})$$

for some coefficients $\alpha_{0j} \in \mathbb{R}$, $\alpha_{kj} \in \mathbb{C}$. Also, let $\|\mathcal{L}\|_{\text{pauli}} := 2(\alpha_0 + \sum_{k=1}^K \alpha_k^2)$ for $\alpha_k := \sum_j |\alpha_{kj}|$. Then, for any $t > 0$ and any positive integer $r \geq \|\mathcal{L}\|_{\text{pauli}} t$, there exists a linear decomposition

$$e^{t\mathcal{L}}(\bullet) = \sum_{v \in \mathcal{S}} c_v \text{Tr}_{\text{anc}}[(X_{\text{anc}} \otimes \mathbf{1}) \widetilde{\mathcal{W}}_v(|+\rangle \langle +|_{\text{anc}} \otimes \bullet)] \quad (\text{B.2})$$

for some index set \mathcal{S} , real values $c_v > 0$, and $(n+1)$ -qubit completely positive trace non-increasing (CPTN) maps $\{\widetilde{\mathcal{W}}_v\}$ such that

$$\sum_{v \in \mathcal{S}} c_v \leq e^{2\|\mathcal{L}\|_{\text{pauli}}^2 t^2 / r}. \quad (\text{B.3})$$

Furthermore, for any v , the $(n+1)$ -qubit CPTN map $\widetilde{\mathcal{W}}_v$ can be effectively simulated by a quantum circuit on the $(n+1)$ -qubit system and additional $3 + \lceil \log_2 M \rceil$ qubits ancilla system with mid-circuit measurement and qubit reset.

Proof of Theorem 1. This proof consists of two parts: (i) proof of a decomposition of the dynamical map $e^{tG} = S(e^{t\mathcal{L}})$ in the form of a linear combination of (the transfer matrix of) superoperators and (ii) proof of an efficient simulation of the superoperators $\widetilde{\mathcal{W}}_v$ using a generalized Hadamard test circuit on the target n -qubit system and a constant-size ancilla system, which does not require doubling the target system size. In the proof, we employ Lemmas 5, 8, 9, and 10 which are proved in the next subsections. Note that from the assumption, we write H/α_0 and L_k/α_k as

$$\frac{H}{\alpha_0} = \sum_{j=1}^m p_{0j} e^{i\theta_{0j}} P_{0j}, \quad \frac{L_k}{\alpha_k} = \sum_{j=1}^M p_{kj} e^{i\theta_{kj}} P_{kj}, \quad (\text{B.4})$$

where $p_{kj} := |\alpha_{kj}|/\alpha_k$ is a probability distribution satisfying $\sum_j p_{kj} = 1$ for all $k = 0, 1, \dots, K$, and the phases $e^{i\theta_{kj}}$ are defined as

$$e^{i\theta_{kj}} := \frac{\alpha_{kj}}{|\alpha_{kj}|}, \quad \forall k, j. \quad (\text{B.5})$$

As for the case $k = 0$, the phase $e^{i\theta_{0j}}$ is equivalent to $\text{sgn}(\alpha_{0j})$.

Now, we construct a decomposition of $e^{tG} = S(e^{t\mathcal{L}})$. Our intermediate goal is to expand the transfer matrix $e^{tG/r}$ of the r -sliced dynamical map $e^{t\mathcal{L}/r}$ in the form

$$e^{tG/r} = \sum_u c_u S(\mathcal{W}_u) \quad (\text{B.6})$$

for some positive coefficients c_u and some superoperators \mathcal{W}_u acting on the target n -qubit system. In particular, we aim to construct such a decomposition with the coefficients $\{c_u\}$ satisfying

$$\sum_u c_u \leq e^{\mathcal{O}(t^2/r^2)} \quad (\text{B.7})$$

in order that the total weight for r -repetition of this decomposition scales as $e^{\mathcal{O}(t^2/r)}$. To this end, we start by expanding the transfer matrix $e^{tG/r}$ via the Taylor expansion as

$$e^{(t/r)G} = \sum_{q=0}^{\infty} \frac{(t/r)^q G^q}{q!} = \sum_{l=0}^{\infty} \frac{(t/r)^{2l}}{(2l)!} G^{2l} \left(\mathbf{1} \otimes \mathbf{1} + \frac{(t/r)}{2l+1} G \right), \quad (\text{B.8})$$

where $G = S(\mathcal{L})$ can be written as

$$\begin{aligned} G &= -i\mathbf{1} \otimes H + iH^T \otimes \mathbf{1} + \sum_{k=1}^K \left(\overline{L}_k \otimes L_k - \frac{1}{2} \mathbf{1} \otimes L_k^\dagger L_k - \frac{1}{2} L_k^T \overline{L}_k \otimes \mathbf{1} \right) \\ &= \alpha_0 \cdot \mathbf{1} \otimes \frac{-iH}{\alpha_0} + \alpha_0 \cdot \frac{iH^T}{\alpha_0} \otimes \mathbf{1} + \sum_{k=1}^K \alpha_k^2 \cdot \left(\frac{\overline{L}_k}{\alpha_k} \otimes \frac{L_k}{\alpha_k} + \frac{1}{2} \mathbf{1} \otimes \frac{(-1)L_k^\dagger L_k}{\alpha_k^2} + \frac{1}{2} \frac{(-1)L_k^T \overline{L}_k}{\alpha_k^2} \otimes \mathbf{1} \right). \end{aligned} \quad (\text{B.9})$$

In what follows, we decompose G^{2l} and $\mathbf{1} \otimes \mathbf{1} + \frac{(t/r)}{2l+1}G$ in Eq. (B.8) toward the final form (B.33). Firstly, we provide a decomposition of G^{2l} up to normalization. Since H/α_0 and L_k/α_k are the convex combinations of Pauli strings with complex phases as in Eq. (B.4), Lemma 9 says that there is a probability distribution $p_G(\mu)$ over some index set $S_G(\ni \mu)$ and two sets $\{U_G(\mu)\}, \{V_G(\mu)\}$ of n -qubit Pauli strings with complex phases (e.g., $e^{i\theta}P$ for some $\theta \in \mathbb{R}$) such that

$$\frac{G}{\|\mathcal{L}\|_{\text{pauli}}} = \sum_{\mu \in S_G} p_G(\mu) \overline{U_G(\mu)} \otimes V_G(\mu) = S \left(\sum_{\mu \in S_G} p_G(\mu) \cdot V_G(\mu) \bullet U_G^\dagger(\mu) \right). \quad (\text{B.10})$$

Here, $\|\mathcal{L}\|_{\text{pauli}}$ defined by

$$\|\mathcal{L}\|_{\text{pauli}} = 2\alpha_0 + \sum_{k=1}^K \alpha_k^2 \cdot \left(1 + \frac{1}{2} \times 2\right) = 2 \left(\alpha_0 + \sum_{k=1}^K \alpha_k^2 \right) \quad (\text{B.11})$$

is the normalization factor introduced to guarantee $\sum_{\mu} p_G(\mu) = 1$. Note that we can efficiently sample the random unitary $\overline{U_G(\mu)} \otimes V_G(\mu)$ according to the probability distribution $p_G(\mu)$ by Algorithm 2. Also, we note that $G/\|\mathcal{L}\|_{\text{pauli}}$ is the transfer matrix of the convex combination of the superoperators $V_G(\mu) \bullet U_G^\dagger(\mu)$ acting on the target system as

$$V_G(\mu) \bullet U_G^\dagger(\mu) : A \mapsto V_G(\mu) A U_G^\dagger(\mu) \quad (\text{B.12})$$

for any operator A . Thus, we straightforwardly obtain the decomposition of $G^{2l}/\|\mathcal{L}\|_{\text{pauli}}^{2l}$ from Eq. (B.10).

Next, we decompose the term $\mathbf{1} \otimes \mathbf{1} + \frac{(t/r)}{2l+1}G$ in Eq. (B.8) into a linear combination of (the transfer matrix of) superoperators. Defining

$$\alpha := 2 \left(\alpha_0 + \frac{1}{2} \sum_{k=1}^K \alpha_k^2 \right) \quad \text{and} \quad \tau_l := \frac{\alpha(t/r)}{2l+1}, \quad (\text{B.13})$$

we rewrite the term $\mathbf{1} \otimes \mathbf{1} + \frac{(t/r)}{2l+1}G = \mathbf{1} \otimes \mathbf{1} + \tau_l G/\alpha$. To satisfy Eq. (B.3), we derive the decomposition whose normalization scales as $1 + \mathcal{O}(\tau_l^2)$.

$$\begin{aligned} \mathbf{1} \otimes \mathbf{1} + \tau_l \frac{G}{\alpha} &= \frac{\alpha_0}{\alpha} \left(\mathbf{1} \otimes \mathbf{1} + (-i\tau_l) \mathbf{1} \otimes \frac{H}{\alpha_0} \right) + \frac{\alpha_0}{\alpha} \left(\mathbf{1} \otimes \mathbf{1} + (+i\tau_l) \frac{H^\text{T}}{\alpha_0} \otimes \mathbf{1} \right) \\ &\quad + \sum_k \frac{\alpha_k^2}{\alpha} \left(\mathbf{1} \otimes \mathbf{1} + \tau_l \left(\frac{\overline{L_k}}{\alpha_k} \otimes \frac{L_k}{\alpha_k} - \frac{1}{2} \mathbf{1} \otimes \frac{L_k^\dagger L_k}{\alpha_k^2} - \frac{1}{2} \frac{L_k^\text{T} \overline{L_k}}{\alpha_k^2} \otimes \mathbf{1} \right) \right) \\ &= \frac{\alpha_0}{\alpha} \left(\mathbf{1} \otimes \mathbf{1} + (-i\tau_l) \mathbf{1} \otimes \frac{H}{\alpha_0} \right) + \frac{\alpha_0}{\alpha} \left(\mathbf{1} \otimes \mathbf{1} + (+i\tau_l) \frac{H^\text{T}}{\alpha_0} \otimes \mathbf{1} \right) \\ &\quad + \sum_k \frac{\alpha_k^2}{\alpha} \left\{ \left(\mathbf{1} - \frac{\tau_l}{2} \frac{L_k^\dagger L_k}{\alpha_k^2} \right) \otimes \left(\mathbf{1} - \frac{\tau_l}{2} \frac{L_k^\dagger L_k}{\alpha_k^2} \right) + \tau_l \frac{\overline{L_k}}{\alpha_k} \otimes \frac{L_k}{\alpha_k} - \frac{\tau_l^2}{4} \frac{L_k^\text{T} \overline{L_k}}{\alpha_k^2} \otimes \frac{L_k^\dagger L_k}{\alpha_k^2} \right\}. \end{aligned} \quad (\text{B.14})$$

To have further detailed decomposition, we apply different treatments for the first and second terms that come from the Hamiltonian H , and the third term that comes from the jumps $\{L_k\}$. For the first and second terms, we follow the technique developed in Ref. [31] (reviewed in Section A 4), to combine the Pauli operators into a single non-Clifford gate. That is, the first term can be written as

$$\begin{aligned} \mathbf{1} \otimes \mathbf{1} + (-i\tau_l) \mathbf{1} \otimes \frac{H}{\alpha_0} &= \sum_{j=1}^m p_{0j} (\mathbf{1} \otimes \mathbf{1} - i\tau_l e^{i\theta_{0j}} \mathbf{1} \otimes P_{0j}) \\ &= \sqrt{1 + \tau_l^2} \sum_{j=1}^m p_{0j} (\mathbf{1} \otimes \exp[-i\theta_l \text{sgn}(\alpha_{0j}) P_{0j}]) \\ &= \sqrt{1 + \tau_l^2} \cdot S \left(\sum_{j=1}^m p_{0j} \cdot \exp[-i\theta_l \text{sgn}(\alpha_{0j}) P_{0j}] \bullet \mathbf{1} \right), \end{aligned} \quad (\text{B.15})$$

where $\theta_l = \arccos(\{1 + \tau_l^2\}^{-1/2})$. Note that the superoperator $\exp[-i\theta_l \text{sgn}(\alpha_{0j}) P_{0j}] \bullet \mathbf{1}$ acts as

$$A \mapsto \exp[-i\theta_l \text{sgn}(\alpha_{0j}) P_{0j}] A \quad (\text{B.16})$$

for any operator A . Similarly, we can write the second term as

$$\mathbf{1} \otimes \mathbf{1} + (+i\tau_l) \frac{H^\top}{\alpha_0} \otimes \mathbf{1} = \sqrt{1 + \tau_l^2} \cdot S \left(\sum_{j=1}^m p_{0j} \cdot \mathbf{1} \bullet \exp[i\theta_l \text{sgn}(\alpha_{0j}) P_{0j}] \right). \quad (\text{B.17})$$

Note that the scaling of the normalization factor $\sqrt{1 + \tau_l^2} = 1 + \mathcal{O}(\tau_l^2)$ with respect to τ_l is crucial to achieve the goal $\sum_u c_u \leq e^{\mathcal{O}(t^2/r^2)}$ as described later.

Thus, as for the terms where the jumps $\{L_k\}$ appear in Eq. (B.14), we also want to have an expression with overhead $1 + \mathcal{O}(\tau_l^2)$; a naive approach is as follows;

$$\begin{aligned} & \overline{\left(\mathbf{1} - \frac{\tau_l L_k^\dagger L_k}{2 \alpha_k^2} \right)} \otimes \left(\mathbf{1} - \frac{\tau_l L_k^\dagger L_k}{2 \alpha_k^2} \right) + \tau_l \frac{\overline{L_k}}{\alpha_k} \otimes \frac{L_k}{\alpha_k} - \frac{\tau_l^2}{4} \frac{\overline{L_k^\dagger L_k}}{\alpha_k^2} \otimes \frac{L_k^\dagger L_k}{\alpha_k^2} \\ &= \left(1 + \frac{\tau_l^2}{2} \right) \times \left\{ \frac{1 + \tau_l^2/4}{1 + \tau_l^2/2} \cdot S \left(\frac{1}{1 + \tau_l^2/4} \mathcal{B}_{kl} \right) + \frac{\tau_l^2/4}{1 + \tau_l^2/2} \cdot (-1) \cdot S \left(\frac{L_k^\dagger L_k}{\alpha_k^2} \bullet \frac{L_k^\dagger L_k}{\alpha_k^2} \right) \right\}, \end{aligned} \quad (\text{B.18})$$

where the superoperator \mathcal{B}_{kl} is the CP map defined as

$$\begin{aligned} \mathcal{B}_{kl}(\bullet) &:= B_{kl,0} \bullet B_{kl,0}^\dagger + B_{kl,1} \bullet B_{kl,1}^\dagger \\ &\equiv \left(\mathbf{1} - \frac{\tau_l L_k^\dagger L_k}{2 \alpha_k^2} \right) \bullet \left(\mathbf{1} - \frac{\tau_l L_k^\dagger L_k}{2 \alpha_k^2} \right)^\dagger + \sqrt{\tau_l} \frac{L_k}{\alpha_k} \bullet \left(\sqrt{\tau_l} \frac{L_k}{\alpha_k} \right)^\dagger. \end{aligned} \quad (\text{B.19})$$

Here, we defined the operators $B_{kl,0}$ and $B_{kl,1}$ in the equation. A straightforward approach to realize \mathcal{B}_{kl} is to find a CPTN map \mathcal{K} such that $\mathcal{K} + (1 + \tau_l^2/4)^{-1} \mathcal{B}_{kl}$ becomes a CPTP map because the superoperator $(1 + \tau_l^2/4)^{-1} \mathcal{B}_{kl}$ is a CPTN map. We obtain $(1 + \tau_l^2/4)^{-1} \mathcal{B}_{kl}$ by partially measuring a quantum circuit with (possibly a large number of) additional qubits and/or gates, which is in principle possible using, e.g., the Stinespring dilation theorem [53]. However, such a naive approach to simulate $S(\mathcal{B}_{kl})$ is computationally hard in general, especially for finding a companion CPTN map \mathcal{K} .

To overcome this difficulty, we develop a new technique that allows us to exactly simulate the CP map \mathcal{B}_{kl} much easier than the above approach, with the help of random sampling of *correction* superoperators. We summarize this technique in Lemma 5 and Lemma 8, which will be formally proven in the next subsection. Using Lemma 5 and Lemma 8 (note that from the assumption of Theorem 1, we have $\tau_l \in [0, 3]$ for any l), the CP map \mathcal{B}_{kl} can be decomposed as

$$S(\mathcal{B}_{kl}) = S(\mathcal{B}_{kl}^{\text{approx}}) + S(\mathcal{R}_{kl}), \quad (\text{B.20})$$

where \mathcal{R}_{kl} is the correction superoperator with the magnitude of $\mathcal{O}(\tau_l^2)$ whose transfer matrix is given by

$$\begin{aligned} R_{kl} \equiv S(\mathcal{R}_{kl}) &:= \sum_{\lambda=0}^1 \left(\frac{\tau_l^2}{8} \overline{B_{kl,\lambda}} \otimes B_{kl,\lambda} D_k + \frac{\tau_l^2}{8} \overline{B_{kl,\lambda} D_k} \otimes B_{kl,\lambda} - \frac{\tau_l^4}{64} \overline{B_{kl,\lambda} D_k} \otimes B_{kl,\lambda} D_k \right) \\ &= \sum_{\lambda=0}^1 \gamma_{l,\lambda}^2 \left(\frac{\tau_l^2}{8} \frac{\overline{B_{kl,\lambda}}}{\gamma_{l,\lambda}} \otimes \frac{B_{kl,\lambda}}{\gamma_{l,\lambda}} D_k + \frac{\tau_l^2}{8} \frac{\overline{B_{kl,\lambda} D_k}}{\gamma_{l,\lambda}} \otimes \frac{B_{kl,\lambda}}{\gamma_{l,\lambda}} + \frac{\tau_l^4}{64} (-1) \frac{\overline{B_{kl,\lambda} D_k}}{\gamma_{l,\lambda}} \otimes \frac{B_{kl,\lambda} D_k}{\gamma_{l,\lambda}} \right), \end{aligned} \quad (\text{B.21})$$

for $\gamma_{l,\lambda} > 0$ defined as

$$\gamma_{l,0} := 1 + \frac{\tau_l}{2}, \quad \gamma_{l,1} := \sqrt{\tau_l}. \quad (\text{B.22})$$

Also, the CP map $\mathcal{B}_{kl}^{(\text{approx})}$ and the operator D_k are defined as

$$\mathcal{B}_{kl}^{(\text{approx})}(\bullet) := \sum_{\lambda=0,1} B'_{kl,\lambda} \bullet (B'_{kl,\lambda})^\dagger, \quad B'_{kl,\lambda} := B_{kl,\lambda} \left(\mathbf{1} - \frac{\tau_l^2}{8} D_k \right), \quad (\text{B.23})$$

and

$$\frac{\tau_l^2}{4} D_k := B_{kl,0}^\dagger B_{kl,0} + B_{kl,1}^\dagger B_{kl,1} - \mathbf{1} = \frac{\tau_l^2}{4} \frac{(L_k^\dagger L_k)^2}{\alpha_k^4}. \quad (\text{B.24})$$

As described in Lemma 5, we can explicitly construct a quantum circuit with the use of additional $3 + \lceil \log_2 M \rceil$ ancilla qubits that simulates the CP (more precisely, CPTN) map $\mathcal{B}_{kl}^{(\text{approx})}$ by measuring or discarding the ancilla qubits at the end of this circuit; See Remark 1. On the other hand, since $B_{kl,\lambda}/\gamma_{l,\lambda}$ and D_k are the convex combinations of Pauli strings with complex phases, Lemma 8 yields the following decomposition

$$\frac{R_{kl}}{\|R_{kl}\|_{\text{pauli}}} = \sum_{\mu \in S_{R_{kl}}} p_{R_{kl}}(\mu) \overline{U_{R_{kl}}(\mu)} \otimes V_{R_{kl}}(\mu), \quad (\text{B.25})$$

where the normalization factor $\|R_{kl}\|_{\text{pauli}}$ is defined as

$$\|R_{kl}\|_{\text{pauli}} := \sum_{\lambda=0}^1 \gamma_{l,\lambda}^2 \frac{\tau_l^2}{4} \left(1 + \frac{\tau_l^2}{16} \right) = \frac{\tau_l^2}{4} + \frac{\tau_l^3}{2} + \frac{5\tau_l^4}{64} + \frac{\tau_l^5}{32} + \frac{\tau_l^6}{256}. \quad (\text{B.26})$$

Here, $p_{R_{kl}}(\mu)$ is a probability distribution over the index set $S_{R_{kl}}$, and $U_{R_{kl}}(\mu), V_{R_{kl}}(\mu)$ are n -qubit Pauli strings with complex phases for all $\mu \in S_{R_{kl}}$. The random unitary $\overline{U_{R_{kl}}(\mu)} \otimes V_{R_{kl}}(\mu)$ can be efficiently sampled according to the probability distribution $p_{R_{kl}}(\mu)$ by Algorithm 3. Therefore, we now have an algorithm for exactly simulating the CP map \mathcal{B}_{kl} .

Having shown the grouped form of all components in Eq. (B.14), we combine the Eqs. (B.14), (B.15), (B.17), and (B.20) and proceed to derive a new decomposition of $e^{(t/r)G}$. Combining the Eqs. (B.14), (B.15), (B.17), and (B.20), we can write $\mathbf{1} \otimes \mathbf{1} + \tau_l G/\alpha$ as

$$\begin{aligned} \mathbf{1} \otimes \mathbf{1} + \tau_l \frac{G}{\alpha} &= \frac{\alpha_0}{\alpha} \left(\mathbf{1} \otimes \mathbf{1} + (-i\tau_l) \mathbf{1} \otimes \frac{H}{\alpha_0} \right) + \frac{\alpha_0}{\alpha} \left(\mathbf{1} \otimes \mathbf{1} + (+i\tau_l) \frac{H^\text{T}}{\alpha_0} \otimes \mathbf{1} \right) \\ &\quad + \sum_k \frac{\alpha_k^2}{\alpha} \left\{ \left(\mathbf{1} - \frac{\tau_l}{2} \frac{L_k^\dagger L_k}{\alpha_k^2} \right) \otimes \left(\mathbf{1} - \frac{\tau_l}{2} \frac{L_k^\dagger L_k}{\alpha_k^2} \right) + \tau_l \frac{\overline{L_k}}{\alpha_k} \otimes \frac{L_k}{\alpha_k} - \frac{\tau_l^2}{4} \frac{L_k^\text{T} \overline{L_k}}{\alpha_k^2} \otimes \frac{L_k^\dagger L_k}{\alpha_k^2} \right\} \\ &= 2 \frac{\alpha_0}{\alpha} \sqrt{1 + \tau_l^2} \frac{S \left(\sum_{j=1}^m p_{0j} \cdot \exp[-i\theta_l \text{sgn}(\alpha_{0j}) P_{0j}] \bullet \mathbf{1} \right) + S \left(\sum_{j=1}^m p_{0j} \cdot \mathbf{1} \bullet \exp[-i\theta_l \text{sgn}(\alpha_{0j}) P_{0j}] \right)^\dagger}{2} \\ &\quad + \sum_k \frac{\alpha_k^2}{\alpha} \left(S(\mathcal{B}_{kl}) - \frac{\tau_l^2}{4} S \left(\frac{L_k^\dagger L_k}{\alpha_k^2} \bullet \frac{L_k^\dagger L_k}{\alpha_k^2} \right) \right) \\ &= 2 \frac{\alpha_0}{\alpha} \sqrt{1 + \tau_l^2} \frac{S \left(\sum_{j=1}^m p_{0j} \cdot \exp[-i\theta_l \text{sgn}(\alpha_{0j}) P_{0j}] \bullet \mathbf{1} \right) + S \left(\sum_{j=1}^m p_{0j} \cdot \mathbf{1} \bullet \exp[-i\theta_l \text{sgn}(\alpha_{0j}) P_{0j}] \right)^\dagger}{2} \\ &\quad + \sum_k \frac{\alpha_k^2}{\alpha} \left(S(\mathcal{B}_{kl}^{(\text{approx})}) + \|R_{kl}\|_{\text{pauli}} S \left(\frac{\mathcal{R}_{kl}}{\|R_{kl}\|_{\text{pauli}}} \right) + \frac{\tau_l^2}{4} S \left((-1) \frac{L_k^\dagger L_k}{\alpha_k^2} \bullet \frac{L_k^\dagger L_k}{\alpha_k^2} \right) \right) \\ &= \left(2 \frac{\alpha_0}{\alpha} \sqrt{1 + \tau_l^2} + \sum_{k=1}^K \frac{\alpha_k^2}{\alpha} \left(1 + \|R_{kl}\|_{\text{pauli}} + \frac{\tau_l^2}{4} \right) \right) \sum_{k=0}^K \sum_{\nu=1}^3 q_{kl} p_{\Gamma,kl,\nu} \Gamma_{kl,\nu}, \end{aligned} \quad (\text{B.27})$$

where we define the probability distributions $\{q_{kl}\}, \{p_{\Gamma,kl,\nu}\}$ as

$$q_{0l} \propto 2 \frac{\alpha_0}{\alpha} \sqrt{1 + \tau_l^2}, \quad q_{kl} \propto \frac{\alpha_k^2}{\alpha} \left(1 + \|R_{kl}\|_{\text{pauli}} + \frac{\tau_l^2}{4} \right) \quad (\text{for } k = 1, 2, \dots, K), \quad (\text{B.28})$$

and

$$p_{\Gamma,0l,\nu} := \frac{1}{2}(\delta_{1\nu} + \delta_{2\nu}), \quad p_{\Gamma,kl,\nu} := \frac{\delta_{1\nu} + \|R_{kl}\|_{\text{pauli}}\delta_{2\nu} + (\tau_l^2/4)\delta_{3\nu}}{1 + \|R_{kl}\|_{\text{pauli}} + \tau_l^2/4} \quad (\text{for } k = 1, 2, \dots, K). \quad (\text{B.29})$$

The transfer matrix of superoperator, which we denote as $\Gamma_{kl,\nu}$, is given by

$$\Gamma_{0l,1} := S \left(\sum_{j=1}^m p_{0j} \cdot \exp[-i\theta_l \text{sgn}(\alpha_{0j}) P_{0j}] \bullet \mathbf{1} \right), \quad \Gamma_{0l,2} := S \left(\sum_{j=1}^m p_{0j} \cdot \mathbf{1} \bullet \exp[-i\theta_l \text{sgn}(\alpha_{0j}) P_{0j}]^\dagger \right), \quad (\text{B.30})$$

and for $k = 1, 2, \dots, K$,

$$\Gamma_{kl,1} := S(\mathcal{B}_{kl}^{\text{(approx)}}), \quad \Gamma_{kl,2} := S \left(\frac{\mathcal{R}_{kl}}{\|R_{kl}\|_{\text{pauli}}} \right) = S \left(\sum_{\mu \in \mathcal{S}_{R_{kl}}} p_{R_{kl}}(\mu) \cdot V_{R_{kl}}(\mu) \bullet U_{R_{kl}}^\dagger(\mu) \right), \quad (\text{B.31})$$

$$\Gamma_{kl,3} := S \left((-1) \frac{L_k^\dagger L_k}{\alpha_k^2} \bullet \frac{L_k^\dagger L_k}{\alpha_k^2} \right) = S \left(\sum_{j_1, j_2, j_3, j_4=1}^M p_{kj_1} p_{kj_2} p_{kj_3} p_{kj_4} e^{i(-\theta_{kj_1} + \theta_{kj_2} - \theta_{kj_3} + \theta_{kj_4} + \pi)} P_{kj_1} P_{kj_2} \bullet P_{kj_3} P_{kj_4} \right). \quad (\text{B.32})$$

Therefore, we arrive at the following decomposition of the dynamical map $e^{(t/r)G}$:

$$\begin{aligned} e^{(t/r)G} &= \sum_{l=0}^{\infty} \frac{(t/r)^{2l}}{(2l)!} G^{2l} \left(\mathbf{1} \otimes \mathbf{1} + \frac{(t/r)}{2l+1} G \right) \\ &= \sum_{l=0}^{\infty} \frac{(t/r)^{2l} \|\mathcal{L}\|_{\text{pauli}}^{2l}}{(2l)!} \left(\frac{G}{\|\mathcal{L}\|_{\text{pauli}}} \right)^{2l} \left(\mathbf{1} \otimes \mathbf{1} + \frac{(t/r)}{2l+1} G \right) \\ &= \sum_{l=0}^{\infty} \frac{(t/r)^{2l} \|\mathcal{L}\|_{\text{pauli}}^{2l}}{(2l)!} \left(2 \frac{\alpha_0}{\alpha} \sqrt{1 + \tau_l^2} + \sum_{k'=1}^K \frac{\alpha_{k'}^2}{\alpha} \left(1 + \|R_{k'l}\|_{\text{pauli}} + \frac{\tau_l^2}{4} \right) \right) \\ &\quad \times \sum_{k=0}^K \sum_{\nu=1}^3 q_{kl} p_{\Gamma,kl,\nu} \left(\frac{G}{\|\mathcal{L}\|_{\text{pauli}}} \right)^{2l} \Gamma_{kl,\nu}. \end{aligned} \quad (\text{B.33})$$

This means that the transfer matrix of the dynamical map $e^{(t/r)\mathcal{L}}$ can be written in the form of $\sum_u c_u S(\mathcal{W}_u)$ by implicitly defining c_u and $S(\mathcal{W}_u)$ as

$$c_u \rightarrow \frac{(t/r)^{2l} \|\mathcal{L}\|_{\text{pauli}}^{2l}}{(2l)!} \left(2 \frac{\alpha_0}{\alpha} \sqrt{1 + \tau_l^2} + \sum_{k'=1}^K \frac{\alpha_{k'}^2}{\alpha} \left(1 + \|R_{k'l}\|_{\text{pauli}} + \frac{\tau_l^2}{4} \right) \right) q_{kl} p_{\Gamma,kl,\nu} \geq 0, \quad (\text{B.34})$$

$$S(\mathcal{W}_u) \rightarrow \left(\frac{G}{\|\mathcal{L}\|_{\text{pauli}}} \right)^{2l} \Gamma_{kl,\nu}. \quad (\text{B.35})$$

In addition, the sum of $c_u \geq 0$ can be evaluated as

$$\begin{aligned} \sum_u c_u &= \sum_{l=0}^{\infty} \frac{(t/r)^{2l} \|\mathcal{L}\|_{\text{pauli}}^{2l}}{(2l)!} \left(2 \frac{\alpha_0}{\alpha} \sqrt{1 + \tau_l^2} + \sum_{k'=1}^K \frac{\alpha_{k'}^2}{\alpha} \left(1 + \|R_{k'l}\|_{\text{pauli}} + \frac{\tau_l^2}{4} \right) \right) \\ &= \sum_{l=0}^{\infty} \frac{(t/r)^{2l} \|\mathcal{L}\|_{\text{pauli}}^{2l}}{(2l)!} \left(\frac{2\alpha_0}{\alpha} \sqrt{1 + \tau_l^2} + \left(\sum_{k'=1}^K \frac{\alpha_{k'}^2}{\alpha} \right) \left(1 + \frac{\tau_l^2}{2} + \frac{\tau_l^3}{2} + \frac{5\tau_l^4}{64} + \frac{\tau_l^5}{32} + \frac{\tau_l^6}{256} \right) \right) \\ &\leq \sum_{l=0}^{\infty} \frac{(t/r)^{2l} \|\mathcal{L}\|_{\text{pauli}}^{2l}}{(2l)!} \left(1 + \frac{(\tau_l')^2}{2} + \frac{(\tau_l')^3}{2} + \frac{5(\tau_l')^4}{64} + \frac{(\tau_l')^5}{32} + \frac{(\tau_l')^6}{256} \right) \\ &\leq \exp \left(\frac{c \|\mathcal{L}\|_{\text{pauli}}^2 t^2}{r^2} \right) \end{aligned} \quad (\text{B.36})$$

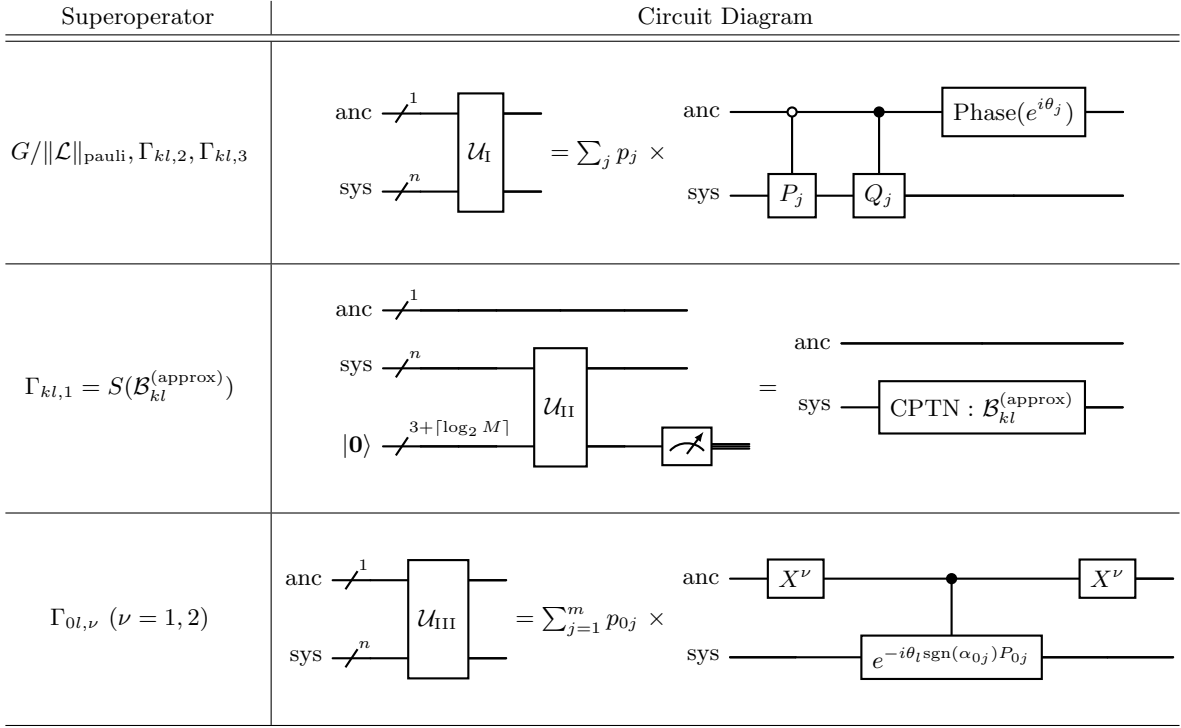


FIG. 4. Quantum circuits for the superoperators in \mathcal{W}_u . The Phase gate is defined as $e^{i\theta_j} |0\rangle\langle 0| + |1\rangle\langle 1|$. The index k runs from 1 to K .

for any constant value $c \geq 1.66$. The first inequality follows from the facts: $\sqrt{1+x^2} \leq 1+x^2/2$ for any $x \geq 0$ and $\tau'_l := \|\mathcal{L}\|_{\text{pauli}}(t/r)/(2l+1) \geq \tau_l$. The final inequality follows from Lemma 10. Using the notation $e^{(t/r)G} = \sum_u c_u S(\mathcal{W}_u)$, we obtain the full decomposition of $e^{tG} = S(e^{t\mathcal{L}})$ as

$$e^{tG} = \left(e^{(t/r)G} \right)^r = \sum_{u_1, \dots, u_r} c_{u_1} \cdots c_{u_r} S(\mathcal{W}_{u_1}) \cdots S(\mathcal{W}_{u_r}). \quad (\text{B.37})$$

The sum of the coefficients $c_{u_1} \cdots c_{u_r}$ satisfies

$$\sum_{u_1, \dots, u_r} c_{u_1} \cdots c_{u_r} = \left(\sum_u c_u \right)^r \leq \exp \left(\frac{c \|\mathcal{L}\|_{\text{pauli}}^2 t^2}{r} \right). \quad (\text{B.38})$$

This completes the proof of Eq. (B.3), where we particularly choose $c = 2 > 1.66$.

Finally, we prove that the transfer matrix form Eq. (B.37) can be reduced to the expression with the $(n+1)$ -qubit CPTN maps as Eq. (B.2). At the same time, this will also reveal a concrete simulation method of the above decomposition (B.37) on quantum circuits without doubling the target system size. The key observation is that for any u , the superoperator \mathcal{W}_u can be simulated by using a generalized Hadamard test. The main components of constructing a quantum circuit for \mathcal{W}_u are the following type-I, II, III circuits illustrated in Fig. 4. We here summarize the properties of the quantum circuits; see Appendix B 3 for more details.

- The type-I circuit \mathcal{U}_I is a mixed unitary channel that has the following action for any linear operator A on the $(n+1)$ -qubit system

$$\mathcal{U}_I : \begin{pmatrix} A_{00} & A_{01} \\ A_{10} & A_{11} \end{pmatrix} \mapsto \begin{pmatrix} * & \Phi(A_{01}) \\ \mathcal{J} \circ \Phi \circ \mathcal{J}(A_{10}) & * \end{pmatrix}, \quad (\text{B.39})$$

where $A_{ij} := (\langle i|_{\text{anc}} \otimes \mathbf{1}) A (|j\rangle_{\text{anc}} \otimes \mathbf{1})$, and \mathcal{J} is the anti-linear map defined as

$$\mathcal{J} : A \mapsto \mathcal{J}(A) := A^\dagger. \quad (\text{B.40})$$

The n -qubit superoperator $S(\Phi)$ becomes $S(\mathcal{L})/\|\mathcal{L}\|_{\text{pauli}}$, $\Gamma_{kl,2}$, $\Gamma_{kl,3}$ by choosing the corresponding probability p_j , complex phase $e^{i\theta_j}$, and n -qubit Pauli strings (P_j, Q_j) according to Eqs. (B.10), (B.25), (B.32), respectively.

- The type-II circuit $\mathcal{I}_{\text{anc}} \otimes \mathcal{U}_{\text{II}}$ effectively simulates the CPTN map $\mathcal{I}_{\text{anc}} \otimes \mathcal{B}_{kl}^{(\text{approx})}$ by measuring (or discarding) the additional ancilla qubits by the computational basis measurement. \mathcal{I}_{anc} denotes the identity channel. The TN property arises from the multiplication of 0 to the final outputs if the measurement result is not all zero. Also, the action of $\mathcal{I}_{\text{anc}} \otimes \mathcal{B}_{kl}^{(\text{approx})}$ can be written as

$$\mathcal{I}_{\text{anc}} \otimes \mathcal{B}_{kl}^{(\text{approx})} : \begin{pmatrix} A_{00} & A_{01} \\ A_{10} & A_{11} \end{pmatrix} \mapsto \begin{pmatrix} * & \mathcal{B}_{kl}^{(\text{approx})}(A_{01}) \\ \mathcal{B}_{kl}^{(\text{approx})}(A_{10}) & * \end{pmatrix}. \quad (\text{B.41})$$

The quantum circuit \mathcal{U}_{II} with the classical post-processing instruction can be constructed by Lemma 5 from the description of \mathcal{B}_{kl} . This circuit needs to introduce an (at most) additional $3 + \lceil \log_2 M \rceil$ qubits for any k, l . After the (mid-circuit) measurement for the additional ancilla qubits, these qubits are reset to the initial state for the next type-II circuit.

- The type-III circuit \mathcal{U}_{III} is a mixed unitary channel that has the following action for any linear operator A on the $(n+1)$ -qubit system

$$\mathcal{U}_{\text{III}} : \begin{pmatrix} A_{00} & A_{01} \\ A_{10} & A_{11} \end{pmatrix} \mapsto \begin{pmatrix} * & \Phi'(A_{01}) \\ \mathcal{J} \circ \Phi' \circ \mathcal{J}(A_{10}) & * \end{pmatrix}, \quad (\text{B.42})$$

where the n -qubit superoperator $S(\Phi')$ becomes $\Gamma_{0l,\nu}$ ($\nu = 1, 2$) by choosing the index $\nu = 1, 2$.

Thus, \mathcal{U}_{I} , \mathcal{U}_{II} , or \mathcal{U}_{III} according to the superoperator $\Gamma_{kl,\nu}$ followed by $2l$ sequential applications of \mathcal{U}_{I} for the superoperator $\mathcal{L}/\|\mathcal{L}\|_{\text{pauli}}$ yields a quantum circuit $\widetilde{\mathcal{W}}_u$ such that

$$\widetilde{\mathcal{W}}_u : \begin{pmatrix} A_{00} & A_{01} \\ A_{10} & A_{11} \end{pmatrix} \mapsto \begin{pmatrix} * & \mathcal{W}_u(A_{01}) \\ \mathcal{J} \circ \mathcal{W}_u \circ \mathcal{J}(A_{10}) & * \end{pmatrix}, \quad (\text{B.43})$$

where we used the facts $\mathcal{J}^2 = \mathcal{I}$ and $\mathcal{J} \circ \mathcal{B}_{kl}^{(\text{approx})} \circ \mathcal{J} = \mathcal{B}_{kl}^{(\text{approx})}$ for any k, l . An example of $\widetilde{\mathcal{W}}_u$ is shown in Fig. 5. This result immediately leads to

$$\widetilde{\mathcal{W}}_{u_1} \circ \cdots \circ \widetilde{\mathcal{W}}_{u_r} : \begin{pmatrix} A_{00} & A_{01} \\ A_{10} & A_{11} \end{pmatrix} \mapsto \begin{pmatrix} * & \mathcal{W}_{u_1} \circ \cdots \circ \mathcal{W}_{u_r}(A_{01}) \\ \mathcal{J} \circ \mathcal{W}_{u_1} \circ \cdots \circ \mathcal{W}_{u_r} \circ \mathcal{J}(A_{10}) & * \end{pmatrix}, \quad (\text{B.44})$$

where we used $\mathcal{J}^2 = \mathcal{I}$ again. Therefore, we obtain

$$\begin{aligned} & \sum_{u_1, u_2, \dots, u_r} c_{u_1} c_{u_2} \cdots c_{u_r} \text{Tr}_{\text{anc}} \left[(X_{\text{anc}} \otimes \mathbf{1}) \widetilde{\mathcal{W}}_{u_1} \circ \cdots \circ \widetilde{\mathcal{W}}_{u_r} (|+\rangle\langle +|_{\text{anc}} \otimes \bullet) \right] \\ &= \sum_{u_1, u_2, \dots, u_r} c_{u_1} c_{u_2} \cdots c_{u_r} \frac{1}{2} \left(\sum_{q=0}^1 \mathcal{J}^q \circ \mathcal{W}_{u_1} \circ \cdots \circ \mathcal{W}_{u_r} \circ \mathcal{J}^q \right) (\bullet) \\ &= \frac{1}{2} \left\{ \sum_{q=0}^1 \sum_{u_1, u_2, \dots, u_r} c_{u_1} c_{u_2} \cdots c_{u_r} \mathcal{J}^q \circ \mathcal{W}_{u_1} \circ \cdots \circ \mathcal{W}_{u_r} \circ \mathcal{J}^q \right\} (\bullet) \\ &= \frac{1}{2} \left\{ \sum_{q=0}^1 \mathcal{J}^q \circ e^{t\mathcal{L}} \circ \mathcal{J}^q \right\} (\bullet) = e^{t\mathcal{L}}(\bullet), \end{aligned} \quad (\text{B.45})$$

where for the final equality we used $\mathcal{J} \circ e^{t\mathcal{L}} \circ \mathcal{J} = e^{t\mathcal{L}}$ due to the Hermitian preserving property of $e^{t\mathcal{L}}$. This completes the proof of Theorem 1. \square

We here remark on the effective simulation of CPTN maps using quantum circuits and classical post-processing.

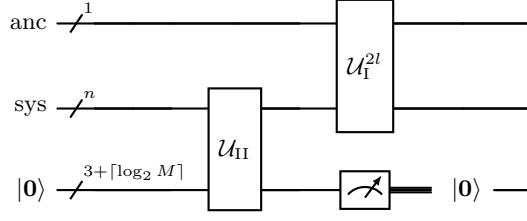
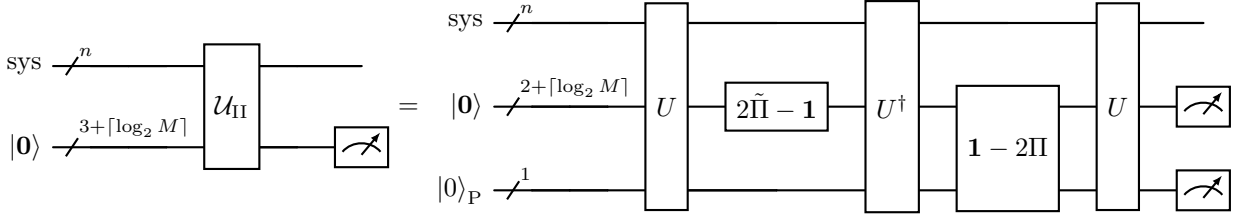


FIG. 5. Quantum circuit $\widetilde{\mathcal{W}}_u$ for $S(\mathcal{W}_u) = \left(\frac{G}{\|\mathcal{L}\|_{\text{pauli}}}\right)^{2l} \Gamma_{kl,\nu}$ when $\Gamma_{kl,\nu} = S(\mathcal{B}_{kl}^{(\text{approx})})$. The $|\mathbf{0}\rangle$ after the measurement denotes the qubit reset operation.

Remark 1 (Effective simulation of CPTN map $\mathcal{B}_{kl}^{(\text{approx})}$). From the Lemma 5, the quantum circuit \mathcal{U}_{II} with measurement for $\mathcal{B}_{kl}^{(\text{approx})}$ has the following form



where $\tilde{\Pi} := \mathbf{1} \otimes |\mathbf{0}\rangle \langle \mathbf{0}| \otimes I_P$, $\Pi := \mathbf{1} \otimes |\mathbf{0}\rangle \langle \mathbf{0}| \otimes |0\rangle \langle 0|_P$, and U is a quantum circuit satisfying

$$\tilde{\Pi}U\Pi = \frac{1}{2} (B_{kl,0} \otimes |\mathbf{0}\rangle \langle \mathbf{0}| \otimes |0\rangle \langle 0|_P + B_{kl,1} \otimes |\mathbf{0}\rangle \langle \mathbf{0}| \otimes |1\rangle \langle 0|_P). \quad (\text{B.46})$$

The final measurement on $3 + \lceil \log_2 M \rceil$ qubits is given by the following two-outcome POVM $\{\Pi_b\}_{b=0,1}$

$$\Pi_0 := \tilde{\Pi}, \quad \Pi_1 := \mathbf{1} - \tilde{\Pi}, \quad (\text{B.47})$$

which can be simulated by the computational basis measurement. Let us consider a general case that we measure an observable O on the target system after the process for $\mathcal{B}_{kl}^{(\text{approx})}$ i.e., \mathcal{U}_{II} followed by the measurement of $\{\Pi_b\}_{b=0,1}$. In a single trial of the whole process, we obtain measurement outcomes (o, b) for the observable O and the POVM $\{\Pi_b\}_{b=0,1}$, respectively. Using the measurement outcomes, we can estimate $\text{Tr}[O\mathcal{B}_{kl}^{(\text{approx})}(\rho)]$ for any input state ρ , in an unbiased manner. That is, the mean of $o\delta_{b0}$ is given by

$$\begin{aligned} \mathbb{E}[o\delta_{b0}] &= \sum_{o,b} o\delta_{b0} \text{Tr} [|o\rangle \langle o| \otimes \mathbf{1} \cdot \Pi_b \cdot \mathcal{U}_{\text{II}}(\rho \otimes |\mathbf{0}\rangle \langle \mathbf{0}|)] \\ &= \sum_o o \text{Tr} \left[|o\rangle \langle o| \text{Tr}_{\text{sys}} \left[\tilde{\Pi} \mathcal{U}_{\text{II}}(\rho \otimes |\mathbf{0}\rangle \langle \mathbf{0}|) \right] \right] \\ &= \text{Tr} \left[O\mathcal{B}_{kl}^{(\text{approx})}(\rho) \right], \end{aligned} \quad (\text{B.48})$$

where Tr_{sys} denotes the partial trace over all the qubits except for the target system, and $\{|o\rangle\}$ are the eigenstates of O . The final equality follows from Eq. (B.57) in the next subsection. In this way, we can effectively simulate CPTN maps, using classical post-processing for final outputs, without an additional increase in estimators' variance.

2. Exact and efficient simulation of general CP maps

In the proof of Theorem 1 in the previous subsection, we employed the CP map \mathcal{B} in the operator form as follows:

$$S(\mathcal{B}) = \overline{B_0} \otimes B_0 + \overline{B_1} \otimes B_1, \quad (\text{B.49})$$

where B_0 and B_1 are defined as, for $\tau > 0$,

$$B_0 = \mathbf{1} - \frac{1}{2} \frac{L^\dagger L}{\alpha^2} \tau, \quad B_1 = \frac{L}{\alpha} \sqrt{\tau}. \quad (\text{B.50})$$

Here, L is a jump operator described by a linear combination of unitaries U_i and coefficients $\alpha_i > 0$:

$$L = \sum_{i=1}^M \alpha_i U_i, \quad \alpha = \sum_{i=1}^M \alpha_i. \quad (\text{B.51})$$

Cleve et al. [23] introduced a quantum algorithm, using LCU for channels and OAA for isometry, to deterministically implement a target CPTP map as we reviewed in Section A.3. In addition, the algorithm is available for a CP map \mathcal{A} without a TP property. Initially, LCU for channels itself can effectively simulate the target CP map exactly up to normalization $p \in [0, 1]$ as $p\mathcal{A}$, by measuring an observable in ancilla qubits (e.g., measuring the observable $\mathbf{1}_P \otimes |\mathbf{0}\rangle\langle\mathbf{0}|$ in Eq. (A.25)). It means that we require the multiplication of $1/p$ to final outputs for compensating the normalization, which leads to classical sampling overhead. To avoid the overhead, OAA is used to increase the normalization factor toward 1. However, it introduces an approximation error between the resulting map $\mathcal{A}^{(\text{approx})}$ and the target map \mathcal{A} , i.e., $\mathcal{A}^{(\text{approx})} \approx \mathcal{A}$, unless \mathcal{A} is a CPTP map. We call this procedure a *standard method* for deterministic implementation of an approximate CP map $\mathcal{A}^{(\text{approx})} \approx \mathcal{A}$.

Now we seek an exact and efficient (i.e. low-overhead) simulation method of the CP map \mathcal{B} to prove Theorem 1. However, the $1/p$ overhead from LCU for channels is too large, and an approximation error by OAA is not acceptable for our case. Here, we first identify the approximated map $\mathcal{B}^{(\text{approx})}$ and its error that is implemented by the standard method. Then, we propose a new method to simulate \mathcal{B} exactly by developing a recovery operation for the approximation error with the help of classical sampling, while benefiting from the overhead reduction by OAA.

Lemma 3 (Exact form of approximated CPTN map by the standard method). *Let B_k be linear operators for $k = 1, \dots, K$, and we assume that each B_k can be written by a linear combination of unitary operators as $B_k := \sum_i c_{ki} U_{ki}$ with $c_{ki} \geq 0$ satisfying $\sum_k (\sum_i c_{ki})^2 \leq 4$. Also, we write $\sum_k B_k^\dagger B_k = \mathbf{1} + \delta D$ for some $\delta > 0$ and a Hermitian operator D with $\|D\|_\infty \leq 1$. Then the standard method, described in Section A.3, for a target map $\mathcal{B} = \sum_k B_k \bullet B_k^\dagger$ yields the CPTN map $\mathcal{B}^{(\text{approx})}$ such that*

$$\mathcal{B}^{(\text{approx})} = \sum_k B'_k \bullet (B'_k)^\dagger, \quad B'_k := B_k \left(\mathbf{1} - \frac{\delta}{2} D \right). \quad (\text{B.52})$$

Furthermore, the exact form of $\mathcal{B}^{(\text{approx})}$ is given by

$$\mathcal{B}^{(\text{approx})} = \mathcal{B} - \mathcal{R}, \quad \mathcal{R} = \sum_k \left(\frac{\delta}{2} B_k \bullet D B_k^\dagger + \frac{\delta}{2} B_k D \bullet B_k^\dagger - \frac{\delta^2}{4} B_k D \bullet D B_k^\dagger \right). \quad (\text{B.53})$$

Proof. We follow the standard method mentioned in Subsection A.3 and carefully evaluate the approximation error. Since B_k are given by linear combinations of unitaries, we can construct unitaries W_k satisfying

$$W_k |\mathbf{0}\rangle |\psi\rangle = \frac{1}{\sum_i c_{ki}} |\mathbf{0}\rangle B_k |\psi\rangle + |\tilde{\perp}_\psi\rangle, \quad (\text{B.54})$$

where $|\mathbf{0}\rangle$ is an initial state on an ancilla system, and $|\tilde{\perp}_\psi\rangle$ denotes an unnormalized state satisfying $\langle\mathbf{0}| \cdot |\tilde{\perp}_\psi\rangle = 0$. Let U , Π , $\tilde{\Pi}$, and W be given in the same manner as in the original OAA procedure described in Subsection A.3;

$$\begin{aligned} U_{\text{R,P}} |\mathbf{0}\rangle_{\text{P}} &= \frac{1}{\sqrt{\sum_k (\sum_i c_{ki})^2}} \sum_k (\sum_i c_{ki}) |k\rangle_{\text{P}}, \quad U = R_y \otimes \left(\sum_k |k\rangle\langle k|_{\text{P}} \otimes W_k \right) U_{\text{R,P}}, \\ \tilde{\Pi} &= |\mathbf{0}\rangle\langle\mathbf{0}| \otimes \mathbf{1}_{\text{P}} \otimes |\mathbf{0}\rangle\langle\mathbf{0}| \otimes \mathbf{1}, \quad \Pi = |\mathbf{0}\rangle\langle\mathbf{0}| \otimes |\mathbf{0}\rangle\langle\mathbf{0}|_{\text{P}} \otimes |\mathbf{0}\rangle\langle\mathbf{0}| \otimes \mathbf{1}, \\ W &= \frac{1}{\sqrt{p}} \tilde{\Pi} U \Pi, \quad p = 1/4. \end{aligned} \quad (\text{B.55})$$

Now we evaluate the error in OAA procedure when W is not a partial isometry. The action of the OAA unitary $V_{\text{OAA}} := U(\mathbf{1} - 2\Pi)U^\dagger(2\tilde{\Pi} - \mathbf{1})U$ satisfies

$$\begin{aligned} \tilde{\Pi} V_{\text{OAA}} \Pi &= -4\sqrt{p}^3 W W^\dagger W + 3\sqrt{p} W = -4\sqrt{p}^3 W \left(\mathbf{1} + \delta \tilde{D} \right) + 3\sqrt{p} W \\ &= W \left(\mathbf{1} - \frac{\delta}{2} \tilde{D} \right), \end{aligned} \quad (\text{B.56})$$

where we used $W^\dagger W = |0\rangle\langle 0| \otimes |0\rangle\langle 0|_{\mathbb{P}} \langle 0|_{\mathbb{P}} \otimes |\mathbf{0}\rangle\langle \mathbf{0}| \otimes (\sum_k B_k^\dagger B_k) = \Pi(\mathbf{1} + \delta\tilde{D})$ with $\tilde{D} := \mathbf{1}_{\text{sys}} \otimes D$. Therefore, the standard method prepares $W(\mathbf{1} - \delta\tilde{D}/2)$, and thus, it yields the CPTN map $\mathcal{B}^{(\text{approx})}$ as

$$\text{Tr}_{\overline{\text{sys}}}[\tilde{\Pi}V_{\text{OAA}}(|0\rangle\langle 0| \otimes |0\rangle\langle 0|_{\mathbb{P}} \otimes |\mathbf{0}\rangle\langle \mathbf{0}| \otimes \bullet)V_{\text{OAA}}^\dagger] = \sum_k B'_k \bullet (B'_k)^\dagger = \mathcal{B}^{(\text{approx})}, \quad (\text{B.57})$$

where $\text{Tr}_{\overline{\text{sys}}}$ denotes the partial trace over all the qubits except for the target system, and

$$B'_k = B_k \left(\mathbf{1} - \frac{\delta}{2} D \right). \quad (\text{B.58})$$

The projection $\tilde{\Pi}$ and the tracing out can be realized by measuring the ancilla qubits except the purifier and the classical post-processing where we multiply the final output by zero whenever the ancilla-measurement result does not coincide with $|0\rangle|\mathbf{0}\rangle$. We remark that this post-processing does not introduce additional cost differently from the post-selection since we purpose to implement a CPTN map.

The difference \mathcal{R} between \mathcal{B} and $\mathcal{B}^{(\text{approx})}$ is determined by the direct calculation as follows:

$$\begin{aligned} \mathcal{R} &= \mathcal{B} - \mathcal{B}^{(\text{approx})} \\ &= \sum_k \left(B_k \bullet B_k^\dagger - B_k \left(\mathbf{1} - \frac{\delta}{2} D \right) \bullet \left(\mathbf{1} - \frac{\delta}{2} D \right) B_k^\dagger \right) \\ &= \sum_k \left(\frac{\delta}{2} B_k \bullet D B_k^\dagger + \frac{\delta}{2} B_k D \bullet B_k^\dagger - \frac{\delta^2}{4} B_k D \bullet D B_k^\dagger \right). \end{aligned} \quad (\text{B.59})$$

□

While the CPTN property of $\mathcal{B}^{(\text{approx})}$ necessarily follows from its construction (B.57), we remark that this CPTN property is tied with the assumption $\sum_k (\sum_i c_{ki})^2 \leq 4$ required for R_y to be well-defined unitary, as shown below. Let us observe that the assumption $\sum_k (\sum_i c_{ki})^2 \leq 4$ implies

$$\|\mathbf{1} + \delta D\|_\infty = \left\| \sum_k B_k^\dagger B_k \right\|_\infty \leq \sum_k \|B_k^\dagger B_k\|_\infty \leq \sum_k \left\| \sum_i c_{ki} U_{ki} \right\|_\infty^2 \leq \sum_k (\sum_i c_{ki} \|U_{ki}\|_\infty)^2 \leq \sum_k (\sum_i c_{ki})^2 \leq 4. \quad (\text{B.60})$$

Then, we have $\mathbf{1} + \delta D \leq \|\mathbf{1} + \delta D\|_\infty \mathbf{1} \leq 4$, which implies $3 - \delta D \geq 0$. Therefore, we have

$$\sum_k B_k^\dagger B'_k = \left(\mathbf{1} - \frac{\delta}{2} D \right) \sum_k B_k^\dagger B_k \left(\mathbf{1} - \frac{\delta}{2} D \right) = \left(\mathbf{1} - \frac{\delta}{2} D \right) (\mathbf{1} + \delta D) \left(\mathbf{1} - \frac{\delta}{2} D \right) = \mathbf{1} - \frac{\delta^2}{4} D^2 (3 - \delta D) \leq \mathbf{1}, \quad (\text{B.61})$$

which is equivalent to the CPTN property.

Although the procedure in Lemma 3 follows the standard method, we additionally obtain the exact representation of CPTN map $\mathcal{B}^{(\text{approx})}$ and approximation-error map \mathcal{R} . This identification opens the way to exactly and efficiently simulate the general CP map \mathcal{B} via constructing $\mathcal{B}^{(\text{approx})}$ by the standard method and compensating its error \mathcal{R} by classical sampling. This technique is one of our key contributions. Furthermore, this error recovery operation can be efficient as shown below.

Lemma 4 (Decomposition of \mathcal{R}). *Let $\{B_k\}$, D , δ , \mathcal{R} be as in Lemma 3. In addition, we assume that D can be described as a linear combination of unitaries form:*

$$D = \sum_i q_i V_i \quad (\text{B.62})$$

with unitaries V_i and $q_i > 0$ satisfying $\sum_i q_i = 1$. Then, \mathcal{R} can be decomposed into a convex combination of superoperators formed as $A_i \bullet B_i^\dagger$ up to a normalization factor C , where A_i and B_i are some unitaries. The normalization factor C is determined as follows

$$C = \frac{1}{p} \left(\delta + \frac{\delta^2}{4} \right) \quad (\text{B.63})$$

where $1/p = \sum_k (\sum_i c_{ki})^2$.

Proof. By defining $b_k = \sum_i c_{ki}$, we obtain

$$\begin{aligned} \mathcal{R} &= \sum_k \left(\frac{\delta}{2} B_k \bullet DB_k^\dagger + \frac{\delta}{2} B_k D \bullet B_k^\dagger - \frac{\delta^2}{4} B_k D \bullet DB_k^\dagger \right) \\ &= C \sum_k \frac{pb_k^2}{\delta + \frac{\delta^2}{4}} \left(\frac{\delta}{2} \frac{B_k}{b_k} \bullet D \frac{B_k^\dagger}{b_k} + \frac{\delta}{2} \frac{B_k}{b_k} D \bullet \frac{B_k^\dagger}{b_k} + \frac{\delta^2}{4} \cdot (-1) \cdot \frac{B_k}{b_k} D \bullet D \frac{B_k^\dagger}{b_k} \right), \end{aligned} \quad (\text{B.64})$$

and $C = \frac{1}{p} \left(\delta + \frac{\delta^2}{4} \right)$. Since B_k/b_k and D are convex combinations of unitaries, we can write the terms in the round bracket as a convex combination of superoperators with an asymmetric form of unitaries. \square

Importantly, the convex combination of superoperators \mathcal{R}/C can be effectively simulated by the random sampling of Hadamard test circuits. The concrete procedure for the simulation is provided in the next subsection. In this method, C corresponds to the sampling overhead to maintain the norm of \mathcal{R} . As a result, we have an exact decomposition of a target CP map \mathcal{B} :

$$\mathcal{B} = (1 + C) \times \left(\frac{1}{1 + C} \mathcal{B}^{(\text{approx})} + \frac{C}{1 + C} \frac{\mathcal{R}}{C} \right). \quad (\text{B.65})$$

The total overhead in this decomposition is given by $1 + C$. C corresponds to the sampling overhead to maintain the norm.

The efficiency of methods depends on p and δ . If we prepare the exact CP map \mathcal{B} by LCU for channels like Eq. (A.25), we have

$$\sqrt{p} \left(\sum_k |k\rangle_{\text{P}} \otimes |\mathbf{0}\rangle \otimes B_k |\psi\rangle \right) + |\perp\rangle \quad (\text{B.66})$$

for any state $|\psi\rangle$. With the same post-processing as OAA, this provides a CPTN map $p\mathcal{B}$. For the rescaling, we need additional sampling overhead $1/p$. By comparing the overheads, we observe that the method with $\mathcal{B}^{(\text{approx})}$ and the recovery operation \mathcal{R} is more efficient than the approach with only the use of the LCU method when δ satisfies

$$\delta \leq 2(-1 + \sqrt{2 - p}). \quad (\text{B.67})$$

The OAA with the recovery operation is available for general CP maps, and this has advantages over encoding by simply applying the LCU for channels when δ is small, i.e., \mathcal{B} is close to a TP map. This inherits the characteristics of OAA. Our target map (B.50) is a good example where this method has a substantial effect.

Now, let us analyze the case in which the map specified by Lindblad-type operators Eqs. (B.50) and (B.51). This example is a fundamental case for Lindblad simulation, with a single jump operator. For the case, we provide a detailed description of the implementation of $\mathcal{B}^{(\text{approx})}$ and calculate the circuit complexity to verify the efficiency. Through the following analysis, we assume the access of a unitary gate W_L such that

$$\langle \langle \mathbf{0} | \otimes \mathbf{1} \rangle \cdot W_L \cdot (|\mathbf{0}\rangle \otimes \mathbf{1}) = \frac{L}{\alpha} \quad (\text{B.68})$$

using a l ancilla qubits with initial state $|\mathbf{0}\rangle$. Such W_L can be prepared with $l = \lceil \log_2(M) \rceil$ ancilla qubits by LCU. We apply Lemma 3 to B_0 and B_1 and obtain the following.

Lemma 5 (CPTN map $\mathcal{B}^{(\text{approx})}$ for $B_0 \bullet B_0^\dagger + B_1 \bullet B_1^\dagger$). *Let L be a linear operator defined by Eq. (B.51), and W_L be a unitary satisfying Eq. (B.68) requiring l ancilla qubits. Let B_0 and B_1 be linear operators defined by Eq. (B.50) with $\tau \in [0, 3]$. Let D be a Hermitian operator defined by*

$$\frac{\tau^2}{4} D := \sum_{k=0}^1 B_k^\dagger B_k - \mathbf{1} = \frac{\tau^2}{4} \frac{(L^\dagger L)^2}{\alpha^4}. \quad (\text{B.69})$$

Defining modified operators $B'_k = B_k \left(\mathbf{1} - \frac{\tau^2}{4} \frac{D}{2} \right)$ for $k = 0, 1$, we can effectively simulate the CPTN map $\mathcal{B}^{(\text{approx})} := \sum_{k=0}^1 B'_k \bullet (B'_k)^\dagger$ with use of a quantum circuit that has the following non-Clifford cost:

- Single-qubit gates: 12,

- *NOT gates controlled by at most $(l + 2)$ qubits: 5,*
- *Unitary gates W_L and its inverse: 3,*
- *Controlled version of W_L and its inverse: 3,*
- *Additional ancilla qubits, excluding the target system qubits: $l + 3$*
- *The computational basis measurements for the $l + 3$ ancilla qubits*

and a classical post-processing for the measurement outcomes.

To prove the Lemma 5, firstly we propose the explicit circuit implementations of W_{B_0} and W_B that satisfy

$$(\langle \mathbf{0} | \otimes \langle \mathbf{0} | \otimes \mathbf{1}) \cdot W_{B_0} \cdot (|0\rangle \otimes |\mathbf{0}\rangle \otimes \mathbf{1}) = \mathbf{1} - \frac{L^\dagger L}{2\alpha^2} \tau, \quad (\text{B.70})$$

$$(\mathbf{1}_P \otimes \langle \mathbf{0} | \otimes \mathbf{1}) \cdot W_B \cdot (|0\rangle_P |\mathbf{0}\rangle |\psi\rangle) = \frac{1}{\sqrt{1+\tau}} \sum_{k=0}^1 |k\rangle_P \otimes B_k |\psi\rangle, \quad (\text{B.71})$$

respectively. Actually, the proposed implementation is more efficient than just preparing $L^\dagger L$.

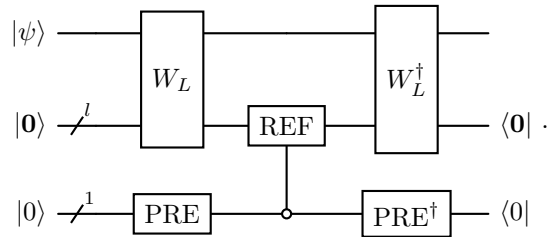
Lemma 6. *Let L be a linear operator defined by Eq. (B.51), and W_L be a unitary satisfying Eq. (B.68) requiring l ancilla qubits. τ denotes a time satisfying $\tau \in [0, 4]$. The unitary W_{B_0} satisfying Eq. (B.70), can be constructed by using*

- *Single-qubit non-Clifford gates: 2,*
- *NOT gates controlled by at most l qubits: 1,*
- *Unitary gate W_L and its inverse: 2,*
- *Additional ancilla qubits, excluding the target system qubits: $l + 1$.*

Proof. Let us define the PREPARE circuit for a single qubit as follows:

$$\text{PRE} : |0\rangle \mapsto \sqrt{\frac{\tau}{4}} |0\rangle + \sqrt{1 - \frac{\tau}{4}} |1\rangle, \quad (\text{B.72})$$

and the reflection REF as $\text{REF} = \mathbf{1} - 2|\mathbf{0}\rangle\langle\mathbf{0}|$, on l ancilla qubits. Then, we consider the following circuit.



With noting that $(\langle \mathbf{0} | \otimes \mathbf{1}) \cdot W_L^\dagger \cdot \text{REF} \cdot W_L \cdot (|\mathbf{0}\rangle \otimes \mathbf{1}) = \mathbf{1} - 2L^\dagger L/\alpha^2$, we obtain

$$\begin{aligned} |\mathbf{0}\rangle |\mathbf{0}\rangle |\psi\rangle &\rightarrow \left(\sqrt{\frac{\tau}{4}} |0\rangle + \sqrt{1 - \frac{\tau}{4}} |1\rangle \right) |\mathbf{0}\rangle |\psi\rangle \\ &\rightarrow \sqrt{\frac{\tau}{4}} |0\rangle \left(\mathbf{1} - 2\frac{L^\dagger L}{\alpha^2} \right) |\psi\rangle + \sqrt{1 - \frac{\tau}{4}} |1\rangle |\psi\rangle \\ &\rightarrow \left(\mathbf{1} - \frac{L^\dagger L}{2\alpha^2} \tau \right) |\psi\rangle \end{aligned} \quad (\text{B.73})$$

for an arbitrary state $|\psi\rangle$. Therefore, the circuit provides the W_{B_0} that requires $l + 1$ -ancilla qubit, and calling W_L and W_L^\dagger once each, and 2 PREPARE circuits. \square

We remark that a straightforward LCU implementation of $L^\dagger L/\alpha^2$ requires at most $\lceil \log_2 M^2 \rceil$ ancilla qubits, whereas our implementation reduces them to $\lceil \log_2 M \rceil + 1$. This indicates that Lemma 6 is a more memory-efficient implementation.

Next we prepare the $W_{\mathcal{B}}$ using the proposed W_{B_0} and W_L .

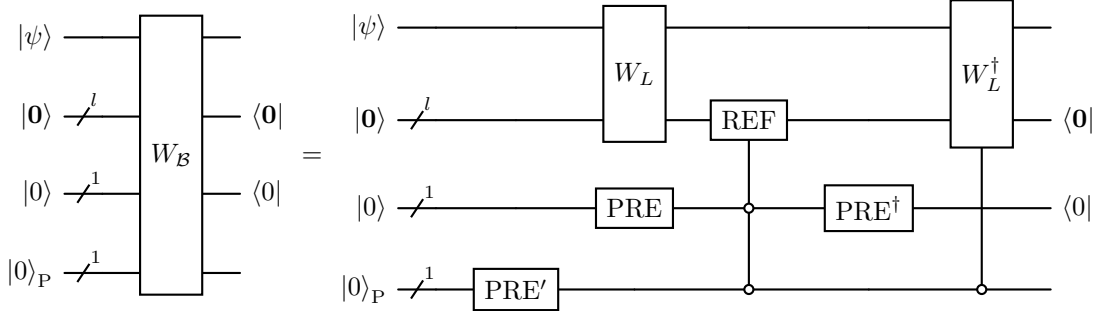
Lemma 7. *Let L be a linear operator defined by Eq. (B.51), and W_L be a unitary satisfying Eq. (B.68) requiring l ancilla qubits. Let B_0 and B_1 be linear operators defined by Eq. (B.50). τ denotes a time satisfying $\tau \in [0, 4]$. The unitary $W_{\mathcal{B}}$ satisfying Eq. (B.71), can be constructed by using*

- Single-qubit non-Clifford gates: 3,
- NOT gates controlled by at most $(l + 1)$ qubits: 1,
- Unitary gate W_L : 1,
- Controlled version of W_L^\dagger : 1,
- Additional ancilla qubits, excluding system qubits: $l + 2$.

Proof. Define another PREPARE circuit on a single qubit for a purifier ancilla P as

$$\text{PRE}' : |0\rangle_{\text{P}} \mapsto \frac{1}{\sqrt{1+\tau}}(|0\rangle_{\text{P}} + \sqrt{\tau}|1\rangle_{\text{P}}). \quad (\text{B.74})$$

Referring to Lemma 6, we design the circuit as:



The circuit can be considered as the controlled application of W_L or W_{B_0} depending on the ancilla's state. Then, we obtain

$$\begin{aligned} |0\rangle_{\text{P}} |0\rangle |0\rangle |\psi\rangle &\rightarrow \frac{1}{\sqrt{1+\tau}}(|0\rangle_{\text{P}} + \sqrt{\tau}|1\rangle_{\text{P}}) |0\rangle |0\rangle |\psi\rangle \\ &\rightarrow \frac{1}{\sqrt{1+\tau}} \left(|0\rangle_{\text{P}} \left(\mathbf{1} - \frac{L^\dagger L}{2\alpha^2} \tau \right) |\psi\rangle + |1\rangle_{\text{P}} \cdot \sqrt{\tau} \frac{L}{\alpha} |\psi\rangle \right). \end{aligned} \quad (\text{B.75})$$

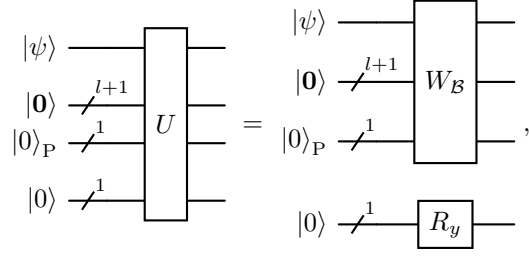
The statement holds by directly counting the gates and qubits of the circuit diagrams above. \square

Now we are ready to prove Lemma 5.

Proof of Lemma 5. Define a rotation gate R_y to maintain the success probability as

$$R_y : |0\rangle \mapsto \frac{\sqrt{1+\tau}}{2} |0\rangle + \sqrt{\frac{3-\tau}{4}} |1\rangle \quad (\text{B.76})$$

for $\tau \in [0, 3]$. Here, $W_{\mathcal{B}}$ can be constructed by the circuit in Lemma 7, and we define $U = (R_y \otimes \mathbf{1})(\mathbf{1} \otimes W_{\mathcal{B}})$ as the circuit:



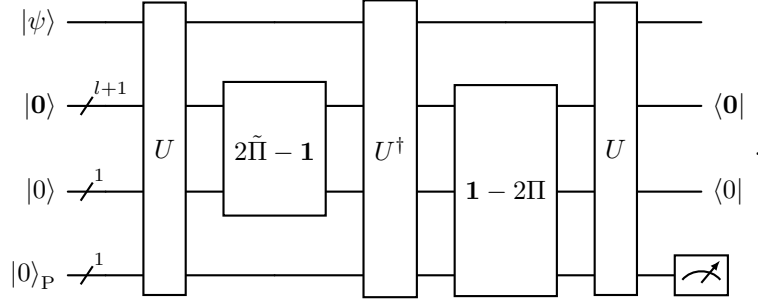
and the projectors as

$$\tilde{\Pi} = |0\rangle\langle 0| \otimes \mathbf{1}_P \otimes |0\rangle\langle 0| \otimes \mathbf{1}, \quad \Pi = |0\rangle\langle 0| \otimes |0\rangle\langle 0|_P \otimes |0\rangle\langle 0| \otimes \mathbf{1}. \quad (\text{B.77})$$

This unitary U satisfies

$$\tilde{\Pi}U\Pi = \frac{1}{2} \sum_{k=0,1} |0\rangle\langle 0| \otimes |k\rangle\langle 0|_P \otimes |0\rangle\langle 0| \otimes B_k. \quad (\text{B.78})$$

The remaining steps follow the procedure of Lemma 3, and then we confirm that the CPTN map $\mathcal{B}^{(\text{approx})} = \sum_{k=0}^1 B'_k \bullet (B'_k)^\dagger$ can be implemented deterministically. The corresponding circuit is depicted as follows:



For the visualization, the bottom two registers are swapped. Note that $2\tilde{\Pi} - \mathbf{1}$ consists of a single NOT gate controlled by at most $(l+1)$ qubits, and $\mathbf{1} - 2\Pi$ consists of a NOT gate controlled by at most $(l+2)$ qubits. From the circuit above and Lemma 7, the number of gates can be directly counted as follows:

- Single-qubit gate: $12 = (3+1) \times 3$
- NOT gate controlled by at most $(l+2)$ qubits: $5 = 3+2$
- Unitary gate W_L and its inverse: 3,
- Controlled version of W_L and its inverse: 3,
- Additional ancilla qubits, excluding system qubits: $l+3$.

All $l+3$ ancilla qubits are measured by the computational basis, and we perform classical post-processing depending on the measurement outcome. That is, partially tracing the purifier register out, we multiply the final output by zero whenever the other $l+2$ ancilla qubits measurement result does not coincide with $|0\rangle|0\rangle$. \square

In the Lindblad case, we can derive a correction superoperator \mathcal{R} immediately.

Lemma 8 (Correction superoperator \mathcal{R} for $B_0 \bullet B_0^\dagger + B_1 \bullet B_1^\dagger$). *Let $L, \{B_k\}, D, \tau$, and $\{B'_k\}$ be as in Lemma 5. Then, the correction superoperator \mathcal{R} , representing the difference between the target CP map $\mathcal{B} := \sum_{k=0}^1 B_k \bullet B_k^\dagger$ and the approximated CPTN map $\mathcal{B}^{(\text{approx})} := \sum_{k=0}^1 B'_k \bullet (B'_k)^\dagger$ effectively simulated by Lemma 5, can be written as*

$$\mathcal{R} := \mathcal{B} - \mathcal{B}^{(\text{approx})} = \sum_{k=0}^1 \left(\frac{\tau^2}{8} B_k \bullet DB_k^\dagger + \frac{\tau^2}{8} B_k D \bullet B_k^\dagger - \frac{\tau^4}{64} B_k D \bullet DB_k^\dagger \right). \quad (\text{B.79})$$

Furthermore, the transfer matrix of \mathcal{R} can be described as a linear combination of unitaries, that is,

$$S(\mathcal{R}) = \sum_i c_i \bar{V}_i \otimes U_i, \quad (\text{B.80})$$

for some unitaries U_i, V_i and $c_i \geq 0$. The sum of coefficients is determined as

$$\sum_i c_i = \frac{1}{4}\tau^2 + \frac{1}{2}\tau^3 + \frac{5}{64}\tau^4 + \frac{1}{32}\tau^5 + \frac{1}{256}\tau^6. \quad (\text{B.81})$$

Also, if L is written as a linear combination of Pauli strings, i.e., $L = \sum_i \alpha_i P_i$ where $\{P_i\}$ are Pauli strings, and $\alpha_i \in \mathbb{C}$, and $\alpha = \sum_i |\alpha_i|$, then $S(\mathcal{R})/(\sum_i c_i)$ is a convex combination of Pauli strings with complex phases.

Proof. From the direct calculation, we obtain

$$\begin{aligned} \mathcal{R} &= \mathcal{B} - \mathcal{B}^{(\text{approx})} \\ &= \sum_{k=0}^1 B_k \bullet B_k^\dagger - B_k \left(\mathbf{1} - \frac{\tau^2 D}{8} \right) \bullet \left(\mathbf{1} - \frac{\tau^2 D}{8} \right) B_k^\dagger \\ &= \sum_{k=0}^1 \left(\frac{\tau^2}{8} B_k \bullet DB_k^\dagger + \frac{\tau^2}{8} B_k D \bullet B_k^\dagger - \frac{\tau^4}{64} B_k D \bullet DB_k^\dagger \right) \end{aligned} \quad (\text{B.82})$$

or,

$$S(\mathcal{R}) = \sum_{k=0}^1 \left(\frac{\tau^2}{8} \overline{B_k D} \otimes B_k + \frac{\tau^2}{8} \overline{B_k} \otimes B_k D - \frac{\tau^4}{64} \overline{B_k D} \otimes B_k D \right). \quad (\text{B.83})$$

Since L/α is a convex combination of unitaries, $B_0/(1 + \tau/2)$ and $B_1/\sqrt{\tau}$ are convex combinations of unitaries, as is D . Then, from the Lemma 9, normalized \mathcal{R} can be written as a linear combination of unitaries. The normalization factor is

$$\begin{aligned} C &= \left(1 + \frac{\tau}{2}\right)^2 \left(\frac{\tau^2}{8} + \frac{\tau^2}{8} + \frac{\tau^4}{64}\right) + \tau \left(\frac{\tau^2}{8} + \frac{\tau^2}{8} + \frac{\tau^4}{64}\right) \\ &= \frac{1}{4}\tau^2 + \frac{1}{2}\tau^3 + \frac{5}{64}\tau^4 + \frac{1}{32}\tau^5 + \frac{1}{256}\tau^6, \end{aligned} \quad (\text{B.84})$$

which is consistent with Lemma 4 where $1/p = (1 + \tau/2)^2 + \tau$ and $\delta = \tau^2/4$. In addition, if L/α is expanded by Pauli strings, B_0, B_1 , and D in \mathcal{R} can be written in Pauli strings. Then we obtain \mathcal{R} as a convex combination of Pauli strings. \square

To conclude the subsection, we discuss the effectiveness of our OAA and recovery operation method in this case. We can prepare the exact map \mathcal{B} using the LCU for channel $W_{\mathcal{B}}$,

$$\sqrt{p} \left(\sum_{k=0}^1 |k\rangle_{\text{P}} \otimes |\mathbf{0}\rangle \otimes B_k |\psi\rangle \right) + |\perp\rangle. \quad (\text{B.85})$$

This provides a CPTN map $p\mathcal{B}$ with normalization factor $1/p = 1 + \tau$ from Eq. (B.71). The overhead for rescaling is equal to $1 + \tau$, and the linear dependence on τ is not suitable for our random compilation purposes. Our new OAA and recovery operation method can also yield the exact CPTN map via

$$\frac{1}{1+C}\mathcal{B} = \frac{1}{1+C}\mathcal{B}^{(\text{approx})} + \frac{C}{1+C}\frac{\mathcal{R}}{C}. \quad (\text{B.86})$$

Therefore, the method requires additional $1 + C = 1 + \mathcal{O}(\tau^2)$ overhead for rescaling. Comparing the overheads, the OAA with the recovery operation improves the overhead from $1 + \tau$ to $1 + \mathcal{O}(\tau^2)$, and the improvement is quadratic with respect to τ . This compression is a crucial fact that leads to our decomposition in Theorem 1. OAA can be regarded as an essential quantum resource usage corresponding to non-Clifford gates in the case of randomized LCU for Hamiltonian simulation (Section A 4).

3. Circuit simulation of superoperators

As we derived in Eq. (B.33), the time propagator $e^{Gt/r}$ can be decomposed into a (rescaled) convex combination of products of four-type superoperators having the following forms: $e^{i\theta\bar{P}} \otimes Q$, $S(\mathcal{B}_{kl}^{(\text{approx})})$, $\mathbf{1} \otimes e^{-i\theta P}$, and $e^{-i\theta\bar{P}} \otimes \mathbf{1}$, where P and Q are some n -qubit Pauli strings. In the previous subsection, we showed explicit circuits for $\mathcal{B}^{(\text{approx})}$. Next, we focus on the construction of the other superoperators, more specifically, an asymmetric superoperator

$$\mathcal{F}_{U,V}(\bullet) := U \bullet V^\dagger, \quad S(\mathcal{F}_{U,V}) = \bar{V} \otimes U \quad (\text{B.87})$$

and its convex combination $\Phi_{p,\mathcal{F}} = \sum_i p_i \mathcal{F}_i$ with $\mathcal{F}_i(\bullet) = U_i \bullet V_i^\dagger$ for some unitaries U, V, U_i , and V_i . In the following, we provide a framework to simulate a linear combination of superoperators (LCS) \mathcal{F}_i using quantum circuits with some additional ancilla system.

The simulation of $\mathcal{F}_{U,V}$ is inspired by Hadamard test circuits. First, by the analogy with the Hadamard test, we consider the following circuit $\tilde{\mathcal{F}}_{U,V}$:

$$\begin{array}{c} |+\rangle \\ \rho \end{array} \begin{array}{c} \boxed{\tilde{\mathcal{F}}_{U,V}} \\ \hline \end{array} \begin{array}{c} |+\rangle \\ \rho \end{array} := \begin{array}{c} |+\rangle \\ \rho \end{array} \begin{array}{c} \text{---} \circ \text{---} \\ \text{---} \boxed{U} \text{---} \boxed{V} \text{---} \end{array} = \frac{1}{2} \begin{pmatrix} & * & \\ \mathcal{J} \circ \mathcal{F}_{U,V} \circ \mathcal{J}(\rho) & & \mathcal{F}_{U,V}(\rho) \\ & * & \end{pmatrix},$$

where \mathcal{J} is an anti-linear map to transform an operator into its complex conjugate, i.e., $\mathcal{J} : A \mapsto \mathcal{J}(A) := A^\dagger$ for any operator A . The circuit provides an encoding of the map $\mathcal{F}_{U,V}$ on $(0, 1)$ -component of the dilated density matrix $(|+\rangle\langle+| \otimes \rho)$ together with the conjugate $\mathcal{J} \circ \mathcal{F}_{U,V} \circ \mathcal{J} = \mathcal{F}_{V,U}$ on $(1, 0)$ -component. Thus, we can use the unitary circuit $\tilde{\mathcal{F}}_{U,V}$ on the $(n+1)$ qubits to simulate the superoperator $\mathcal{F}_{U,V}$ on (a part of) the dilated density matrix. Actually, measuring X, Y on the top 1 qubit, we can effectively simulate the superoperator $\mathcal{F}_{U,V}$ as

$$\text{Tr}_{\text{anc}} \left[(X - iY)_{\text{anc}} \otimes \mathbf{1} \cdot \tilde{\mathcal{F}}_{U,V} (|+\rangle\langle+|_{\text{anc}} \otimes \bullet) \right] = \mathcal{F}_{U,V}(\bullet). \quad (\text{B.88})$$

Note that $\tilde{\mathcal{F}}_{U,V}$ is a unitary channel, even if $\mathcal{F}_{U,V}$ is not a CPTP map. This observation can be generalized as follows.

Proposition 1 (Linear combination of superoperators (LCS)). *Let $\Phi_{c,\mathcal{F}} = \sum_i c_i \mathcal{F}_i$ be n -qubit superoperators with real coefficients $c := \{c_i\}$ and superoperators $\mathcal{F}_i(\bullet) := \mathcal{F}_{U_i, V_i}(\bullet) = U_i \bullet V_i^\dagger$ for some unitaries U_i and V_i . Let $\tilde{\Phi}_{c,\mathcal{F}}$ be a linear combination of unitary channels:*

$$\tilde{\Phi}_{c,\mathcal{F}} := \sum_i c_i \tilde{\mathcal{F}}_i \quad (\text{B.89})$$

for unitary channels $\tilde{\mathcal{F}}_i = \tilde{\mathcal{F}}_{U_i, V_i}$ defined as

$$\tilde{\mathcal{F}}_{U,V}(\bullet) := (|0\rangle\langle 0| \otimes U + |1\rangle\langle 1| \otimes V) \bullet (|0\rangle\langle 0| \otimes U^\dagger + |1\rangle\langle 1| \otimes V^\dagger). \quad (\text{B.90})$$

Then, the action of $\tilde{\Phi}_{c,\mathcal{F}}$ acting on $(n+1)$ qubits can be written with the superoperator $\Phi_{c,\mathcal{F}}$ as

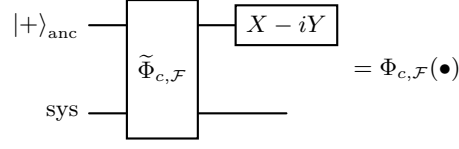
$$\tilde{\Phi}_{c,\mathcal{F}} : \begin{pmatrix} A_{00} & A_{01} \\ A_{10} & A_{11} \end{pmatrix} \mapsto \begin{pmatrix} & * & \Phi_{c,\mathcal{F}}(A_{01}) \\ \mathcal{J} \circ \Phi_{c,\mathcal{F}} \circ \mathcal{J}(A_{10}) & & * \end{pmatrix}, \quad (\text{B.91})$$

where $A_{ij} := (|i\rangle_{\text{anc}} \otimes \mathbf{1}) A (|j\rangle_{\text{anc}} \otimes \mathbf{1})$ and \mathcal{J} is the anti-linear map $\mathcal{J} : A \mapsto A^\dagger$. Furthermore, we can effectively simulate $\Phi_{c,\mathcal{F}}$ using the unitary channels $\{\tilde{\mathcal{F}}_i\}$ by measuring $(X - iY)$ on the ancilla qubit as

$$\text{Tr}_{\text{anc}} \left[(X - iY)_{\text{anc}} \otimes \mathbf{1} \cdot \tilde{\Phi}_{c,\mathcal{F}} (|+\rangle\langle+|_{\text{anc}} \otimes \bullet) \right] = \Phi_{c,\mathcal{F}}(\bullet). \quad (\text{B.92})$$

by the circuit depicted in Fig. 6. If $\Phi_{c,\mathcal{F}}$ is a Hermitian-preserving map, then we can omit the Y measurement as

$$\text{Tr}_{\text{anc}} \left[X_{\text{anc}} \otimes \mathbf{1} \cdot \tilde{\Phi}_{c,\mathcal{F}} (|+\rangle\langle+|_{\text{anc}} \otimes \bullet) \right] = \Phi_{c,\mathcal{F}}(\bullet). \quad (\text{B.93})$$

FIG. 6. A circuit to effectively simulate $\Phi_{c,\mathcal{F}}$

Proof. From the direct calculation, we have

$$\tilde{\mathcal{F}}_{U,V} : \begin{pmatrix} A_{00} & A_{01} \\ A_{10} & A_{11} \end{pmatrix} \mapsto \begin{pmatrix} * & \mathcal{F}_{U,V}(A_{01}) \\ \mathcal{J} \circ \mathcal{F}_{U,V} \circ \mathcal{J}(A_{10}) & * \end{pmatrix} \quad (\text{B.94})$$

for any unitaries U and V . Thus,

$$\begin{aligned} \tilde{\Phi}_{c,\mathcal{F}} \left(\begin{pmatrix} A_{00} & A_{01} \\ A_{10} & A_{11} \end{pmatrix} \right) &= \sum_i c_i \tilde{\mathcal{F}}_i \left(\begin{pmatrix} A_{00} & A_{01} \\ A_{10} & A_{11} \end{pmatrix} \right) \\ &= \begin{pmatrix} * & \sum_i c_i \mathcal{F}_i(A_{01}) \\ \sum_i c_i \mathcal{J} \circ \mathcal{F}_i \circ \mathcal{J}(A_{10}) & * \end{pmatrix} \\ &= \begin{pmatrix} * & \Phi_{c,\mathcal{F}}(A_{01}) \\ \mathcal{J} \circ \Phi_{c,\mathcal{F}} \circ \mathcal{J}(A_{10}) & * \end{pmatrix}. \end{aligned} \quad (\text{B.95})$$

Particularly, for a matrix $|+\rangle\langle+| \otimes \rho$,

$$\tilde{\Phi}_{c,\mathcal{F}}(|+\rangle\langle+| \otimes \rho) = \begin{pmatrix} * & \Phi_{c,\mathcal{F}}(\rho)/2 \\ \mathcal{J} \circ \Phi_{c,\mathcal{F}} \circ \mathcal{J}(\rho)/2 & * \end{pmatrix} \quad (\text{B.96})$$

holds. By measuring $X - iY$ on the ancilla qubit, we obtain

$$\begin{aligned} \text{Tr}_{\text{anc}} \left[((X - iY)_{\text{anc}} \otimes \mathbf{1}) \cdot \tilde{\Phi}_{c,\mathcal{F}}(|+\rangle\langle+|_{\text{anc}} \otimes \rho) \right] &= \frac{1}{2} (\Phi_{c,\mathcal{F}}(\rho) + \mathcal{J} \circ \Phi_{c,\mathcal{F}}(\rho) \circ \mathcal{J} + \Phi_{c,\mathcal{F}}(\rho) - \mathcal{J} \circ \Phi_{c,\mathcal{F}} \circ \mathcal{J}(\rho)) \\ &= \Phi_{c,\mathcal{F}}(\rho). \end{aligned} \quad (\text{B.97})$$

Similarly, if $\Phi_{c,\mathcal{F}}$ is a HP map,

$$\text{Tr}_{\text{anc}} \left[(X_{\text{anc}} \otimes \mathbf{1}) \cdot \tilde{\Phi}_{c,\mathcal{F}}(|+\rangle\langle+|_{\text{anc}} \otimes \rho) \right] = \frac{1}{2} (\Phi_{c,\mathcal{F}}(\rho) + \mathcal{J} \circ \Phi_{c,\mathcal{F}}(\rho) \circ \mathcal{J}) = \Phi_{c,\mathcal{F}}(\rho). \quad (\text{B.98})$$

□

In particular, for a probability distribution $p_i \geq 0$ satisfying $\sum_i p_i = 1$, $\tilde{\Phi}_{p,\mathcal{F}}$ becomes a mixed unitary channel that can be realized on quantum circuits $\{\tilde{\mathcal{F}}_i\}$ with random application of the circuits according to the probability p_i .

Remark 2. Let $\{U_i\}$ and $\{V_i\}$ be n -qubit unitary operators. Define a convex combination of $\mathcal{F}_i(\bullet) := U_i \bullet V_i^\dagger$ as

$$\Phi_{p,\mathcal{F}}(\bullet) = \sum_i p_i \mathcal{F}_i(\bullet) \quad (\text{B.99})$$

with $p_i > 0$ and $\sum_i p_i = 1$. Then, $\Phi_{p,\mathcal{F}}$ can be effectively simulated by the mixed unitary channel

$$\tilde{\Phi}_{p,\mathcal{F}} := \sum_i p_i \tilde{\mathcal{F}}_i \quad (\text{B.100})$$

acting on $(n + 1)$ qubits as

$$\sum_i p_i \tilde{\mathcal{F}}_i : \begin{pmatrix} A_{00} & A_{01} \\ A_{10} & A_{11} \end{pmatrix} \mapsto \begin{pmatrix} * & \Phi_{p,\mathcal{F}}(A_{01}) \\ \mathcal{J} \circ \Phi_{p,\mathcal{F}} \circ \mathcal{J}(A_{10}) & * \end{pmatrix}. \quad (\text{B.101})$$

In the proof of Theorem 1, we consider an alternating sequence of n -qubit superoperators in the form of

$$\mathcal{W} = \mathcal{B}^{(l)} \circ \Phi_{p^{(l)}, \mathcal{F}^{(l)}} \circ \cdots \circ \mathcal{B}^{(1)} \circ \Phi_{p^{(1)}, \mathcal{F}^{(1)}}, \quad (\text{B.102})$$

where $\{\mathcal{B}^{(l)}\}$ are CPTN maps, and $\{\Phi_{p^{(l)}, \mathcal{F}^{(l)}}\}$ are convex combinations of asymmetric forms $\mathcal{F}_i^{(l)} = U_i^{(l)} \bullet V_i^{(l)\dagger}$ for some unitaries $U_i^{(l)}, V_i^{(l)}$. Referring to Eq. (B.102), we define $(n+1)$ -qubit CPTN map $\widetilde{\mathcal{W}}$ for the alternating sequence \mathcal{W} :

$$\widetilde{\mathcal{W}} := \mathcal{I}_{\text{anc}} \otimes \mathcal{B}^{(l)} \circ \widetilde{\Phi}_{p^{(l)}, \mathcal{F}^{(l)}} \circ \cdots \circ \mathcal{I}_{\text{anc}} \otimes \mathcal{B}^{(1)} \circ \widetilde{\Phi}_{p^{(1)}, \mathcal{F}^{(1)}}. \quad (\text{B.103})$$

This can be obtained by simply replacing CPTN maps \mathcal{B} with $\mathcal{I}_{\text{anc}} \otimes \mathcal{B}$ and $\Phi_{p, \mathcal{F}}$ with $\widetilde{\Phi}_{p, \mathcal{F}}$ in \mathcal{W} , respectively. Using $\widetilde{\mathcal{W}}$, we can simulate a convex combination of the superoperators \mathcal{W} , which is a key technique to prove our main Theorem 1.

Proposition 2. For any index u , let \mathcal{W}_u be a sequence in the form of Eq. (B.102), and $\Phi_{p, \mathcal{W}} := \sum_u p_u \mathcal{W}_u$ is a convex combination of \mathcal{W}_u with a probability distribution $\{p_u\}$. In addition, we assume that $\Phi_{p, \mathcal{W}}$ is a Hermitian-preserving map for the probability distribution $\{p_u\}$. Then, defining $\widetilde{\Phi}_{p, \mathcal{W}} := \sum_u p_u \widetilde{\mathcal{W}}_u$, we have

$$\text{Tr}_{\text{anc}} \left[X_{\text{anc}} \otimes \mathbf{1} \cdot \left(\widetilde{\Phi}_{p, \mathcal{W}} \right)^r (|+\rangle\langle +|_{\text{anc}} \otimes \bullet) \right] = \Phi_{p, \mathcal{W}}^r(\bullet) \quad (\text{B.104})$$

for any positive integer r , where the corresponding circuit diagram is shown in Fig. 7. Furthermore, the same map $\Phi_{p, \mathcal{W}}^r$ can be simulated by cutting the wire of the ancilla qubit at each iteration using mid-circuit measurement and qubit reset without additional sampling overheads, as shown in Fig. 8, i.e., the following equation holds:

$$\left(\text{Tr}_{\text{anc}} \left[X_{\text{anc}} \otimes \mathbf{1} \cdot \widetilde{\Phi}_{p, \mathcal{W}} (|+\rangle\langle +|_{\text{anc}} \otimes \bullet) \right] \right)^r = \Phi_{p, \mathcal{W}}^r(\bullet). \quad (\text{B.105})$$

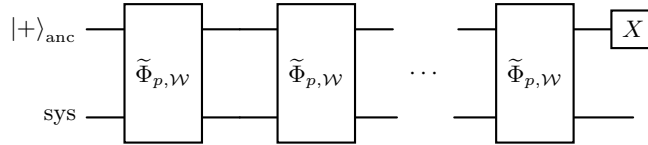


FIG. 7. A circuit to simulate $\Phi_{p, \mathcal{W}}^r$

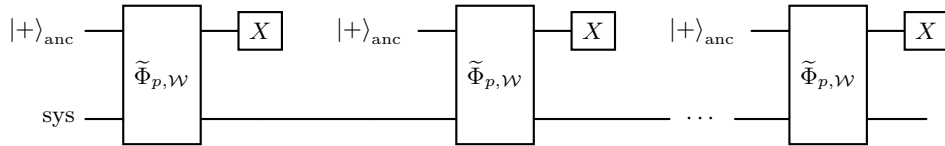


FIG. 8. A circuit to simulate $\Phi_{p, \mathcal{W}}^r$ with mid-circuit measurement and qubit reset

Proof. The action of $\mathcal{I}_{\text{anc}} \otimes \mathcal{B}$ on $(n+1)$ qubits is obviously

$$\mathcal{I}_{\text{anc}} \otimes \mathcal{B} : \begin{pmatrix} A_{00} & A_{01} \\ A_{10} & A_{11} \end{pmatrix} \mapsto \begin{pmatrix} * & \mathcal{B}(A_{01}) \\ \mathcal{B}(A_{10}) & * \end{pmatrix}, \quad (\text{B.106})$$

where $A_{ij} = (\langle i|_{\text{anc}} \otimes \mathbf{1}) A (|j\rangle_{\text{anc}} \otimes \mathbf{1})$. The composition of $\mathcal{I}_{\text{anc}} \otimes \mathcal{B}$ and $\widetilde{\Phi}_{p, \mathcal{F}}$ can simulate $\mathcal{B} \circ \Phi_{p, \mathcal{F}}$, and their sequence

$\widetilde{\mathcal{W}}$ can also simulate \mathcal{W} . This can be described explicitly as

$$\begin{aligned} \widetilde{\mathcal{W}} &: \begin{pmatrix} A_{00} & A_{01} \\ A_{10} & A_{11} \end{pmatrix} \\ &\mapsto \begin{pmatrix} * & \mathcal{B}^{(l)} \circ \Phi_{p^{(l)}, \mathcal{F}^{(l)}} \circ \dots \circ \mathcal{B}^{(1)} \circ \Phi_{p^{(1)}, \mathcal{F}^{(1)}}(A_{10}) \\ \mathcal{B}^{(l)} \circ \mathcal{J} \circ \Phi_{p^{(l)}, \mathcal{F}^{(l)}} \circ \mathcal{J} \circ \dots \circ \mathcal{B}^{(1)} \circ \mathcal{J} \circ \Phi_{p^{(1)}, \mathcal{F}^{(1)}} \mathcal{J}(A_{01}) & * \end{pmatrix} \\ &= \begin{pmatrix} * & \mathcal{W}(A_{01}) \\ \mathcal{J} \circ \mathcal{W} \circ \mathcal{J}(A_{10}) & * \end{pmatrix}. \end{aligned} \quad (\text{B.107})$$

At the last equality, we use the Hermitian-preserving property of CPTN maps $\mathcal{J} \circ \mathcal{B}^{(l)} \circ \mathcal{J} = \mathcal{B}^{(l)}$ and $\mathcal{J}^2 = \mathcal{I}$. From the same calculation as Proposition 1, we obtain the action of convex combination of $\widetilde{\mathcal{W}}$ as

$$\widetilde{\Phi}_{p, \mathcal{W}} : \begin{pmatrix} A_{00} & A_{01} \\ A_{10} & A_{11} \end{pmatrix} \mapsto \begin{pmatrix} * & \Phi_{p, \mathcal{W}}(A_{01}) \\ \mathcal{J} \circ \Phi_{p, \mathcal{W}} \circ \mathcal{J}(A_{10}) & * \end{pmatrix} = \begin{pmatrix} * & \Phi_{p, \mathcal{W}}(A_{01}) \\ \Phi_{p, \mathcal{W}}(A_{10}) & * \end{pmatrix}, \quad (\text{B.108})$$

since $\Phi_{p, \mathcal{W}}$ is assumed to be a Hermitian-preserving map. Finally, after measuring X on the ancilla qubit, we can simulate the map $\Phi_{p, \mathcal{W}}$:

$$\text{Tr}_{\text{anc}} \left[X_{\text{anc}} \otimes \mathbf{1} \cdot \widetilde{\Phi}_{p, \mathcal{W}} (|+\rangle\langle+|_{\text{anc}} \otimes \bullet) \right] = \Phi_{p, \mathcal{W}}(\bullet). \quad (\text{B.109})$$

By repeating the above r times, Eq. (B.105) is shown straightforwardly. Next, considering the action of the $(\widetilde{\Phi}_{p, \mathcal{W}})^r$, we obtain

$$(\widetilde{\Phi}_{p, \mathcal{W}})^r : \begin{pmatrix} A_{00} & A_{01} \\ A_{10} & A_{11} \end{pmatrix} \mapsto \begin{pmatrix} * & (\Phi_{p, \mathcal{W}})^r(A_{01}) \\ (\Phi_{p, \mathcal{W}})^r(A_{10}) & * \end{pmatrix}. \quad (\text{B.110})$$

Therefore, by repeating $\widetilde{\Phi}_{p, \mathcal{W}}$ r times and measuring X , we obtain Eq. (B.104). \square

These Proposition 1 and 2 provide practical procedures to simulate LCS. In practical scenarios, the circuits Fig. 8 with measurements and resets may be more advantageous than the original ones Fig. 7 in the sense of maintaining coherence.

Here we illustrate a simple example to make the formulation clearer. Let us consider the case of randomized LCU for Hamiltonian simulation. Assume that we have the linear combination of unitaries of $e^{-iHt/r} \approx \sum_m c_m U_m$, where U_m are unitaries, and $c_m > 0$. By defining $c = \sum_m c_m$ and joint distribution $p_{m, m'} = c_m c_{m'} / c^2$, the map of the propagator $e^{-iHt/r}$ can be described as

$$e^{-iHt/r} \bullet e^{iHt/r} \approx c^2 \sum_{m, m'} p_{m, m'} U_m \bullet U_{m'}^\dagger \quad (\text{B.111})$$

Using the LCS notations as

$$\begin{aligned} \mathcal{F}_{m, m'} &= U_m \bullet U_{m'}^\dagger \\ \Phi_{p, \mathcal{F}} &= \sum_{m, m'} p_{m, m'} \mathcal{F}_{m, m'}, \end{aligned} \quad (\text{B.112})$$

we obtain the map for the Hamiltonian simulation below:

$$\text{Tr}_{\text{anc}} \left[X_{\text{anc}} \otimes \mathbf{1} \cdot \left(\widetilde{\Phi}_{p, \mathcal{F}} \right)^r (|+\rangle\langle+|_{\text{anc}} \otimes \bullet) \right] \approx \Phi_{p, \mathcal{F}}^r(\bullet) = \frac{1}{c^{2r}} e^{-iHt} \bullet e^{iHt}. \quad (\text{B.113})$$

where we use the HP property of $\Phi_{p, \mathcal{F}}$, that is,

$$\mathcal{J} \circ \Phi_{p, \mathcal{F}} \circ \mathcal{J} = \sum_{m', m} p_{m', m} U_{m'} \bullet U_m^\dagger = \Phi_{p, \mathcal{F}}. \quad (\text{B.114})$$

An asymmetric superoperator $\mathcal{F}_{m, m'}$ alone does not have HP property since $\mathcal{J} \circ \mathcal{F}_{m, m'} \circ \mathcal{J} = \mathcal{F}_{m', m}$, while a symmetrized combination $(\mathcal{F}_{m, m'} + \mathcal{F}_{m', m})/2$ does. Note that this HP property is always satisfied for the superoperators formed as $(\sum_m c_m U_m) \bullet (\sum_m c_m U_m^\dagger)$ with $c_m \in \mathbb{R}$. This example is consistent with the results of prior studies that used Hadamard test such as [52]. The Fig. 9 shows the circuit example. Moreover, we can cut the wire at each simulation step by the HP property as shown in Proposition 2.

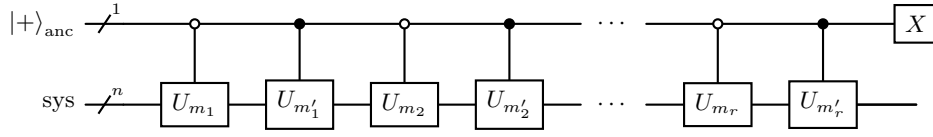


FIG. 9. A circuit example to effectively simulate Hamiltonian dynamics.

4. Technical lemmas

Lemma 9. Let $\{A_k\}$ be convex combinations of unitary operators as

$$A_k := \sum_j p_{kj} U_{kj}. \quad (\text{B.115})$$

Then, $A_1 A_2$ and $A_1 \otimes A_2$ can be written as a convex combination of some unitary operators. Also, for any $\theta_1, \theta_2, \dots \in \mathbb{R}$ and any probability distribution $\{q_k\}_k$, the following operator

$$B := \sum_k q_k e^{i\theta_k} A_k = q_1 e^{i\theta_1} A_1 + q_2 e^{i\theta_2} A_2 + \dots \quad (\text{B.116})$$

can be written as a convex combination of some unitary operators. In addition, if all of $\{U_{kj}\}$ in A_k are Pauli operators with unit complex coefficients (i.e., $e^{i\theta}$ for some $\theta \in \mathbb{R}$), then the operator $A_1 A_2$, $A_1 \otimes A_2$, and B defined above can be written as a convex combination of Pauli operators with unit complex coefficients.

Proof. We can prove this lemma by direct calculations. □

Since Eq. (B.33) already provides the explicit decomposition of $e^{(t/r)G}$, we here derive an inequality to evaluate the sum of coefficients in the decomposition.

Lemma 10. For any constant value $c \geq 1.66$,

$$\sum_{n=0}^{\infty} \frac{x^{2n}}{(2n)!} \gamma\left(\frac{x}{2n+1}\right) \leq \exp(cx^2) \quad (\text{B.117})$$

holds for any $x \in [0, 1]$, where $\gamma(t)$ ($t \in \mathbb{R}$) is defined as

$$\gamma(t) = 1 + \frac{1}{2}t^2 + \frac{1}{2}t^3 + \frac{5}{64}t^4 + \frac{1}{32}t^5 + \frac{1}{256}t^6. \quad (\text{B.118})$$

Proof. It suffices to show

$$\sum_{n=0}^{\infty} \frac{x^{2n}}{(2n)!} \gamma\left(\frac{x}{2n+1}\right) \leq \sum_{n=0}^{\infty} \frac{c^n x^{2n}}{n!}. \quad (\text{B.119})$$

We divide the series into two parts: $n = 0, 1$ and $n \geq 2$. For $n = 0, 1$, we find a constant value c such that

$$\sum_{n=0}^1 \frac{x^{2n}}{(2n)!} \gamma\left(\frac{x}{2n+1}\right) = \gamma(x) + \frac{x^2}{2!} \gamma\left(\frac{x}{3}\right) \leq 1 + cx^2 \quad (\text{B.120})$$

holds for any $x \in [0, 1]$ or equivalently,

$$c \geq \tilde{\gamma}(x) := \left(\frac{1}{2} + \frac{1}{2}x + \frac{5}{64}x^2 + \frac{1}{32}x^3 + \frac{1}{256}x^4\right) + \frac{1}{2!} \gamma\left(\frac{x}{3}\right) \quad (\text{B.121})$$

holds for any $x \in (0, 1]$. Thus, we can take $c \geq 1.66 > \tilde{\gamma}(1)$ for the inequality:

$$\sum_{n=0}^1 \frac{x^{2n}}{(2n)!} \gamma\left(\frac{x}{2n+1}\right) \leq \sum_{n=0}^1 \frac{c^n x^{2n}}{n!}. \quad (\text{B.122})$$

For all $n \geq 2$, $\gamma\left(\frac{x}{2n+1}\right) \leq \gamma(1/5) < 2$ holds under $0 \leq x \leq 1$, and then we have

$$\frac{x^{2n}}{(2n)!} \gamma\left(\frac{x}{2n+1}\right) < x^{2n} \frac{2}{(2n)!} \leq \frac{x^{2n}}{n!}. \quad (\text{B.123})$$

Therefore, if we choose $c \geq 1.66$, the Lemma holds. \square

Appendix C: Proposed method for expectation value estimation

In this section, we first show a truncated version of the decomposition of $e^{t\mathcal{L}}$ in Theorem 1. Then, we prove Theorem 2 for clarifying the performance of our algorithm for expectation values, using the truncated decomposition of $e^{t\mathcal{L}}$.

In Theorem 1, the index set S in the decomposition of $e^{t\mathcal{L}}$ has an infinitely large number of elements. However, for any desired truncation error $\Delta \in (0, 1/e)$, we can construct a finite subset $S_\Delta \subset S$ satisfying the following properties: (i) we can efficiently sample quantum circuits for CPTN maps $\widetilde{\mathcal{W}}_v$ according to the probability distribution proportional to $\{c_v\}_{v \in S_\Delta}$, and furthermore, (ii) the sampled quantum circuits have a logarithmic depth with respect to the truncation error Δ .

Lemma 11 (Truncated version of Theorem 1). *Let \mathcal{L} be an n -qubit Lindblad superoperator with a Hamiltonian H and jump operators $\{L_k\}_{k=1}^K$ that are specified by a linear combination of Pauli strings as*

$$H = \sum_{j=1}^m \alpha_{0j} P_{0j}, \quad L_k = \sum_{j=1}^M \alpha_{kj} P_{kj},$$

for some coefficients $\alpha_{0j} \in \mathbb{R}$, $\alpha_{kj} \in \mathbb{C}$, and let $\|\mathcal{L}\|_{\text{pauli}} := 2(\alpha_0 + \sum_{k=1}^K \alpha_k^2)$ for $\alpha_k := \sum_j |\alpha_{kj}|$. Then, for any $t > 0$, $\Delta \in (0, 1/e)$, and any positive integer $r \geq \|\mathcal{L}\|_{\text{pauli}} t$, there exists an approximate decomposition of $e^{t\mathcal{L}}$ such that

$$\left\| e^{t\mathcal{L}}(\bullet) - \sum_{v \in S_\Delta} c_v \text{Tr}_{\text{anc}}[(X_{\text{anc}} \otimes \mathbf{1}) \widetilde{\mathcal{W}}_v(|+\rangle \langle +|_{\text{anc}} \otimes \bullet)] \right\|_{1 \rightarrow 1} \leq \Delta \quad (\text{C.1})$$

holds for some finite index set S_Δ , $(n+1)$ -qubit completely positive trace non-increasing (CPTN) maps $\{\widetilde{\mathcal{W}}_v\}$, and real values $c_v > 0$ satisfying

$$\sum_{v \in S_\Delta} c_v \leq e^{2\|\mathcal{L}\|_{\text{pauli}}^2 t^2 / r}. \quad (\text{C.2})$$

Furthermore, for any $v \in S_\Delta$, the $(n+1)$ -qubit CPTN map $\widetilde{\mathcal{W}}_v$ can be effectively simulated by using an

$$n + 4 + \lceil \log_2 M \rceil$$

qubits quantum circuit, including mid-circuit measurement and qubit reset, with at most

$$\mathcal{O}\left(r \frac{\log(r/\Delta)}{\log \log(r/\Delta)}\right) \quad (\text{C.3})$$

circuit depth. The corresponding quantum circuits for the CPTN maps $\widetilde{\mathcal{W}}_v$ can be efficiently sampled according to the probability distribution proportional to $c_v > 0$ by Algorithm 1.

Proof of Lemma 11. For a non-negative integer $Q \geq 0$, let $\Lambda_{2Q+1, t/r}$ be a superoperator defined as

$$\Lambda_{2Q+1, t/r} := \sum_{q=0}^{2Q+1} \frac{(t/r)^q \mathcal{L}^q}{q!}. \quad (\text{C.4})$$

This is a truncated series of Eq. (B.8). Thus, using the results in the proof of Theorem 1, we obtain

$$\begin{aligned} S(\Lambda_{2Q+1,t/r}) &= \sum_{l=0}^Q \frac{(t/r)^{2l}}{(2l)!} S(\mathcal{L})^{2l} \left(\mathbf{1} \otimes \mathbf{1} + \frac{(t/r)}{2l+1} S(\mathcal{L}) \right) \\ &= \sum_{l=0}^Q \frac{(t/r)^{2l} \|\mathcal{L}\|_{\text{pauli}}^{2l}}{(2l)!} \left(2 \frac{\alpha_0}{\alpha} \sqrt{1 + \tau_l^2} + \sum_{k=1}^K \frac{\alpha_k^2}{\alpha} \left(1 + \|R_{kl}\|_{\text{pauli}} + \frac{\tau_l^2}{4} \right) \right) \times \sum_{k=0}^K \sum_{\nu=1}^3 q_{kl} P_{\Gamma,kl,\nu} \left(\frac{S(\mathcal{L})}{\|\mathcal{L}\|_{\text{pauli}}} \right)^{2l} \Gamma_{kl,\nu}, \end{aligned} \quad (\text{C.5})$$

where we used the same notation as in the proof of Theorem 1. For simplicity, we write the decomposition as $S(\Lambda_{2Q+1,t/r}) = \sum_{u \in \tilde{\mathcal{S}}_Q} c_u S(\mathcal{W}_u)$ by implicitly defining $c_u \geq 0$, $S(\mathcal{W}_u)$, and a finite index set $\tilde{\mathcal{S}}_Q$. In particular, the superoperator $S(\mathcal{W}_u)$ can always be written as

$$S(\mathcal{W}_u) = \left(\frac{S(\mathcal{L})}{\|\mathcal{L}\|_{\text{pauli}}} \right)^{2l} \Gamma_{kl,\nu}, \quad (\text{C.6})$$

where $\Gamma_{kl,\nu}$ is the transfer matrix of a superoperator defined by Eqs. (B.30)–(B.32). Then, we have

$$S(\Lambda_{2Q+1,t/r}^r) = \sum_{(u_1, u_2, \dots, u_r) \in \tilde{\mathcal{S}}_Q^r} c_{u_1} \cdots c_{u_r} S(\mathcal{W}_{u_1}) \cdots S(\mathcal{W}_{u_r}). \quad (\text{C.7})$$

The sum of coefficients can be evaluated as

$$\begin{aligned} \sum_{(u_1, u_2, \dots, u_r) \in \tilde{\mathcal{S}}_Q^r} c_{u_1} \cdots c_{u_r} &= \left\{ \sum_{l=0}^Q \frac{(t/r)^{2l} \|\mathcal{L}\|_{\text{pauli}}^{2l}}{(2l)!} \left(2 \frac{\alpha_0}{\alpha} \sqrt{1 + \tau_l^2} + \sum_{k=1}^K \frac{\alpha_k^2}{\alpha} \left(1 + \|R_{kl}\|_{\text{pauli}} + \frac{\tau_l^2}{4} \right) \right) \right\}^r \\ &\leq \left\{ \sum_{l=0}^{\infty} \frac{(t/r)^{2l} \|\mathcal{L}\|_{\text{pauli}}^{2l}}{(2l)!} \left(2 \frac{\alpha_0}{\alpha} \sqrt{1 + \tau_l^2} + \sum_{k=1}^K \frac{\alpha_k^2}{\alpha} \left(1 + \|R_{kl}\|_{\text{pauli}} + \frac{\tau_l^2}{4} \right) \right) \right\}^r \\ &\leq \exp \left(\frac{2 \|\mathcal{L}\|_{\text{pauli}}^2 t^2}{r} \right), \end{aligned} \quad (\text{C.8})$$

where we used Eq. (B.36) in the final inequality.

As described in the proof of Theorem 1, the three-type circuits, $\mathcal{U}_I, \mathcal{U}_{II}$, and \mathcal{U}_{III} , illustrated in Fig. 4 simulate the superoperator \mathcal{W}_u . More precisely, for any \mathcal{W}_u , we can explicitly construct a quantum circuit $\tilde{\mathcal{W}}_u$ satisfying

$$\Lambda_{2Q+1,t/r}^r(\bullet) = \sum_{(u_1, u_2, \dots, u_r) \in \tilde{\mathcal{S}}_Q^r} c_{u_1} c_{u_2} \cdots c_{u_r} \text{Tr}_{\text{anc}} \left[(X_{\text{anc}} \otimes \mathbf{1}) \tilde{\mathcal{W}}_{u_1} \circ \cdots \circ \tilde{\mathcal{W}}_{u_r} (|+\rangle\langle +|_{\text{anc}} \otimes \bullet) \right], \quad (\text{C.9})$$

from the fact that $\Lambda_{2Q+1,t/r}^r(\bullet)$ has the Hermitian preserving property. For any $u = (l, k, \nu) \in \tilde{\mathcal{S}}_Q$, the corresponding quantum circuit $\tilde{\mathcal{W}}_u$ consists of a single call of $\mathcal{U}_I, \mathcal{U}_{II}$, or \mathcal{U}_{III} for $\Gamma_{kl,\nu}$ and $2l \leq 2Q$ calls of \mathcal{U}_I for $\mathcal{L}/\|\mathcal{L}\|_{\text{pauli}}$; see Fig. 5 for instance. Since all of the circuits $\mathcal{U}_I, \mathcal{U}_{II}$, and \mathcal{U}_{III} have a constant depth, $\tilde{\mathcal{W}}_u$ has at most $\mathcal{O}(Q)$ depth for all $u \in \tilde{\mathcal{S}}_Q$. Thus, the total depth of quantum circuits $\tilde{\mathcal{W}}_{u_1} \circ \cdots \circ \tilde{\mathcal{W}}_{u_r}$ is given by at most $\mathcal{O}(rQ)$ for any $(u_1, u_2, \dots, u_r) \in \tilde{\mathcal{S}}_Q^r$. Furthermore, we can efficiently sample quantum circuits $\tilde{\mathcal{W}}_u$ (including classical post-processing instructions) according to the probability distribution proportional to the weight $\{c_u\}_{u \in \tilde{\mathcal{S}}_Q}$ as described in Algorithm 1.

Finally, we show that when we take an integer Q as

$$Q \geq \frac{\ln(3r/2\Delta)}{\ln \ln(3r/2\Delta)}, \quad (\text{C.10})$$

then the approximation error of $\Lambda_{2Q+1,t/r}^r(\bullet)$ for $e^{t\mathcal{L}}$ is upper bounded by Δ as

$$\left\| \Lambda_{2Q+1,t/r}^r - e^{t\mathcal{L}} \right\| \leq \Delta \quad (\text{C.11})$$

For any positive integer Q' ,

$$\begin{aligned} \left\| \Lambda_{Q',t/r} - e^{(t/r)\mathcal{L}} \right\|_{1 \rightarrow 1} &= \left\| \sum_{q=Q'+1}^{\infty} \frac{(t/r)^q \mathcal{L}^q}{q!} \right\|_{1 \rightarrow 1} \\ &\leq \sum_{q=Q'+1}^{\infty} \frac{|t/r|^q}{q!} \|\mathcal{L}^q\|_{1 \rightarrow 1} \\ &\leq \sum_{q=Q'+1}^{\infty} \frac{1}{q!} \left(\frac{t \|\mathcal{L}\|_{1 \rightarrow 1}}{r} \right)^q. \end{aligned} \quad (\text{C.12})$$

Here, $\|\mathcal{L}\|_{1 \rightarrow 1} \leq \|\mathcal{L}\|_{\text{pauli}}$ holds as follows. By the triangle inequality and Hölder's inequality, we have for any non-zero operator A ,

$$\begin{aligned} \|\mathcal{L}(A)\|_1 &= \left\| -i[H, A] + \sum_{k=1}^K \left(L_k A L_k^\dagger - \frac{1}{2} \{L_k^\dagger L_k, A\} \right) \right\|_1 \\ &\leq 2\|H\|_\infty \|A\|_1 + 2 \sum_{k=1}^K \|L_k\|_\infty^2 \|A\|_1 \leq 2\|A\|_1 \left(\alpha_0 + \sum_{k=1}^K \alpha_k^2 \right). \end{aligned} \quad (\text{C.13})$$

Hence, $\|\mathcal{L}\|_{1 \rightarrow 1}$ is bounded as

$$\|\mathcal{L}\|_{1 \rightarrow 1} \leq 2 \left(\alpha_0 + \sum_{k=1}^K \alpha_k^2 \right) = \|\mathcal{L}\|_{\text{pauli}}. \quad (\text{C.14})$$

Thus, from the assumption of $r \geq t\|\mathcal{L}\|_{\text{pauli}} \geq t\|\mathcal{L}\|_{1 \rightarrow 1}$, we have

$$\left\| \Lambda_{Q',t/r} - e^{(t/r)\mathcal{L}} \right\|_{1 \rightarrow 1} \leq \sum_{q=Q'+1}^{\infty} \frac{1}{q!} < \frac{1}{(Q')!}. \quad (\text{C.15})$$

Taking $Q' := \lceil 2\kappa / \ln \kappa \rceil$ (≥ 1) for $\kappa := \ln(r/\Delta')$ with $\Delta' \in (0, 1/e)$ and using the Stirling's formula, we can derive that

$$\ln \frac{1}{(Q')!} < Q' - Q' \ln Q' = Q' \ln \kappa \cdot \frac{1 - \ln Q'}{\ln \kappa} \leq -\frac{1}{2} Q' \ln \kappa \leq -\kappa. \quad (\text{C.16})$$

This leads that the approximation error of $\Lambda_{Q',t/r}$ becomes at most Δ'/r , i.e.,

$$\left\| \Lambda_{Q',t/r} - e^{(t/r)\mathcal{L}} \right\|_{1 \rightarrow 1} \leq \Delta'/r. \quad (\text{C.17})$$

Due to Eq. (C.17),

$$\left\| \Lambda_{Q',t/r} \right\|_{1 \rightarrow 1} - \left\| e^{(t/r)\mathcal{L}} \right\|_{1 \rightarrow 1} \leq \left\| \Lambda_{Q',t/r} - e^{(t/r)\mathcal{L}} \right\|_{1 \rightarrow 1} = \Delta'/r \quad (\text{C.18})$$

holds. Hence, we have

$$\left\| \Lambda_{Q',t/r} \right\|_{1 \rightarrow 1} \leq \left\| e^{(t/r)\mathcal{L}} \right\|_{1 \rightarrow 1} + \Delta'/r = 1 + \Delta'/r \quad (\text{C.19})$$

because $\|e^{(t/r)\mathcal{L}}\|_{1 \rightarrow 1} = 1$ holds from Lemma 1 since $e^{(t/r)\mathcal{L}}$ is CPTP. Observing that

$$\|\mathcal{C}^r - \mathcal{D}^r\|_{1 \rightarrow 1} \leq \sum_{k=1}^r \|\mathcal{C}\|_{1 \rightarrow 1}^{k-1} \|\mathcal{C} - \mathcal{D}\|_{1 \rightarrow 1} \|\mathcal{D}\|_{1 \rightarrow 1}^{r-k} \leq r \max\{\|\mathcal{C}\|_{1 \rightarrow 1}, \|\mathcal{D}\|_{1 \rightarrow 1}\}^{r-1} \|\mathcal{C} - \mathcal{D}\|_{1 \rightarrow 1} \quad (\text{C.20})$$

for any linear maps \mathcal{C} and \mathcal{D} , we obtain

$$\begin{aligned} \left\| (\Lambda_{Q',t/r})^r - e^{t\mathcal{L}} \right\|_{1 \rightarrow 1} &\leq r \max\{\|\Lambda_{Q',t/r}\|_{1 \rightarrow 1}, 1\}^{r-1} \left\| \Lambda_{Q',t/r} - e^{(t/r)\mathcal{L}} \right\|_{1 \rightarrow 1} \\ &\leq \Delta' (1 + \Delta'/r)^{r-1} \leq \Delta' e^{\Delta'} \\ &\leq \Delta, \end{aligned} \quad (\text{C.21})$$

where we set $\Delta' := (2/3)\Delta \in (0, 1/e)$ in the final inequality. Therefore, taking Q as $Q \geq Q'/2 = \frac{\ln(3r/2\Delta)}{\ln \ln(3r/2\Delta)}$, the lemma holds. \square

Using quantum circuits sampled by Algorithm 1, we can estimate the target quantity $\text{Tr}[Oe^{t\mathcal{L}}(\rho_0)]$ as follows. First, we generate a quantum circuit $\widetilde{\mathcal{W}}$ by Algorithm 1. This circuit contains (possibly multi-round) mid-circuit measurement and qubit reset as in Fig. 1, and the corresponding POVM $\{\Pi_b\}_{b=0,1}$ in each mid-circuit measurement is given by Eq. (B.47). Then, running the circuit with an initial state $|+\rangle\langle +|_{\text{anc}} \otimes \rho_0$ and measuring the observable $X_{\text{anc}} \otimes O$ at the end of circuit, we obtain measurement outcomes (b_X, b_O) and a collection of mid-circuit measurement outcomes $\mathbf{b} = (b_1, b_2, \dots)$ ($b_i \in \{0, 1\}$). By repeating the above procedure N times independently, we calculate the following quantity

$$\varphi_N := \frac{C}{N} \sum_{i=1}^N b_X^{(i)} b_O^{(i)} \delta_{\mathbf{b}^{(i)}, \mathbf{0}}, \quad (\text{C.22})$$

where the superscript i denotes the index of trials and the positive value C is also the output of Algorithm 1.

From the construction, it can be confirmed that the mean of φ_N becomes

$$\mathbb{E}[\varphi_N] = \sum_{v \in \mathcal{S}_\Delta} c_v \text{Tr}[(X_{\text{anc}} \otimes O) \widetilde{\mathcal{W}}_v(|+\rangle\langle +|_{\text{anc}} \otimes \rho)] \quad (\text{C.23})$$

and this is $(\Delta\|O\|)$ -close to the target value as

$$|\mathbb{E}[\varphi_N] - \text{Tr}[Oe^{t\mathcal{L}}(\rho_0)]| \leq \Delta\|O\| \quad (\text{C.24})$$

due to Eq. (C.1) and the tracial matrix Hölder's inequality. In addition, from the Hoeffding's inequality and the above evaluation, we can say

$$N = \frac{2C^2\|O\|^2 \log(2/\delta)}{(\varepsilon')^2} \quad (\text{C.25})$$

samples are sufficient in order that

$$\Pr(|\varphi_N - \text{Tr}[Oe^{t\mathcal{L}}(\rho_0)]| < \varepsilon' + \Delta\|O\|) \geq 1 - \delta \quad (\text{C.26})$$

holds for given parameters $\varepsilon' > 0$ and $\delta > 0$. Thus, for a target additive error ε , taking $\Delta = \varepsilon/2\|O\|$ and $\varepsilon' = \varepsilon/2$, we conclude that our algorithm estimates the target expectation value within an additive error ε with at least $1 - \delta$ probability, i.e.,

$$\Pr(|\varphi_N - \text{Tr}[Oe^{t\mathcal{L}}(\rho_0)]| < \varepsilon) \geq 1 - \delta. \quad (\text{C.27})$$

Also, the sampling overhead $C = \sum_{v \in \mathcal{S}_\Delta} c_v$ can be $\mathcal{O}(1)$ by setting $r = \mathcal{O}(\|\mathcal{L}\|_{\text{pauli}}^2 t^2)$ because of Eq. (C.2). Consequently, the above construction and analysis complete the proof of Theorem 2.

Theorem 2. *For any Hamiltonian H and jump operators $\{L_k\}_{k=1}^K$ specified by Eq. (2), there exists a quantum algorithm that estimates the expectation value of an observable O for the n -qubit Lindblad dynamics Eq. (1) with the use of additional $4 + \lceil \log_2 M \rceil$ ancilla qubits, where M is the number of Pauli strings contained in a single jump operator L_k . For given additive error ε , δ , and simulation time t , this algorithm outputs an ε -close estimate for the expectation value with at least $1 - \delta$ probability, using $\mathcal{O}(\|O\|^2 \log(1/\delta)/\varepsilon^2)$ samples from the set of quantum circuits the maximal depth of which is*

$$\mathcal{O}\left(\|\mathcal{L}\|_{\text{pauli}}^2 t^2 \frac{\log(\|O\|_\infty \|\mathcal{L}\|_{\text{pauli}} t / \varepsilon)}{\log \log(\|O\|_\infty \|\mathcal{L}\|_{\text{pauli}} t / \varepsilon)}\right).$$

Algorithm 1 Efficient sampling of the random circuit for the approximate decomposition of $e^{t\mathcal{L}}$

Input: Hamiltonian H and jump operators $\{L_k\}_{k=1}^K$ defined by (B.1), simulation time $t > 0$, number of time segments (integer) $r \geq t\|\mathcal{L}\|_{\text{pauli}}$, accuracy parameter $\Delta \in (0, 1/e)$.

Output: Positive value C and description of a sample from the random quantum circuit $\widetilde{\mathcal{W}}$ including classical post-processing, such that its average provides a Δ -approximation of Lindblad dynamics as

$$\left\| C \times \mathbb{E}_{\widetilde{\mathcal{W}}}[\text{Tr}_{\text{anc}}[(X_{\text{anc}} \otimes \mathbf{1})\widetilde{\mathcal{W}}(|+\rangle\langle +|_{\text{anc}} \otimes (\bullet))] - e^{t\mathcal{L}}(\bullet) \right\| \leq \Delta.$$

- 1: Initialize an integer $Q \leftarrow \lceil \ln(3r/2\Delta)/\ln \ln(3r/2\Delta) \rceil$, a phase parameter $\phi \leftarrow 0$, and a list QCList $\leftarrow []$
- 2: Define functions for $l \in \{0, 1, \dots, Q\}$

$$\tau_l := \frac{t/r}{2l+1} \times 2 \left(\alpha_0 + \frac{1}{2} \sum_{k=1}^K \alpha_k^2 \right), \quad \|R_{kl}\|_{\text{pauli}} := \frac{\tau_l^2}{4} + \frac{\tau_l^3}{2} + \frac{5\tau_l^4}{64} + \frac{\tau_l^5}{32} + \frac{\tau_l^6}{256},$$

$$C_l := \frac{(t/r)^{2l} \|\mathcal{L}\|_{\text{pauli}}^{2l}}{(2l)!} \left(2 \frac{\alpha_0}{\alpha} \sqrt{1 + \tau_l^2} + \sum_{k=1}^K \frac{\alpha_k^2}{\alpha} \left(1 + \|R_{kl}\|_{\text{pauli}} + \frac{\tau_l^2}{4} \right) \right) \geq 0$$

- 3: **for** $i = 0$ to $r - 1$ **do**
- 4: Sample $l \in \{0, 1, \dots, Q\}$ from the probability distribution $\{C_l / (\sum_l C_l)\}$
- 5: Sample $k \in \{0, 1, \dots, K\}$ from the probability distribution conditioned by l

$$q_{0l} \propto 2 \frac{\alpha_0}{\alpha} \sqrt{1 + \tau_l^2}, \quad q_{kl} \propto \frac{\alpha_k^2}{\alpha} \left(1 + \|R_{kl}\|_{\text{pauli}} + \frac{\tau_l^2}{4} \right) \quad (\text{for } k = 1, 2, \dots, K)$$

- 6: Sample $\nu \in \{1, 2, 3\}$ from the probability distribution conditioned by l, k

$$p_{\Gamma, 0l, \nu} := \frac{1}{2} (\delta_{1\nu} + \delta_{2\nu}), \quad p_{\Gamma, kl, \nu} := \frac{\delta_{1\nu} + \|R_{kl}\|_{\text{pauli}} \delta_{2\nu} + (\tau_l^2/4) \delta_{3\nu}}{1 + \|R_{kl}\|_{\text{pauli}} + \tau_l^2/4} \quad (\text{for } k = 1, 2, \dots, K)$$

- 7: **if** $k = 0$ **then**
- 8: Sample a Pauli string P_{0j} from H according to the probability distribution $\{p_{0j} := |\alpha_{0j}| / (\sum_j |\alpha_{0j}|)\}$
- 9: Append $\widetilde{\mathcal{F}}_{U,1}$ ($\nu = 1$) or $\widetilde{\mathcal{F}}_{1,U}$ ($\nu = 0$) to QCList, where $U = \exp[-i\theta_l \text{sgn}(\alpha_{0j}) P_{0j}]$,

$$\theta_l := \arccos\left(\{1 + \tau_l^2\}^{-1/2}\right), \quad \widetilde{\mathcal{F}}_{A,B}(\bullet) := (|0\rangle\langle 0| \otimes A + |1\rangle\langle 1| \otimes B) \bullet (|0\rangle\langle 0| \otimes A^\dagger + |1\rangle\langle 1| \otimes B^\dagger)$$

- 10: **else if** $\nu = 1$ with $k > 0$ **then**
- 11: Append $\mathcal{I}_{\text{anc}} \otimes \mathcal{U}_{\text{II}}$, with mid-circuit measurement followed by qubit reset and classical post-processing (see Fig. 4 and Remark 1) for the CPTN map $\mathcal{B}_{kl}^{(\text{approx})}$, to QCList
- 12: **else if** $\nu = 2$ with $k > 0$ **then**
- 13: Call Algorithm 3 and obtain $e^{i\theta} \overline{Q} \otimes P$ with a phase θ and n -qubit Pauli strings $\{P, Q\}$
- 14: Append $\widetilde{\mathcal{F}}_{P,Q}$ to QCList and Update $\phi \leftarrow \phi + \theta$
- 15: **else if** $\nu = 3$ with $k > 0$ **then**
- 16: Sample $j_1, \dots, j_4 \in \{1, 2, \dots, M\}$ independently from the identical distribution $\{p_{kj} := |\alpha_{kj}| / (\sum_j |\alpha_{kj}|)\}$
- 17: Append $\widetilde{\mathcal{F}}_{A,B}$ with $A = P_{kj_1} P_{kj_2}$ and $B = P_{kj_4} P_{kj_3}$ to QCList and Update ϕ as

$$\phi \leftarrow \phi - \theta_{kj_1} + \theta_{kj_2} - \theta_{kj_3} + \theta_{kj_4} + \pi, \quad \theta_{kj} := \arg(\alpha_{kj} / |\alpha_{kj}|)$$

- 18: **end if**
 - 19: **for** $j = 0$ to $2l - 1$ **do**
 - 20: Call Algorithm 2 and obtain $e^{i\theta} \overline{Q} \otimes P$ with a phase θ and n -qubit Pauli strings $\{P, Q\}$
 - 21: Append $\widetilde{\mathcal{F}}_{P,Q}$ to QCList and Update $\phi \leftarrow \phi + \theta$
 - 22: **end for**
 - 23: **end for**
 - 24: Append a Phase gate $\text{Phase}(e^{i\phi}) \otimes \mathbf{1}$ to QCList, where $\text{Phase}(e^{i\phi}) := e^{i\phi} |0\rangle\langle 0|_{\text{anc}} + |1\rangle\langle 1|_{\text{anc}}$
 - 25: **return** Positive value $C := (\sum_l C_l)^r$ and $\widetilde{\mathcal{W}} = \text{QCList}[\text{length}(\text{QCList})-1] \circ \dots \circ \text{QCList}[0]$
-

We note that if we can calculate $\prod_{j=0}^{2l-1} e^{i\theta_j} \overline{Q}_j \otimes P_j =: e^{i\theta'} \overline{Q}' \otimes P'$ classically, we can simply append $\widetilde{\mathcal{F}}_{P',Q'}$ instead of $\widetilde{\mathcal{F}}_{P_{2l-1}, Q_{2l-1}} \circ \dots \circ \widetilde{\mathcal{F}}_{P_0, Q_0}$ on the line 21. This substitution improves the circuit depth.

Algorithm 2 Efficient sampling of the random unitary X_G for $G = S(\mathcal{L})$

Input: Hamiltonian H and jump operators $\{L_k\}_{k=1}^K$ defined by (B.1).

Output: Description of a sample from the random unitary X_G such that $\mathbb{E}[X_G] = G/\|\mathcal{L}\|_{\text{pauli}}$, where $G = S(\mathcal{L})$ and $\|\mathcal{L}\|_{\text{pauli}}$ is defined by Eqs. (B.9) and (B.11). Here, X_G has the form of

$$e^{i\theta\overline{Q}} \otimes P \quad (\text{C.28})$$

for some $\theta \in \mathbb{R}$ and n -qubit Pauli strings $P, Q \in \{I, X, Y, Z\}^{\otimes n}$, with probability 1.

1: Sample $k \in \{0, 1, \dots, K\}$ from the probability distribution p_k ,

$$p_k = \frac{2\alpha_0}{\|\mathcal{L}\|_{\text{pauli}}} \delta_{0k} + \sum_{m=1}^K \frac{2\alpha_m^2}{\|\mathcal{L}\|_{\text{pauli}}} \delta_{mk}.$$

2: **if** $k = 0$ **then**

3: Sample $l \in \{1, 2\}$ with equal probability.

4: Sample $j \in \{1, \dots, m\}$ from the probability distribution

$$p_{0j} = \frac{|\alpha_{0j}|}{\sum_{j=1}^m |\alpha_{0j}|}.$$

5: Set X_G as

$$X_G := \begin{cases} \exp[i(\theta_{0j} - \pi/2)] \cdot \mathbf{1} \otimes P_{0j}, & \text{if } l = 1 \\ \exp[i(\theta_{0j} + \pi/2)] \cdot P_{0j}^T \otimes \mathbf{1}, & \text{if } l = 2 \end{cases} \quad \text{and } e^{i\theta_{0j}} := \frac{\alpha_{0j}}{|\alpha_{0j}|} (\in \{1, -1\})$$

6: **else if** $k \neq 0$ **then**

7: Sample $l \in \{1, 2, 3\}$ with the probability $\{1/2, 1/4, 1/4\}$.

8: Sample $j_1, j_2 \in \{1, \dots, M\}$ independently from the identical probability distribution

$$p_{kj} = \frac{|\alpha_{kj}|}{\sum_{j=1}^M |\alpha_{kj}|}$$

9: Set X_G as

$$X_G := \begin{cases} \exp[i(-\theta_{kj_1} + \theta_{kj_2})] \cdot \overline{P_{kj_1}} \otimes P_{kj_2}, & \text{if } l = 1 \\ \exp[i(-\theta_{kj_1} + \theta_{kj_2} + \pi)] \cdot \mathbf{1} \otimes P_{kj_1} P_{kj_2}, & \text{if } l = 2 \\ \exp[i(\theta_{kj_1} - \theta_{kj_2} + \pi)] \cdot P_{kj_1}^T \overline{P_{kj_2}} \otimes \mathbf{1}, & \text{if } l = 3, \end{cases} \quad \text{and } e^{i\theta_{kj}} := \frac{\alpha_{kj}}{|\alpha_{kj}|}.$$

10: **end if**

11: Modify the phase of X_G to match the form of Eq. (C.28).

12: **return** The description of X_G with a complex phase and Pauli strings.

Algorithm 3 Efficient sampling of the random unitary X_R for the correction superoperator $R = S(\mathcal{R})$

Input: Hamiltonian H and jump operators $\{L_k\}_{k=1}^K$ defined by (B.1), $t > 0$, $r \in \mathbb{N}$, $l \in \{0, 1, \dots\}$, and $k \in \{1, 2, \dots, K\}$.

Output: Description of a sample from the random unitary X_R such that $\mathbb{E}[X_R] = R_{kl}/\|R_{kl}\|_{\text{pauli}}$, where R_{kl} and $\|R_{kl}\|_{\text{pauli}}$ is defined by Eqs. (B.21) and (B.26). Here, X_R has the form of

$$e^{i\theta\overline{Q}} \otimes P$$

for some $\theta \in \mathbb{R}$ and n -qubit Pauli strings $P, Q \in \{I, X, Y, Z\}^{\otimes n}$, with probability 1.

1: Set

$$\tau_l := \frac{t/r}{2l+1} \times 2 \left(\alpha_0 + \frac{1}{2} \sum_{k=1}^K \alpha_k^2 \right), \quad P_{k0} := i\mathbf{1}, \quad \theta_{k0} := 0$$

2: Sample $\lambda \in \{0, 1\}$ from the probability distribution

$$p_\lambda = \frac{1 + \tau_l^2/16}{1 + 2\tau_l + 5\tau_l^2/16 + \tau_l^3/8 + \tau_l^4/64} \left\{ \left(1 + \frac{\tau_l}{2}\right)^2 \delta_{0\lambda} + \tau_l \delta_{1\lambda} \right\}$$

3: Sample $i \in \{0, 1, 2\}$ from the probability distribution

$$p_i = \frac{1}{2 + \tau_l^2/8} \left\{ \delta_{0i} + \delta_{1i} + \frac{\tau_l^2}{8} \delta_{2i} \right\}$$

4: **if** $\lambda = 0$ **then**

5: Sample $(j_1, j_2), (j'_1, j'_2) \in \{0, 1, \dots, M\}^2$ independently from the identical joint probability distribution

$$p_{j_1 j_2} := \frac{1}{1 + \tau_l/2} \delta_{0j_1} \delta_{0j_2} + \frac{\tau_l/2}{1 + \tau_l/2} \sum_{m_1, m_2=1}^M p_{km_1} p_{km_2} \delta_{m_1 j_1} \delta_{m_2 j_2}$$

6: Sample $j_3, \dots, j_{10} \in \{1, \dots, M\}$ independently from the identical distribution $p_{kj} = \frac{|\alpha_{kj}|}{\sum_{j=1}^M |\alpha_{kj}|}$

7: Set X_R as

$$X_R := \begin{cases} \overline{P_{kj_1} P_{kj_2}} \otimes P_{kj'_1} P_{kj'_2} \prod_{\nu=3}^6 P_{kj_\nu} \\ \quad \times \exp[i(\theta_{kj_1} - \theta_{kj_2} - \theta_{kj'_1} + \theta_{kj'_2} - \theta_{kj_3} + \theta_{kj_4} - \theta_{kj_5} + \theta_{kj_6})], & \text{if } i = 0 \\ \overline{P_{kj_1} P_{kj_2} \prod_{\nu=3}^6 P_{kj_\nu}} \otimes P_{kj'_1} P_{kj'_2} \\ \quad \times \exp[i(\theta_{kj_1} - \theta_{kj_2} - \theta_{kj'_1} + \theta_{kj'_2} + \theta_{kj_3} - \theta_{kj_4} + \theta_{kj_5} - \theta_{kj_6})], & \text{if } i = 1 \\ \overline{P_{kj_1} P_{kj_2} \prod_{\nu=3}^6 P_{kj_\nu}} \otimes P_{kj'_1} P_{kj'_2} \prod_{\nu=7}^{10} P_{kj_\nu} \\ \quad \times \exp[i(\theta_{kj_1} - \theta_{kj_2} - \theta_{kj'_1} + \theta_{kj'_2} + \theta_{kj_3} - \theta_{kj_4} + \theta_{kj_5} - \theta_{kj_6} - \theta_{kj_7} + \theta_{kj_8} - \theta_{kj_9} + \theta_{kj_{10}})], & \text{if } i = 2 \end{cases}$$

8: **else if** $\lambda = 1$ **then**

9: Sample $j_1, j'_1, j_2, \dots, j_9 \in \{1, \dots, M\}$ independently from the identical probability distribution $p_{kj} = \frac{|\alpha_{kj}|}{\sum_{j=1}^M |\alpha_{kj}|}$

10: Set X_R as

$$X_R := \begin{cases} \overline{P_{kj_1}} \otimes P_{kj'_1} \prod_{\nu=2}^5 P_{kj_\nu} \\ \quad \times \exp[i(-\theta_{kj_1} + \theta_{kj'_1} - \theta_{kj_2} + \theta_{kj_3} - \theta_{kj_4} + \theta_{kj_5})], & \text{if } i = 0 \\ \overline{P_{kj_1} \prod_{\nu=2}^5 P_{kj_\nu}} \otimes P_{kj'_1} \\ \quad \times \exp[i(-\theta_{kj_1} + \theta_{kj'_1} + \theta_{kj_2} - \theta_{kj_3} + \theta_{kj_4} - \theta_{kj_5})], & \text{if } i = 1 \\ \overline{P_{kj_1} \prod_{\nu=2}^5 P_{kj_\nu}} \otimes P_{kj'_1} \prod_{\nu=6}^9 P_{kj_\nu} \\ \quad \times \exp[i(-\theta_{kj_1} + \theta_{kj'_1} + \theta_{kj_2} - \theta_{kj_3} + \theta_{kj_4} - \theta_{kj_5} - \theta_{kj_6} + \theta_{kj_7} - \theta_{kj_8} + \theta_{kj_9})], & \text{if } i = 2 \end{cases}$$

11: **end if**

12: Modify the phase of X_R to match the form of $e^{i\theta\overline{Q}} \otimes P$

13: **return** The description of X_R with a complex phase and Pauli strings

Appendix D: Numerical analysis

In this section, we numerically demonstrate the validity of the proposed algorithm. Let us consider an example of the spontaneous emission of a two-level system in a zero-temperature heat bath, described by a 1-qubit system with a lowering operator:

$$H = -\frac{\delta}{2}Z - \frac{\Omega}{2}X, \quad (\text{D.1})$$

$$L = \sqrt{\gamma}\frac{X - iY}{2}, \quad (\text{D.2})$$

where δ , Ω and γ are the Rabi frequency, the detuning, the Rabi frequency, and the emission rate, respectively. This model is simple but well-studied [19, 54]. We apply the proposed algorithm for the Lindblad dynamics defined by the H and L and measure the expectation value of the observable $O := |0\rangle\langle 0|$, which corresponds to the state population of the excited state.

The results of the numerical simulation are shown in Fig. 10, and the detailed setup for the demonstration is given in Table II. Through the demonstration, the numerical results are obtained by Qiskit density matrix simulation. Figure 10 (a) shows the comparison between the simulation output and an exact solution obtained by QuTiP [55, 56]. It can be verified that our results are in good agreement with the exact solution.

Furthermore, Fig. 10 (b) shows that the total norm C , which corresponds to the output of Algorithm 1, can be maintained at a constant by an appropriate choice of the number of segments r , where we set $r = \max[\lceil 2\|\mathcal{L}\|_{\text{pauli}}^2 t^2 \rceil, 1]$. This indicates that we need only a few overheads (≈ 1.4) for the rescaling of the sample mean. In addition, it can be seen that the sampling overhead is much smaller than the upper bound shown by Theorem 1. It means that we can expect further cost reduction from the theoretical bound for practical setups.

items	values
dynamics parameters	$\delta = \Omega = \gamma = 1$
simulation time	$t \in \{0.1, 1, 2, 3, 4, 5\}$
initial state	$ 0\rangle\langle 0 $
the number of segments	$r = \max[\lceil 2\ \mathcal{L}\ _{\text{pauli}}^2 t^2 \rceil, 1]$
target error level	$\Delta = 10^{-2}$
the number of samples	$N = 2 \times 10^4$

TABLE II. Numerical simulation setup

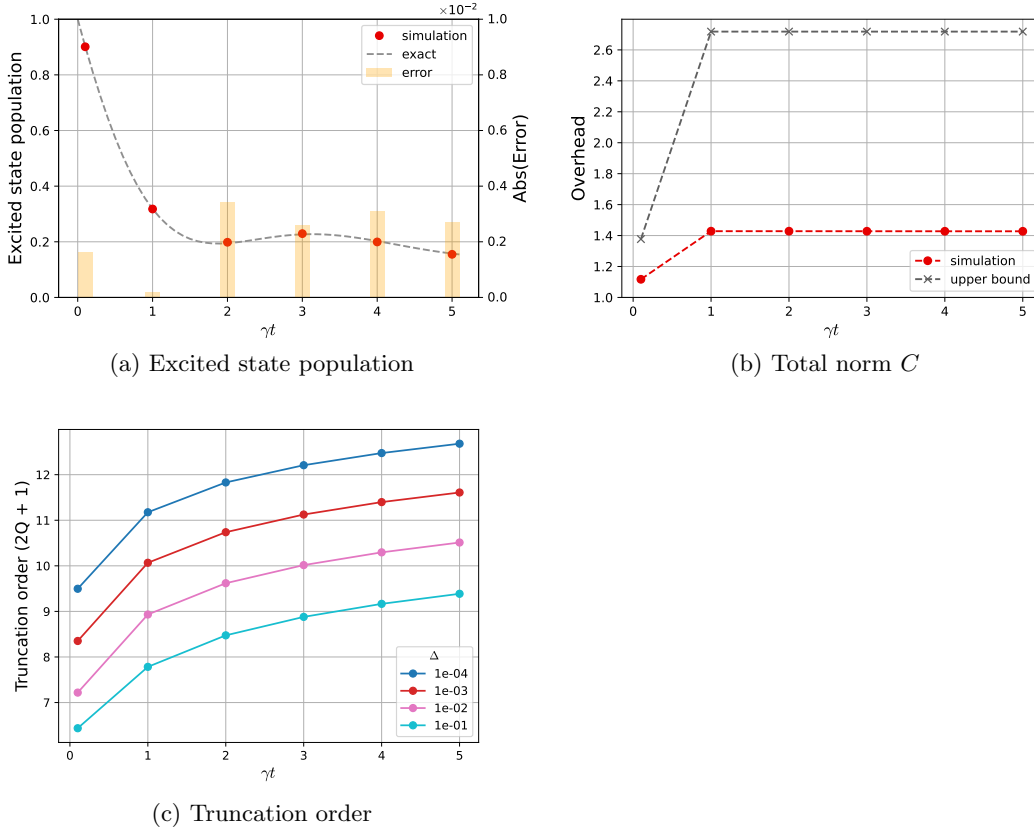


FIG. 10. Numerical simulation of the two-level system with the decay. (a) The comparison of the excited state population between the exact solution and the simulation by the proposed algorithm. The *exact* solution is obtained by QUTiP, and the *simulation* is obtained with Qiskit density matrix simulation. The *error* indicates the absolute error between *exact* and *simulation* for the single experiment on the right axis. For simplicity, we directly sampled $\mathcal{B}^{(\text{approx})}$ instead of OAA circuits. (b) The total norm C with respect to γt . C is less than 1.5 at each time t due to the appropriate choice of $r = \max[\lceil 2\|\mathcal{L}\|_{\text{pauli}}^2 t^2 \rceil, 1]$. The upper bound equals to e for $2\|\mathcal{L}\|_{\text{pauli}}^2 t^2 \geq 1$. (c) Taylor series truncation dependence on required Δ . This varies in time but is bounded at most 11 for our demonstration.